2013

Kinetic and Thermodynamic Studies of Thrombin Inhibitors

Aziz May Abdel
Virginia Commonwealth University

School of Pharmacy
Virginia Commonwealth University

This is to certify that the dissertation prepared by May Hamdy Abdel Aziz entitled "KINETIC AND THERMODYNAMIC STUDIES OF THROMBIN INHIBITORS" has been approved by her committee as satisfactory completion of the dissertation requirement for the degree of

Doctor of Philosophy

Dr. Umesh R Desai, School of Pharmacy

Dr. Glen E Kellogg, School of Pharmacy

Dr. Richard Westkaemper, School of Pharmacy

Dr. Jan Chlebowski, School of Medicine

Dr. H. Tonie Wright, School of Medicine

Dr. Richard Glennon, Chairman of the Department of Medicinal Chemistry

Dr. Victor Yanchick, Dean of the School of Pharmacy

Dr. F. Douglas Boudinot, Dean of the Graduate School

February, 2013

KINETIC AND THERMODYNAMIC STUDIES OF THROMBIN INHIBITORS

A dissertation submitted in partial fulfillment of the requirements for the degree of Doctor of Philosophy at Virginia Commonwealth University

by

MAY HAMDY ABDEL AZIZ

BS in Pharmaceutical Sciences, MS in Pharmaceutical Chemistry

Cairo University, Egypt

Supervisor: UMESH R. DESAI

Professor, Department of Medicinal Chemistry

Virginia Commonwealth University

Richmond, Virginia

February 2013

Acknowledgement

First and above all I would like to thank God for finishing this work, in the face of all obstacles and all odds!

Next, I would love to thank my father, his unconditional love and support have pushed me all my life. If it wasn't for him, I wouldn't have been anywhere I am now.

I am profoundly indebted to Dr. Umesh Desai; he was not only my advisor, he was my mentor and I think he will always be. Not only has he taught me how a true researcher and scientist should be, but also showed me how to be a great teacher and a great mentor. He is my role model when it comes to discipline and productivity. Under his supervision I was given the freedom to think independently and still miraculously float! I do not think I could have found such flexible guidance anywhere else. I will be forever grateful for his understanding and support.

I would like to express my sincere appreciation to my committee members for reading my grant for the oral proposal, then my dissertation. I would also like to thank them for listening to my research presentations, especially Dr. Tonie Wright, my oral examination and then my final defense. They were quite helpful and understanding.

I thank all our collaborators, Drs. Alireza Rezaie, David Farrell, and Paul Bock for providing some of the materials used in this work.

I would like to thank my past and current lab members for listening patiently to my long research presentations each semester and for the funny and friendly environment they created at work. A special attribute goes to Jay Thakkar, Meghan Thompson and Preetpal Sidhu for synthesizing the compounds used in this work.

Words of appreciation should extend to the Department of Medicinal Chemistry for supporting me for the first three years of the program, giving me the chance for a great cultural and educational experience.

Finally I would like to thank my family, especially my little Salma. I have been accidently stealing some of her “Mommy and me” time lately, hopefully she is young enough not to remember that (or read this)!

Table of Contents

List of Tables

List of Figures

Abstract

KINETIC AND THERMODYNAMIC STUDIES OF THROMBIN INHIBITORS

By May Hamdy Abdel Aziz, Ph.D.

A dissertation submitted in partial fulfillment of the requirements for the degree of Doctor of Philosophy at Virginia Commonwealth University.

Virginia Commonwealth University, 2013.

Supervisor: UMESH R. DESAI, professor, department of medicinal chemistry.

Sulfated low molecular weight lignins (LMWLs), $CDSO_3$ and $FDSO_3$, designed recently as macromolecular mimetics of heparin, were found to exhibit potent anticoagulant activity. Small molecules based on the same scaffold, SBD and SBT, showed promising thrombin inhibition. All studied molecules were found to allosterically inhibit thrombin as inferred from Michaelis-Menten kinetics. Absence of competition with hirugen, an exosite 1 ligand, and competition with polymeric heparin points to exosite 2 as the site of interaction for these inhibitors. Site-directed mutagenesis of all positively charged exosite 2 residues showed that Arg93 and Arg175 are the major residues involved in $CDSO_3$ binding. $FDSO_3$ showed a progressively greater defect in inhibition with double point mutations, the triple mutant Arg93,97,101Ala displayed a 50 fold drop in inhibition. A single mutant, Arg173Ala, displayed 22-fold reduction in IC_{50} of SBD, while Arg233Ala was the only mutation that impaired SBT inhibition. Salt-dependence studies showed that $CDSO_3$ had fewer ionic contacts with thrombin, with most of its binding energy derived from non-ionic interactions. $FDSO_3$ on the other hand had a balanced

contribution of ionic and non-ionic forces. Thermodynamic studies showed that both polymers have a positive ΔCp of binding, which proves the involvement of electrostatic forces and signals the burial of the polar residues on thrombin exosite 2. The presence of sodium was found to enhance the binding of $FDSO_3$ at exosite 2. The results identify novel binding sub-sites within exosite 2 that are energetically coupled to thrombin's catalytic function and linked to the sodium binding site. The design of high affinity small molecules based on LMWLs scaffold presents major opportunities for developing clinically relevant, allosteric modulators of thrombin.

Chapter 1: Introduction

1.1. Thrombin and the Coagulation Cascade

Thrombin is a key serine protease that maintains blood hemostasis by balancing, seemingly antithetical, pro- and anti-coagulant actions. Hemostasis is maintained through the sequential activity of a group of enzymes and cofactors that constitute the coagulation cascade. This is a physiologically critical process of consecutive reactions for preventing excessive loss of blood after sustaining injury, but aberrant clot formation can result in life threatening thrombotic disorders such as pulmonary embolism, deep-vein thrombosis, myocardial infarction and unstable angina. More than a half million patients are diagnosed annually in the US for which the treatment of choice is anticoagulants with a global market estimated to reach $12 billion by 2015.[1] Theoretically a drug could target one or more enzyme involved in the chain reaction in order to stop the clot formation, yet most of the developed agents are targeting thrombin and factor Xa (FXa).

The cascade is mainly formed of three stages, initiation, amplification and propagation (Figure 1). This delicate process starts when tissue factor, a protein found on subendothelial cells that are shielded from circulating proteinases is exposed by an injury. After exposure it forms a complex with circulating factor VIIa (FVIIa) to generate factor IXa (FIXa) and factor Xa (FXa) at low levels.[2,3] The latter forms a complex with factor Va (FVa), called the prothrombinase complex (FVa, FXa, Ca^{2+} and phospholipids), which in turn generates a small quantity of thrombin from its zymogen, prothrombin.

The second stage, called amplification, involves the small amount of the so produced thrombin acting as a procoagulant by activating factors XI, VIII and V. It also has a prothrombotic role as it reacts with protease-activated receptors (PARs) leading to platelet activation and aggregation at the site of injury and formation of a plug to prevent hemorrhage.[4] The activated factors initiate the last stage of the cascade, propagation, where factor VIIIa (FVIIIa) complexes with FIXa to form larger quantities of FXa which in turn is involved in formation of larger amounts of the prothrombinase complex that yields bulk quantities of thrombin. Activated platelets expose the fibrinogen receptor on their membrane, which attract and localize fibrinogen from the blood stream to the injury site. The produced thrombin acts as a procoagulant through its cleavage of fibrinogen to generate the fibrin monomers that self-aggregate to form a loose network, which is the initial clot.[5] This procoagulant role is substantiated by its activation of factor XIII (FXIII), which stabilizes the formed clot and thrombin-activatable fibrinolysis inhibitor (TAFI) that inhibits fibrinolysis.

On the other hand, thrombin has another, seemingly contradictory, role through activation of protein C, a natural anticoagulant that cleaves and inactivates factors Va and VIIIa.[6] Normally the affinity of thrombin for the zymogen protein C is low; it increases by a dramatic 1000-fold after binding to thrombomodulin, a receptor on the membrane of endothelial cells. The binding also decreases thrombin's ability to cleave fibrinogen and PAR-1.[7,8] The delicate balance of pro- and anticoagulant activities has established thrombin as the most attractive target for study as well as for developing anticoagulant agents.

Physiologically, the inhibition of excessive coagulation is achieved by regulatory proteins such as antithrombin (AT), a serine protease inhibitor (SERPIN), that mainly targets thrombin, FXa, and FIXa,[9] and to a less extent FVIIa and FXIa[10-12] using the well-established "*mousetrap*" mechanism.[13] The rate of AT inactivation is relatively slow under physiological conditions, but is greatly enhanced in presence of heparin, a glycosaminoglycan (GAG) polysaccharide that increases AT's efficiency by 10^2 – 10^6 fold depending on the targeted protease.[10] This forms the basis for the wide use of heparin as an anticoagulant since 1916.[14] Another natural inhibitor is tissue factor pathway inhibitor, which only targets FXa.[15]

Figure 1. The central role of thrombin in maintaining physiological haemostasis balance. Regulatory proteins are shown in red and inhibitory pathways are in red arrows

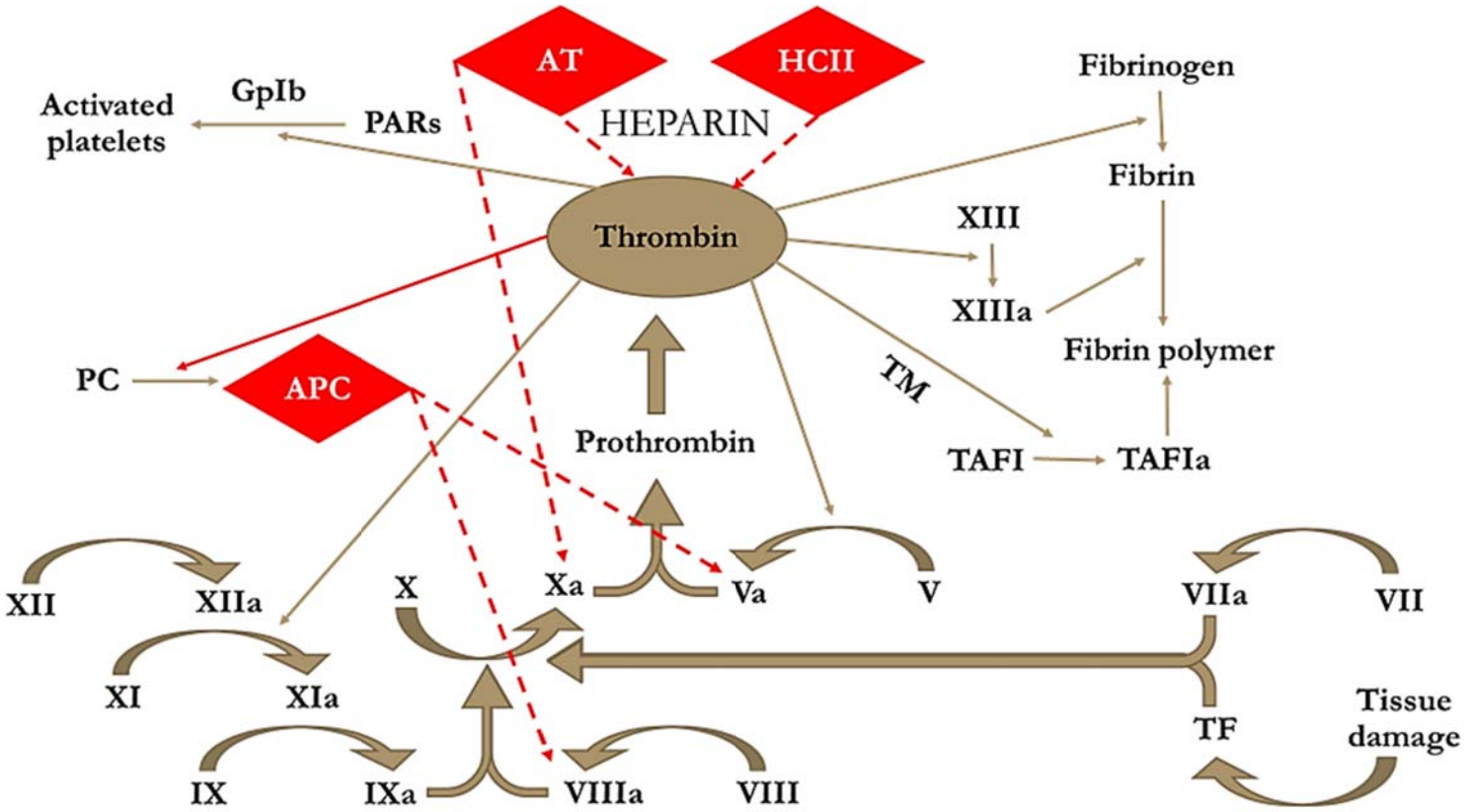

1.2. Anticoagulants in Market

Current treatment options for thrombotic disorders include either direct agents that act on one or more of the enzymes involved in the coagulation cascade or indirect agents that hamper these enzymes' formation or activate their natural inhibitors. The indirect class contains the widely used heparins and vitamin K antagonists (VKAs). Heparin and its variants, low-molecular-weight heparins (LMWH) and fondaparinux (a modified pentasaccharide) induce their effect by activating AT which irreversibly inhibits several coagulation enzymes (Figure 2A). VKAs inhibit necessary post translational modifications required for producing the fully functional proteases. VKAs are the only orally available anticoagulants and include warfarin, dicoumarol, acenocoumarol and phenprocoumon (Figure 2C).[1]

The direct class of inhibitors mainly target thrombin and are thus called direct thrombin inhibitors (DTI). This includes the hirudins and the peptidomimetic inhibitors like ximelagatran and melagatran. A newer direct inhibitor drug developed to target FXa, rivaroxaban, was approved in 2008 in the European Union and Canada, and in 2011 in US markets (Figure 3). These agents have the advantage of possibly inhibiting both free and clot bound enzymes[16-18] and have specificity toward certain targets, which improve its safety profile as well as the likelihood of developing antidote to reverse their effects. Each of the currently used anticoagulants suffer from major adverse consequences. The agents also share the problem of non-oral availability and the higher risk of minor and major bleeds. Anticoagulants as a group ranked first in 2003 and 2004 in number of total deaths from drugs in therapeutic use.[1] Beside this fatal side effect, each anticoagulant in the market suffer other serious complications

including hepatotoxicity, thrombocytopenia and immunogenicity. Discovering safer, orally available, specific and effective new molecules may dramatically alter the anticoagulation therapy of the future.

Figure 2. Indirect anticoagulants, (A) Heparins, (B) Fondaparinux, and (C) VKAs that include warfarin, dicoumarol, acenocoumarol and phenprocoumon

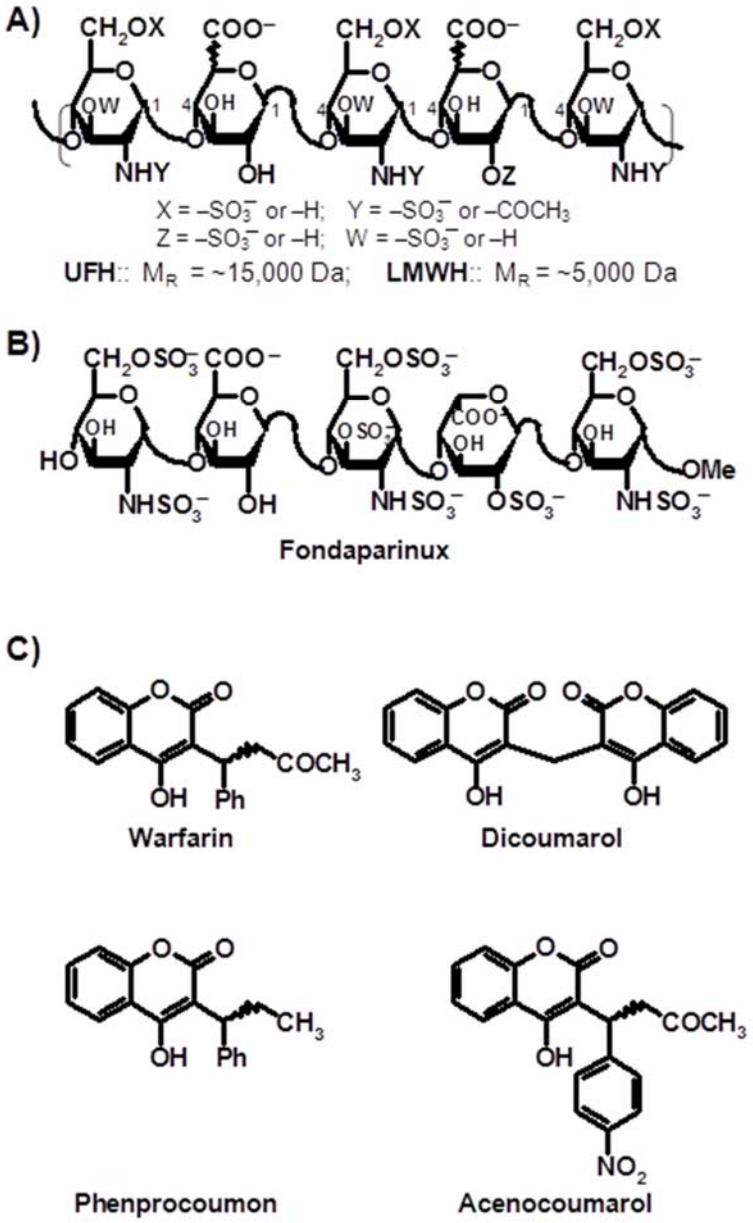

Figure 3. Direct thrombin inhibitors, the peptidomimetics ximelagatran and melagatran and the small molecule recently approved in the market to target FXa, rivaroxaban.

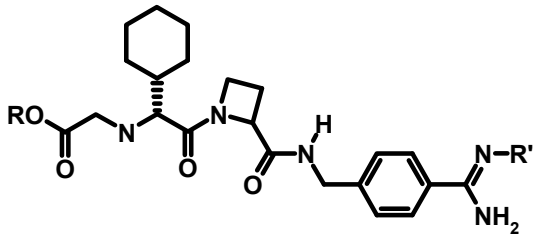

Ximelagatran R = -CH_2CH_3 R' = -OH
Melagatran R = -H; R' = -H

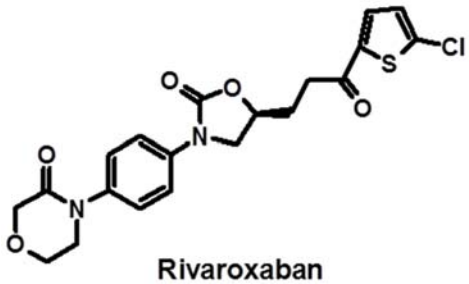

Rivaroxaban

1.3. Indirect Thrombin inhibitors and their Limitations

Unfractionated heparin (UFH) is a linear polydisperse polysaccharide of ~15,000 Da molecular weight with phenomenal structural variability (Figure 2). The backbone is assembled by alternating 1→4-linked uronic acid and glucosamine residues. Sulfate and carboxylate groups decorate the polysaccharide backbone with a high density of ~3.7 negative charge/disaccharide. This makes the molecule the strongest acid in human bodies.[1] The anticoagulant effect is an indirect one that arises through its interaction with antithrombin (AT), the primary physiological inhibitor of the coagulation cascade.

The mechanism of antithrombin activation by the heparin chains involves two pathways. In one mechanism a specific sequence on the heparin chain that has high affinity for antithrombin, a pentasaccharide called DEFGH (K_D = 50 nM)[1], binds and induces a conformational change in AT that activates the serpin against its targets.[19-21] This pathway is sufficient to induce full inhibition for FXa by accelerating the reaction by almost 300-fold in absence of calcium.[9,10,22,23] The structure of synthetic fondaparinux and idraparinux is based on this sequence. The other pathway involves the full-length heparin chains (at least 18 residues[24-26]) acting by bridging or template mechanism, which prevails in the case of antithrombin inhibition of thrombin.[27] The same high affinity sequence binds to antithrombin, followed by non-specific binding of the protease to another part of the long heparin chain. Thrombin then diffuses along the polymer to interact with the serpin forming a ternary complex with 1000-4000 fold accelerated rate (Figure 4). The length of the chain required for this mechanism renders many LMWHs and pentasaccharide anticoagulants ineffective in

accelerating AT-thrombin inhibition. In the presence of calcium, heparin inhibition of FXa and FIXa proceeds via a combination of the two pathways.

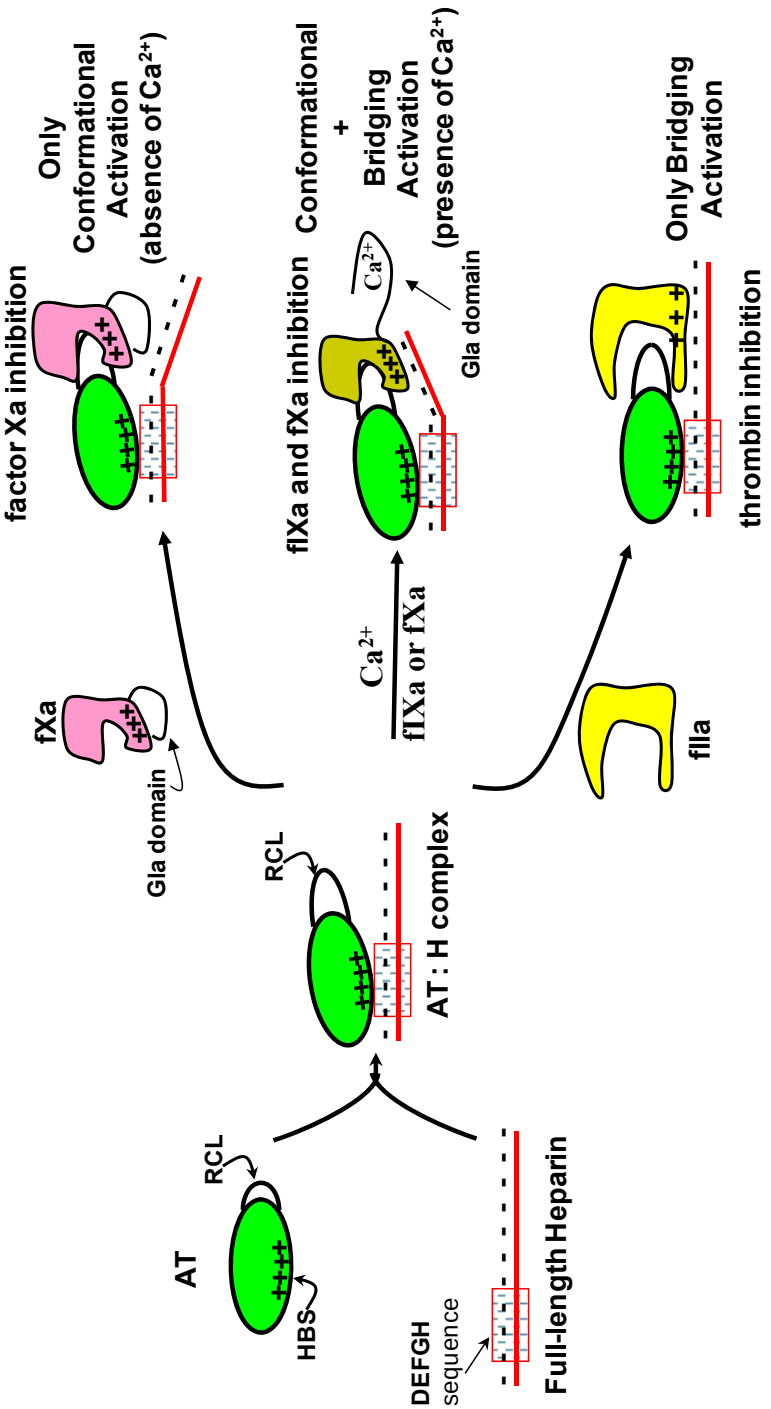

Figure 4. Heparin mechanism of inhibition for different factors via its complex with antithrombin

The risks of bleeds with heparin are the highest in its class, yet it has a suitable antidote: protamine sulfate, a linear polymer with positively charged nitrogen groups that neutralize heparin's negative charges. Beside this problem, heparin has the problem of intra- and inter-patient variability, which requires close monitoring and dose adjustment. This is mainly attributed to the low selectivity of heparin, which binds to many targets, some of which are proteins that become elevated variably in pathological conditions, which reduces its efficacy. Heparin induced thrombocytopenia (HIT) is another fatal adverse reaction of heparin, where the platelet count drops between 4 to 14 days after beginning treatment, and osteoporosis associated with chronic usage.[29] A serious allergic reaction was reported in 2007 following heparin administration that resulted in at least 81 reported deaths, the symptoms included hypotension, nausea, vomiting, diarrhea and abdominal pain. The samples were discovered to be contaminated with up to 30% of oversulfated chondroitin sulfate (OSCS).[1]

The problem is more complicated with regard to clot-bound thrombin. Heparin is incapable of binding to it and thus, this form of thrombin is resistant to inhibition by antithrombin rendering the patients susceptible to the restart of clotting.[14,16-18] The molecular dissection of the interaction revealed that the thrombin on the clot surface is bound to γ' chain of fibrin via its exosite 2, the same binding site as heparin. Thus, it competes with heparin chains for binding and hampers antithrombin inactivation.[30-32] The γ' fibrin(ogen) peptide is a useful tool, like heparin, as a natural ligand that binds to exosite 2 of thrombin.

Low molecular weight heparin (LMWH) is a smaller version (M_R 5,000 Da) with lower polyanionic charges created by chemical or enzymatic depolymerization of heparin.[22] It has the

advantage of higher bioavailability and longer duration of action (12 h)[1] along with lower occurrence of bleeding and less patient variability.[33,34] Unfortunately the efficacy of protamine as an antidote is only partial, unlike that of heparin. This could be due to the fact that it is more efficient in neutralizing long polymeric chains.[1]

Other smaller versions of heparin include the pentasaccharide fondaparinux, which is a highly specific sequence (DEFGH) in heparin that interact with antithrombin, lacks HIT and has predictable patient response.[35] On the other side of the coin, protamine sulfate is completely useless for reversal of fondaparinux toxicity, so in the event of a major hemorrhage there is no current antidote.[33,36] Another pentasaccharide developed is idraparinux, which has a long duration requiring only once a week injections. Owing to its structural similarity with fondaparinux, it is probably going to share its side effects.[37,38] Clinical trials using idraparinux were stopped due to the increased risk of bleeding.[39] A biotinylated version (SSR126517E) is being developed, since it could be neutralized by injecting avidin.[40]

1.4. Direct Thrombin Inhibitors and their Limitations

DTIs include agents that target the active site and/or exosite 1 of thrombin and work through either competitive or mixed-type inhibition mechanism to reduce the enzyme catalytic activity. This class includes hirudin and its analogues, which are extremely potent peptides derived from the leech *hirudo medicinalis.* These induce major bleeding episodes with no effective antidote.[41] Its peptidic nature causes the formation of antibodies that seem to delay its clearance, thus increasing its efficacy.[42] This heightened potency (20 fM for hirudin) renders the inhibition almost irreversible.

Two other analogues derived from hirudin are also available, lepirudin and desirudin, which lack the sulfate group at Y63 of hirudin and contain two residues at the N-terminus of hirudin substituted with Leu-Thr and Val-Val, respectively. A smaller version that belong to the same class of "hirulogs" is bivalirudin, which was developed with lower potency (1-2 nM) and shorter half-life. It has the advantage of lower immunological reactions and more predictable response. The only designed peptidomimetic to reach the market is argatroban, but its usage is limited by short life in plasma.[1] To address the oral bioavailability challenge another agent was developed, ximelagatran, which acts as a pro-drug for melagatran. It was approved in Europe, but the US FDA did not approve it because of hepatotoxicity reports.[43] It was withdrawn from European markets due to several cases of liver failure.[44] Another agent, dabigatran etexilate, was the only approved orally available DTI in US market (Figure 5).[1,45] It was soon joined in 2011 by rivaroxaban, which is a fXa direct inhibitor.

Figure 5. Some of the direct thrombin inhibitors available in the market. Figure is adapted directly from reference 1.

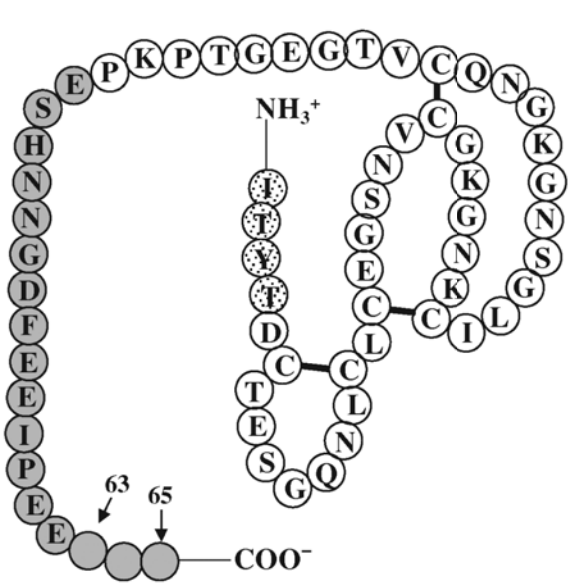

Residue	63	64	65
Hirudin	Tyr^{63}-OSO_3^-	Gln	Leu
Lepirudin	Tyr^{63}	Leu	Thr
Desirudin	Tyr^{63}	Val	Val

Bivalirudin

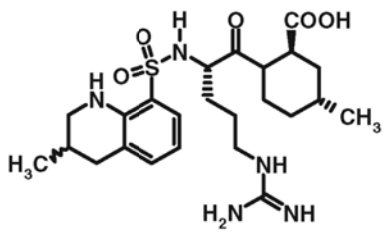

Argatroban

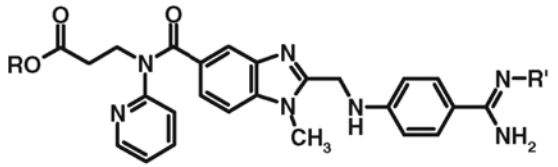

Dabigatran etexilate R = $-CH_2CH_3$ R′ = $-COO-nC_6H_{13}$
Dabigatran R = –H; R′ = –H

1.5. Exosite 2 Ligands and New Opportunities

Exclusive natural exosite 2 ligands, e.g., GAGs, do not affect the catalytic activity of thrombin, although its binding does affect the thrombin active site as monitored by active site inhibited labeled enzyme. Thus, GAGs do not function as DTIs.[46,47] Recently, low molecular weight lignins (LMWLs) were designed in our lab by chemo-enzymatic synthesis as heparin mimetics. In LMWLs a hydrophobic backbone is decorated by sulfate and carboxylate groups (Figure 6). Despite the fact that they structurally resemble heparin, which were able to directly inhibit thrombin in an antithrombin-independent manner, unlike heparin that requires the presence of the serpin for inhibition.[27] These molecules proved in initial studies to be the only macromolecules to reduce significantly the k_{CAT} of small chromogenic substrates by binding in or near exosite 2.[48,49]

Three polymers were synthesized $CDSO_3$, $FDSO_3$, and $SDSO_3$ from the corresponding 4-hydroxycinnamic acid monomers, caffeic acid (CA), ferulic acid (FA), or sinapic acid (SA). Two types of common linkages present in the sulfated molecules include the β-O-4 and β-5 linkages (Figure 7). The concept of the design was aiming to achieve binding at exosite 2 using the same recognition elements utilized by heparin, i.e., the arginine and lysine residues in exosite 2. Using those polymeric polydispersed structures as a guide, smaller molecules (dimers and trimers) were designed with similar scaffolds that were found to decrease the enzyme's activity by different degrees, the first in this class of DTIs (Figure 8).[50]

Figure 6. Design concept for designing a heparin mimetic with an aromatic scaffold, with **(A)** heparin representative example of disaccharide unit and **(B)** LMWLs dimeric unit.

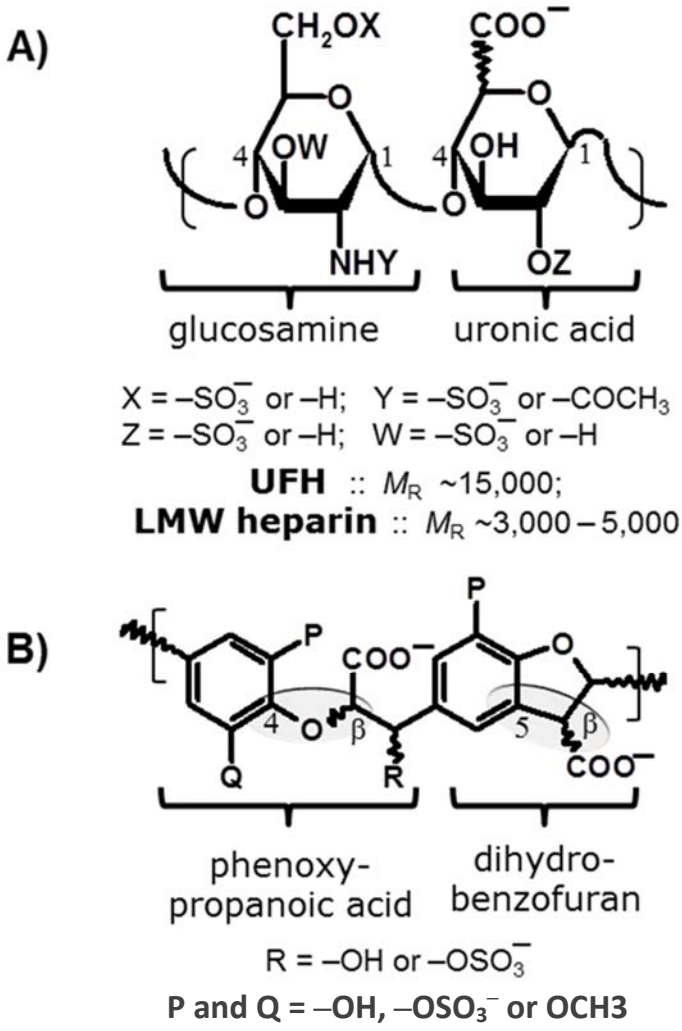

Figure 7. Chemo-enzymatic synthesis steps for the three LMWLs oligomers, $CDSO_3$, $FDSO_3$ and $SDSO_3$. Possible linkages are shown in shaded ovals.

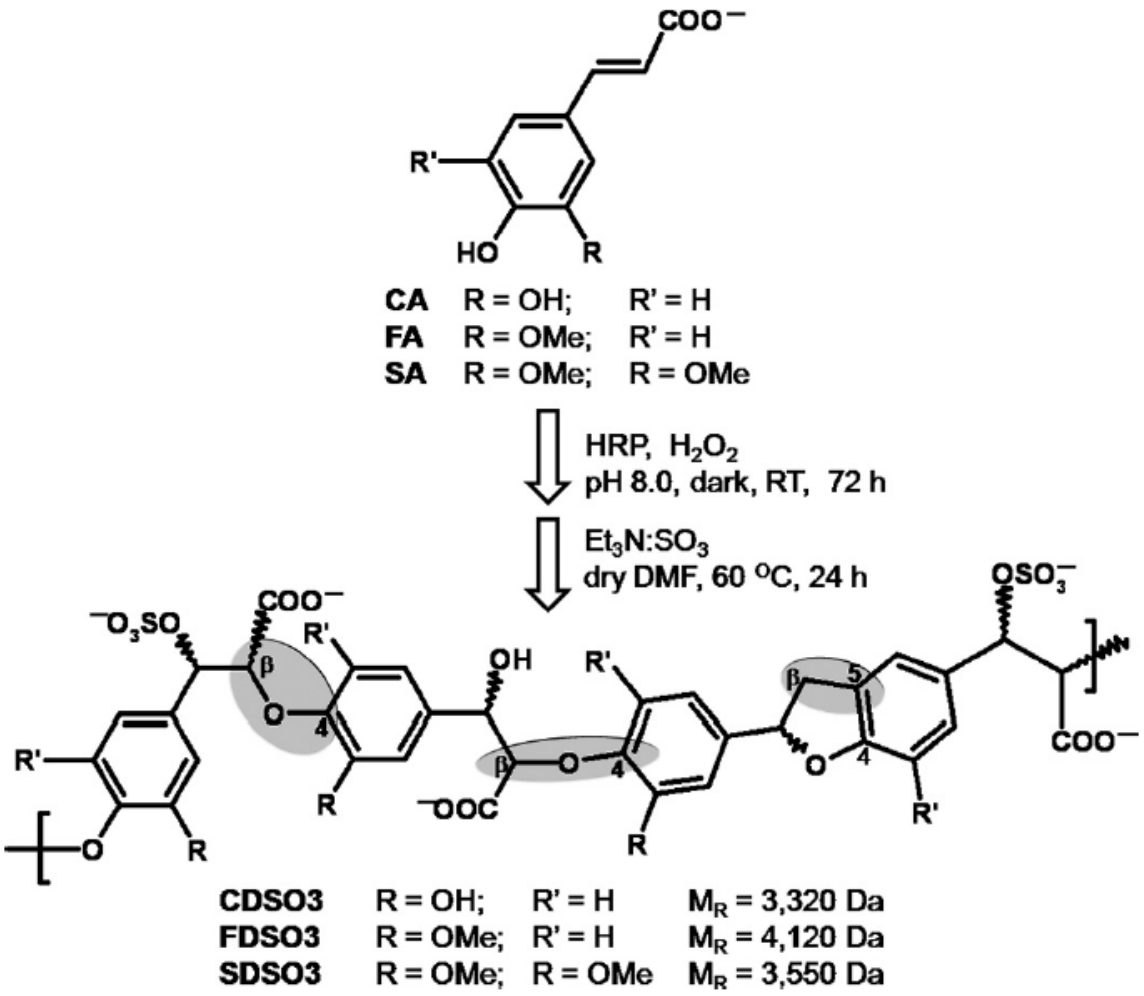

Figure 8. A monomeric unit of benzofuran showing the design concept behind small molecule allosteric inhibitors for thrombin derived from LMWLs scaffold.

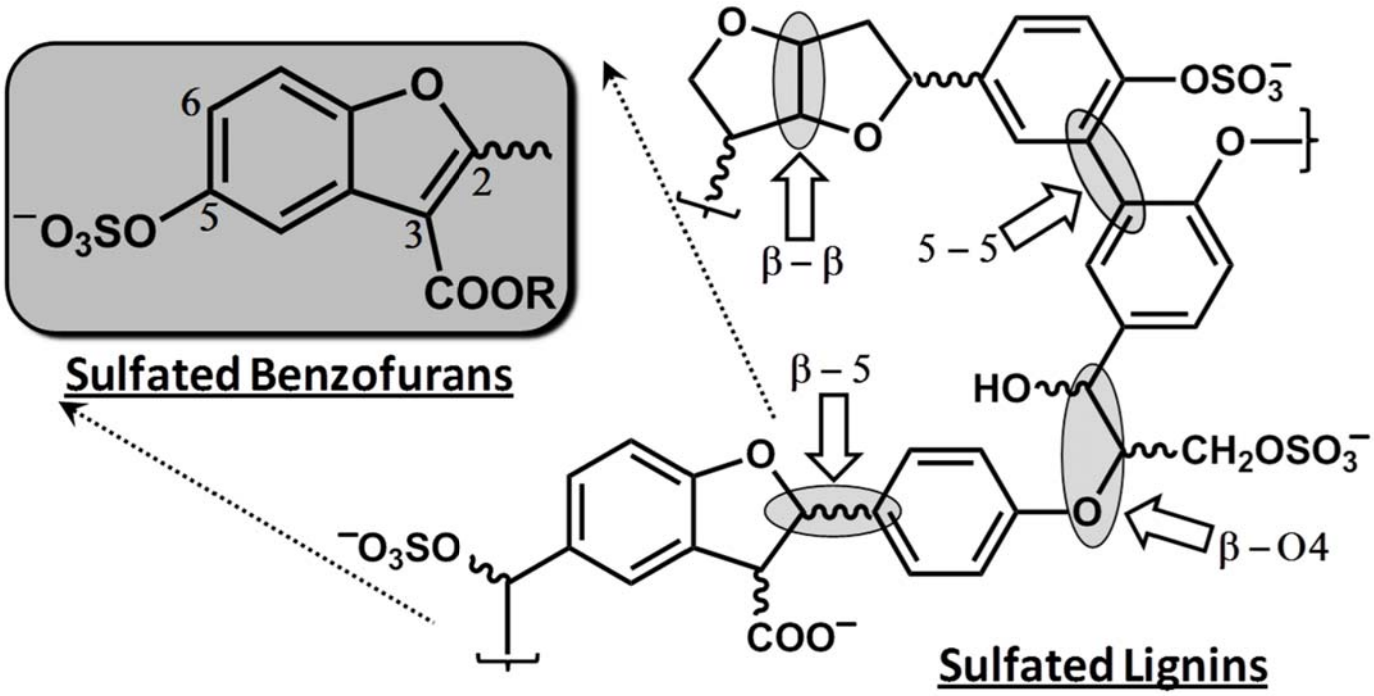

1.6. Thrombin Structure

Thrombin belongs to a wide class of enzymes activated by monovalent cations.[51,52] Several kinases and molecular chaperones require potassium for activation, while galactosidases and clotting proteases are activated by sodium.[53] In the case of thrombin, sodium is not required for catalysis, but its presence greatly enhances the enzyme catalytic activity, so it is considered an allosteric effector.[54-56] The first crystal structure solved for thrombin was in 1992[57] with now almost 300 structures available in the PDB.[58] Like all members of the chymotrypsin family, the enzyme has a characteristic fold, where two six-stranded β-barrels come together to form the catalytic triad H57, D102 and S195 at their boundary.[59] The active site pocket has surrounding ridges of neighboring secondary structures, especially the 60-and γ-loops, that determine the enzyme specificity for its substrates.[60-62] It has two polypeptide chains, the A chain with 36 residues and the B chain with 259 residues, linked by a disulfide bridge between C1 and C122.

In addition to its catalytic site, thrombin has three other separate domains, a sodium binding site and anion binding exosites 1 and 2 (Figure 9). Sodium is known to enhance thrombin's catalytic activity, while exosites 1 and 2 control its interactions with natural ligands that modulate specificity. Exosite 1 is characterized by the presence of basic residues as well as hydrophobic patches covering its surface that causes electrostatic steering and complementarity for natural ligands like PARs. On the opposite side of the enzyme lies exosite 2, formed by the C-terminal and its adjacent domain and has similar characteristic

electropositive exterior. This site is most famous for its interaction with polyanionic ligands like GAG chains of heparin.[53]

Figure 9. Surface representation of thrombin with electrostatic potentials. More red emphasizes more basic surfaces. Important domains are labeled for clarity; image created from PDB file 1XMN using Sybyl 7.2.

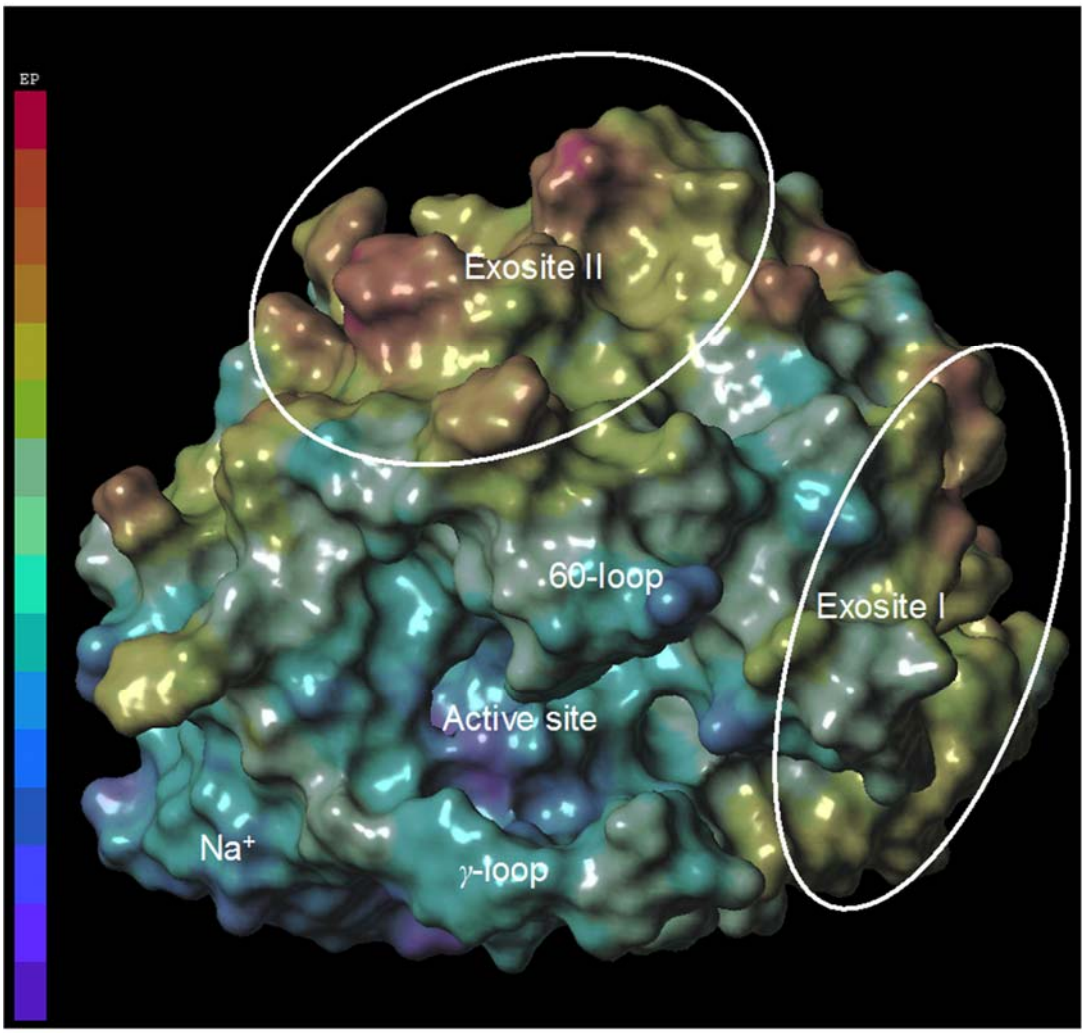

Some ligands interact simultaneously with two sites; hirudin, for example, engages the active site as well as exosite 1.[63] Several other natural ligands bind both exosites, such as fibrinogen, which mainly interacts with exosite 1, while the acidic part of its γ' chain binds with high affinity to exosite 2.[64] Thrombomodulin hydrophobic domain interacts with exosite 1, while its terminal chondroitin sulfate sequence binds to exosite 2.[65] Double binding with both exosites is also seen with some inhibitors like bothrojaracin.[66] Lately, the GpIb receptor was postulated to bind to thrombin in a model that involves each exosite involved with a different GpIb molecule, suggesting a more complex binding events where both exosites interplay.[67]

Lastly, the sodium binding site is a remote 16 – 20 Å away from the catalytic triad, yet a mere 5 Å from D189 of S1 site. The specificity of the enzyme for Na^+ is high, almost 10-fold higher than other monovalent cations like Li^+, K^+ or Rb^+.[68] Binding causes thrombin activation and enhances its procoagulant functions.

1.7. Thrombin Allosteric Network

Binding at sodium binding site or at either one of the exosites has different, sometimes contradictory, effects on the enzyme's active site. Allosteric signals after ligand binding are transmitted in the form of conformational changes at the active site that may or may not lead to changes in the enzyme specificity and/or catalytic efficiency in a ligand specific manner.[62,65] The traditional view of enzyme specificity is focused on the residues of the enzyme that constitute the active site. This was lately challenged in the case of thrombin and other coagulation factors in general. It is well recognized now that extended surfaces away from the

catalytic triad (i.e., exosites) play an important role in shaping the enzyme specificity as well as its efficiency.[69,70]

1.7.1. Sodium and Active Site

Thrombin catalytic efficiency is enhanced towards small chromogenic substrates as well as its natural macromolecular ligands after sodium binding. This led to the now well described designation of "fast" thrombin, when bound to sodium, which mainly acts on fibrinogen and PARs, while Na^+ free "slow" thrombin with better catalysis geared towards protein C activation.[60] The catalytic ability is not lost in the absence of sodium, so the monovalent cation is considered an allosteric effector rather than a cofactor.[71] To assess the effect of sodium binding on the structure of the whole enzyme, the intrinsic fluorescence of thrombin mutants, where the nine tryptophans of thrombin were mutated one at a time to phenylalanine, was monitored upon binding of sodium. All mutants experienced a change in the fast phase of fluorescence increase that correlates with the kinetics of Na^+ binding to thrombin. This indicated a global effect of sodium binding on the structure of the enzyme.[72]

The thermodynamics of sodium binding was studied by monitoring the value of K_A as a function of temperature. Binding of sodium is accompanied by a large enthalpy gain of -22 kcal/mol arising from the formation of the metal six coordination interactions with thrombin,[51,73] which is surprisingly compensated by a large entropy loss of -64 cal/mol.K. The entropy loss was explained by the ordering of water molecules inside a channel that links the sodium site with the specificity pocket and active site.[73,74] This water network was postulated to transmit the allosteric signal from the sodium binding site to the active site by extending H-

bonds from the sodium atom to the Oγ atom of S195 located 15 Å away in the active site and leading to generation of the so called "fast" thrombin form upon sodium binding (Figure 10).[73] The entropy change was accompanied by a large negative heat capacity change upon Na^+ binding.[68,75,76]

Figure 10. Difference between sodium bound thrombin (fast form in blue) and free thrombin (slow form in yellow) showing the main residues involved in sodium binding. Figure shows sodium as a yellow ball and illustrates the water network connecting sodium to the active site residues in fast (red balls) and slow (green balls) forms. The figure is adapted directly from reference 53.

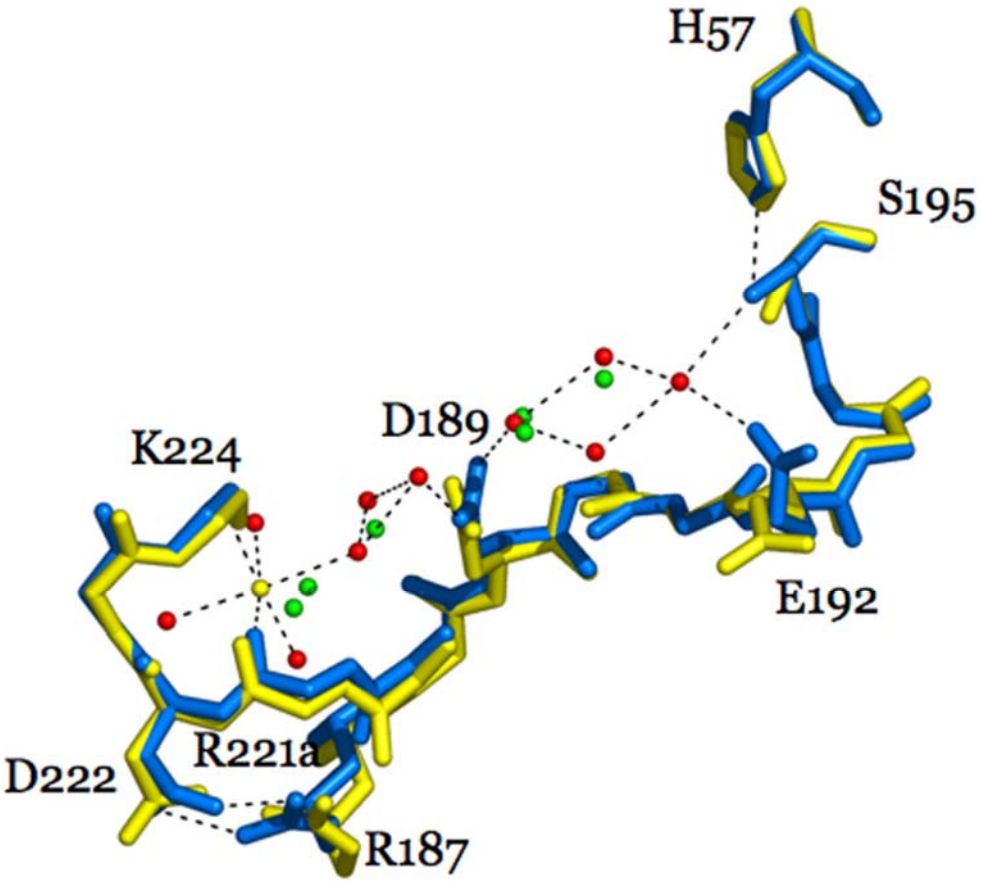

The measured affinity of sodium was 110 mM (pH 8, I = 800 mM at 37 °C).The physiological sodium concentration is 140 mM and the prevalent thinking was that sodium is thus 60% in the fast – sodium bound – form and 40% in the slow free form.[53] These figures have been lately challenged by measuring the affinity of sodium near physiological conditions, which provided a much higher affinity for thrombin (K_D = 5 mM), and would render the enzyme almost saturated with sodium in blood.[77]

1.7.2. Exosite 1 and Active Site

Binding of thrombomodulin to exosite 1 alters the specificity of thrombin from fibrinogen cleavage to activation of protein C, which acts as a switch to shift thrombin from a procoagulant to an anticoagulant enzyme. Hirudin binds through hydrophobic interactions to the active site while its C-terminal dodecapeptide (residues 54-65), called hirugen, binds to exosite 1 (Figure 11).[63] When hirugen alone binds, it causes alteration of thrombin catalytic efficiency (K_{CAT}/K_M) for small chromogenic substrates. Kinetic studies show that the catalytic efficiency increases or decreases by almost 2-fold according to the used substrate.[65,78] On the other hand binding of active site inhibitors leads to increasing affinity of exosite 1 ligands, which proves the thermodynamic linkage between the two sites.[79] Detailed studies were conducted on a self-inhibited thrombin mutant, where the entire 215-219 β-strand is collapsed leading to blocked access to the active site. Binding of a fragment of PAR-1 receptor to exosite 1 of thrombin led to a large conformational change that modified the strand and reestablished the access to the active site.[80] A recent study using NMR proved that binding of sodium or exosite 1 ligands individually stabilize thrombin, but the fully active conformation is only attained when binding occurs at both, or when the active site is occupied.[81]

Figure 11. Thrombin complex with the acidic C-terminal of hirudin (hirugen). Electrostatic potential of thrombin surface is presented where more blue indicates more basic surface. Hirugen is depicted in stick representation with carbon in yellow, oxygen in red and nitrogen in blue. Figure adapted from reference 60.

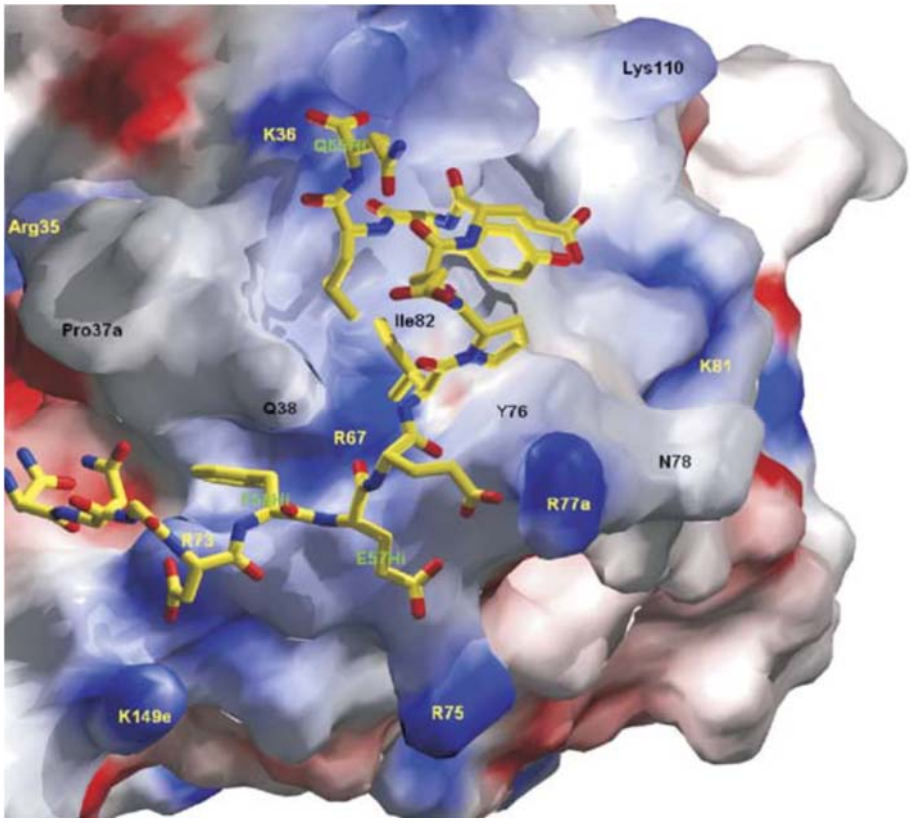

1.7.3. Exosite 2 and Active Site

Binding of heparin to exosite 2 of thrombin leads to its irreversible inactivation by antithrombin by the bridging mechanism. Testing with small chromogenic and fluorogenic peptide substrates proves that heparin does not have an effect on the catalytic efficiency of the enzyme.[46,47,82] Our lab recently reported the first molecules that binds to thrombin exosite 2 and directly causes thrombin inhibition. The molecules were designed based on heparin structure with the polysaccharide backbone replaced with an aromatic scaffold that bears the same combination of sulfate groups. Instead of inhibiting thrombin in the presence of AT using the bridging mechanism like heparin, these lignin based polymeric chains were able to inhibit thrombin independent of AT in an allosteric manner.[48,49] This added another layer to the complexity of thrombin allostery, proving for the first time an energetic link exists between exosite 2 and the active site that could be tweaked to inhibit the enzyme if triggered by the suitable effector. These polymers were used as a template upon which smaller molecules were designed that were found to impart the same action of inhibiting the enzyme catalytic activity.[50]

1.7.4. Exosite 1 and 2

There are a large number of studies, often contradictory, debating the interconnection between thrombin exosites. Some studies report contrasting fluorescence signals of fluorescein-FPR-thrombin when hirudin binds to exosite 1 and the prothrombin F2 fragment binds to exosite 2. These results showed that binding at the two exosites is mutually exclusive as binding of one ligand led to displacement of the other.[83] A study corroborated those early findings, showing that binding different exosite 2 ligands altered γ_A/γ_A fibrinogen peptide or

fibrinogen binding and prolonged clotting time. The study also included direct binding studies by surface plasmon resonance (SPR) in which ligands bound at one exosite decrease or abolish binding at the second.[84] Controversially, another study reports the same peptides bind simultaneously without changing each other's K_D, implying that a ternary complex can be formed with both exosites occupied.[85]

Thrombin is an attractive target in the coagulation cascade. The market has a myriad of anticoagulants that target this key serine protease, yet none of those agents is ideal. The complex structure of thrombin and the intricate allosteric network that regulates its functions is striking. It offers the possibility to design agents that act with new mechanisms to achieve the required inhibition and at the same time avoid the side effects of conventional therapy. The recently designed LMWLs offer a rare chance of modulating thrombin catalytic machinery via an allosteric mechanism that utilizes a direct energetic link between exosite 2 and thrombin active site. This link was not known to exist before, with literature mainly highlighting linkages that connect the active site, sodium binding site and exosite 1. This is mainly due to the fact that few molecules beside GAGs bind to exosite 2, and none leads to inhibition of thrombin. Rational design of smaller molecules based on the polymeric structures led to identification of a new series of compounds that act in the same allosteric manner to inhibit thrombin. Further studies were needed to identify the exact site of binding of these molecules and to dissect the nature of their interaction. These studies would be extremely useful in understanding this new model of inhibition and further design better agents acting by the same mechanism.

Chapter 2: Rationale

2.1. Background

Coagulation enzymes are trypsin-like serine proteases with very similar structures. Designing a specific inhibitor is difficult, especially due to the high conservation of their active site architecture. Yet, specificity can be engineered using the subtle differences between them. An interesting aspect is that nature tends to be less meticulous in conserving allosteric sites in comparison to active sites, which offers a better chance of selectivity. With the high risk of bleeding associated with current therapies, allosteric modulators offer the chance of controlling the enzyme catalytic efficiency better than through total blockage with competitive inhibitors. Keeping a part of the enzyme physiological activity can be the key to preventing some of the current drugs side effects. Another advantage is the possibility of preventing toxicity by administering a silent allosteric molecule that competes with the allosteric inhibitor for the same binding site so as to act as antidote, if needed. As most of the marketed drugs are injectable, there is a need for designing novel inhibitors bearing scaffolds with drug-like properties, improved pharmacokinetics and water solubility that confers oral bioavailability. Of all the molecules available in the market, rivaroxaban seems to be the closest to what is considered an ideal anticoagulant.[1]

2.2. Heparins

Typically, it is difficult to rationally target an allosteric site of an enzyme, which implies that the discovery of allosteric inhibitors is mainly based on serendipity. Our lab has been developing heparin mimetics as thrombin inhibitors. Heparin is a polydisperse, highly sulfated

heterogeneous polymer that binds to exosite 2 of thrombin, which is an electropositive domain. This domain includes basic residues that bind to heparin's sulfate groups, mainly Arg93, Arg101, Arg233, Lys236, and Lys240 (Figure 12).[86]

Figure 12. Surface representation of thrombin exosite 2 with electrostatic potential, where the more basic the residue is, the bluer it is colored. Heparin derived hexasaccharide is co-crystallized and shown in stick representation (carbon in white, oxygen in red and sulfur in yellow). Sulfate groups are shown interacting with labeled key arginines and lysines. Figure directly adapted from reference 86.

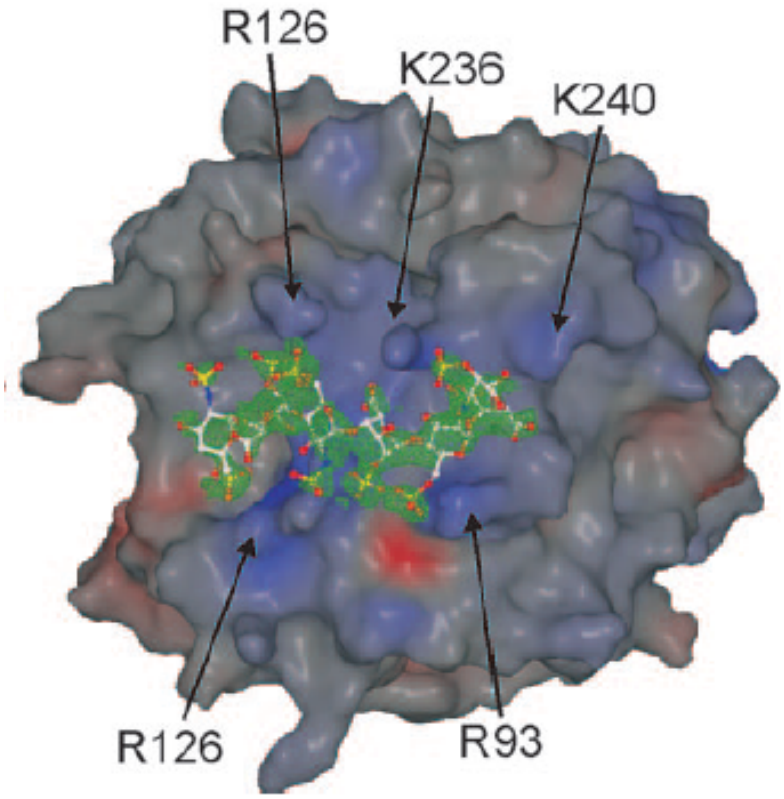

In vitro, heparin binds to thrombin with a wide range of affinity, depending on the molecular weight of heparin chain used, the salt concentration of the experimental buffer, pH and the nature of thrombin used (free or inhibited). The interaction is electrostatic, which renders it highly sensitive to salt concentration. Using active thrombin, lower molecular weight heparin chains (M_r 7,900) bound with K_D 6 – 10 μM, while longer chains (M_r 17,300) bound with K_D 2 μM, at physiological conditions of 150 mM NaCl.[28] Another experiment reproduced a similar value of 1 μM affinity for high molecular weight heparin (M_r 11,000), yet reported a huge increase in affinity (K_D 5.8 nM) when NaCl was removed from the buffer.[87] Similar figures were previously obtained in a third study conducted without NaCl that showed a K_D of 1.7 nM.[88] The affinity of active site inhibited thrombin showed a different discrepancy, where in 100 mM NaCl the K_D was measured to be 35 nM.[89] This highlights the importance of the ionic strength of the buffer.

Heparin and LMWH serve merely as molecular bridges that brings thrombin closer to its natural serpin inhibitor, antithrombin, accelerating the inhibition by almost 1,000 – 4,000 fold.[22] Many heparin mimetics have been designed, but their anticoagulant mechanism is similar to heparin, thus carrying heparin's side effects.[1] Based on heparin structure, our lab advanced low molecular weight lignins (LMWLs) as heparin mimetics. The design was based on the idea of replacing the polysaccharide backbone in heparin with a less problematic, more drug-like aromatic scaffold decorated by sulfate and carboxylate groups that would interact with the basic residues of exosite 2 on thrombin surface.

2.3. Exosite 2 Allosteric Inhibitors

Three polymeric molecules were synthesized: $CDSO_3$, $FDSO_3$ and $SDSO_3$ from the corresponding 4-hydroxycinnamic acid monomers, caffeic acid, ferulic acid or sinapic acid.[49] Initial investigation showed that unlike heparin, which requires antithrombin for inhibition, the sulfated lignins were able to ***directly*** inhibit thrombin. Further work with $CDSO_3$ confirmed that it inhibits thrombin allosterically through exosite 2.[48] To develop smaller molecules based on the sulfated lignin scaffold, our laboratory designed a series of sulfated benzofuran dimers and trimers that also showed good thrombin inhibition capability.[50] To better understand how LMWLs and the sulfated benzofurans interacted with thrombin at the molecular level, two of the sulfated lignins ($CDSO_3$ and $FDSO_3$) (Figure 7) and two sulfated benzofurans, a dimer (SBD) and a trimer (SBT) were selected for further studies (Figure 13).

Figure 13. Structure of the benzofuran compounds selected for further studies, a dimeric compound SBD and trimeric one SBT.

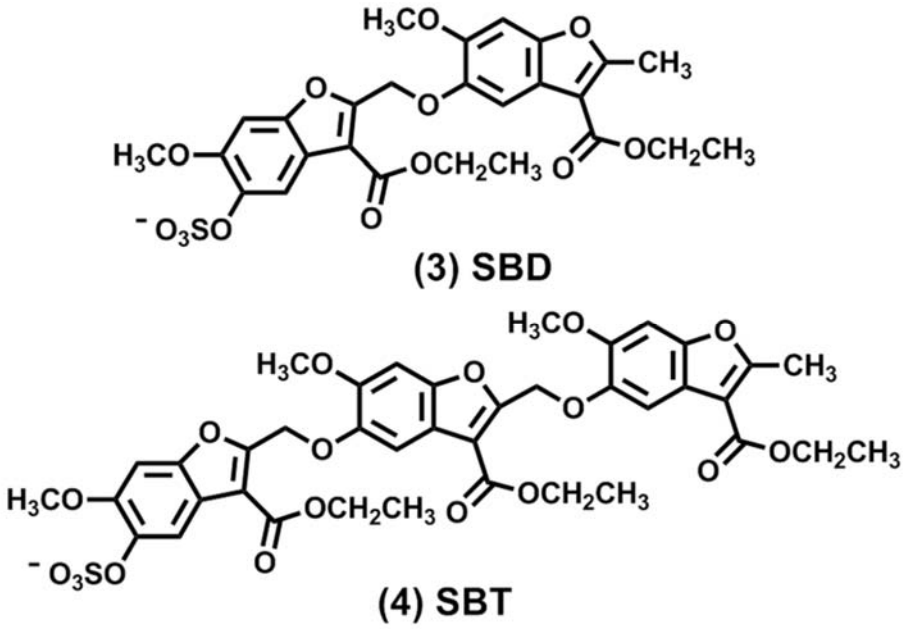

There are many questions that need further exploration with these mechanistically novel molecules. Do they all bind at the same binding site? If they all bind at exosite 2, do they have the same orientation or binding mode? What are the types of forces involved in their interactions? The two polymers studied, $CDSO_3$ and $FDSO_3$, have similar polydispersity in scaffold, linkage and sulfation pattern. Physicochemical studies indicated that $FDSO_3$ is more negatively charged, which allows it to form more ionic interactions with the thrombin surface.[90] The most notable difference was in the side chains. $CDSO_3$ had a larger number of hydroxyl groups since the synthesis starts with the more polar caffeic acid compared to the more hydrophobic methoxy group in ferulic acid, which is the building unit of $FDSO_3$. This promoted the idea that $CDSO_3$ will probably have a better chance of hydrogen-bonding with exosite 2 polar residues. Binding of both polymers was expected to follow the polyelectrolyte theory of binding like heparin, where interaction is highly dependent on the salt concentration of the medium.

The small molecules were, on the other hand, an uncharted area; their design was based on the polymeric chains, but will they actually act as allosteric modulators? Will they bind to exosite 2 as well? These were the first synthetic small molecules that were designed to inhibit thrombin via an allosteric mechanism. The first step was to check if they bind in exosite 2 using a competitive enzyme inhibition assay. As the molecules contained one sulfate group each, they were expected to interact with one of the basic lysines or arginines in exosite 2. It was hard to predict whether extending the chain from two to three units would affect the binding and the mode of inhibition.

As the first thrombin inhibitors to bind at exosite 2, LMWLs offer an attractive chance to further investigate the allostery of thrombin. Is there a direct energetic link between exosite 2, where the molecules bind, and the active site? There are no studies in the literature that discuss this link, simply because, other than these molecules, there are no reported molecules that inhibit thrombin through this exosite. As it is also known that sodium changes the conformation of the enzyme from the slow to the fast form, do the polymers decrease sodium affinity to the enzyme and thereby inactivate thrombin or is it a direct linkage between exosite 2 and the active site? It was also interesting to see if the conformational change to the fast form is correlated with the binding affinity of the polymers, which would clarify the linkage between exosite 2 and sodium binding site.

These studies will shed new light on the complex allosteric network of thrombin and the modulation of its catalytic functions as well as aid in further development of new molecules that act by the same new mechanism. In the following chapters I will present the detailed work done to analyze the site of binding of these novel molecules and identify the key residues involved in their interaction. A detailed study of the salt dependence of $CDSO_3$ and $FDSO_3$ binding as well as their thermodynamics will be discussed.

Chapter 3: Identification of the Binding Site and Key Residues Required for Interaction of LMWLs on Thrombin

3.1. INTRODUCTION

Allosteric regulation of coagulation enzymes, especially factors IIa, Xa, IXa, and XIa, is a fundamental property exploited by nature.[1,91] The primary allosteric regulator of these coagulation enzymes is heparin, an animal-derived, phenomenally complex, linear polysaccharide. Polymeric heparin binds to those factors in a site remote from the active site of the enzymes and enhances their inhibition by AT.[10] Although heparins have been used as anticoagulants for the past eight decades, they are beset with a number of adverse reactions including enhanced bleeding risk, immunological reaction, poor oral bioavailability, patient-to-patient response variability, narrow therapeutic index, possibility of contamination and others.[1,92,93] Yet, few macromolecular mimetics of heparin have been developed so far because of their massive structural complexity, difficulty of synthesis and lack of effective macromolecule design tools.

To address some of these issues, we recently designed synthetic macromolecules, called sulfated LMWLs, as inhibitors of coagulation.[48,49,94] Chemo-enzymatically synthesized sulfated LMWLs are sulfated oligomers of varying lengths and substitution patterns that attempt to mimic the structural diversity of heparins.[49] However, they are completely unlike LMWH with respect to the nature of their backbone. In contrast to the highly anionic, carbohydrate scaffold of the heparins, sulfated LMWLs possess an aromatic scaffold decorated with fewer sulfate and carboxylate groups. The combination of a hydrophobic scaffold with

anionic groups generates physicochemical properties that induce novel protein recognition characteristics.[90] In this respect, sulfated LMWLs are proving to be unlike any other class of anticoagulants investigated to-date, including the heparins, the coumarins, the hirudins, the peptidomimetics and the small molecule direct inhibitors.[1,95]

Functionally, the three designed sulfated LMWLs – $CDSO_3$, $FDSO_3$ and $SDSO_3$– display a plasma and blood anticoagulation profile similar to that of LMWH.[94] The focus of this work will be mainly on two of these polymers that are structurally related, $CDSO_3$ and $FDSO_3$. Physicochemical studies indicated that $FDSO_3$ is more negatively charged, which allows it to form more ionic interactions with thrombin surface.[90] The most obvious difference is in the side chains: $CDSO_3$ has larger number of hydroxyl groups since the synthesis starts with the more polar caffeic acid compared to the more hydrophobic methoxy group in ferulic acid, which is the building unit of $FDSO_3$ (Figure 14). Enzyme inhibition studies showed that these molecules potently inhibit thrombin, factor Xa and plasmin in an antithrombin–independent manner.[49,96] Mechanistic inhibition studies have shown that $CDSO_3$ utilizes exosite 2 of thrombin to induce inhibition.[48] This novel mechanism distinguishes those inhibitors from the heparins, which do not directly inhibit any coagulation enzyme. In fact, sulfated LMWLs appear to be the only molecules that allosterically induce inhibition of thrombin through an exclusive exosite 2 interaction.

To elucidate the site of binding of sulfated LMWLs, we focused on $FDSO_3$, a prototype molecule. We utilized Michaelis-Menten kinetics and competitive enzyme inhibition assays to identify its binding site. In these experiments a competitor known to bind to either exosite 1 or

2 of thrombin is added to the medium and the inhibition by $FDSO_3$ was monitored. If the competitor binds to the same site as the studied molecule, increasing the competitor concentration would lead to a progressive decrease in $FDSO_3$ inhibition. Three competitors were used, hirugen peptide analogue [5F]-Hir[54-65](SO_3^-) (HirP) for exosite 1 and unfractionated heparin (UFH) as well as an octasaccharide fragment derived from heparin (H8) for exosite 2. We also studied the inhibition properties of $CDSO_3$ and $FDSO_3$ against a panel of single, double and triple site-directed thrombin mutants, where all basic residues in exosite 2 are mutated to Ala to abolish its charge. Sulfate and carboxylate groups of $CDSO_3$ and $FDSO_3$ utilize the lysine and arginine basic amino acids lining thrombin exosite 2. We hypothesized that by modifying one or more of those residues to alanine, the key residues vital to binding can be identified.

3.2. EXPERIMENTAL

3.2.1. Proteins, LMWLs, Chemicals and Reagents.

Sulfated dehydropolymers $CDSO_3$ and $FDSO_3$ (Figure 14) were synthesized in two steps from 4-hydroxycinnamic acid monomers, caffeic acid and ferulic acid, using chemo-enzymatic synthesis.[49] Human α-thrombin was purchased from Haematologic Technologies (Essex Junction, VT). Chromogenic substrates Spectrozyme TH (H-*D*-hexahydrotyrosol-Ala-Arg-*p*-nitroanilide) and S2238 (H-*D*-Phe-Pip-Arg–*p*-nitroanilide) were purchased from American Diagnostica (Greenwich, CT) and ANASPEC (Fremont, CA), respectively. Unfractionated porcine heparin was purchased from Sigma (St. Louis, MO). Heparin octasaccharide H8 was purchased from V-Labs (Covington, LA). Hirugen analog, Tyr^{63}-

sulfated hirudin$^{54-65}$ labeled with 5-(carboxy) fluorescein ([5F]-Hir[54-65](SO_3^-)) (HirP), was a gift from the Bock laboratories and its preparation was described earlier.[97] All other chemicals were analytical reagent grade from either Sigma Chemicals (St. Louis, MO) or Fisher (Pittsburgh, PA) and used as such.

3.2.2. Recombinant Thrombin Mutants

Recombinant wild-type and mutant thrombins were prepared in the Rezaie laboratory at St. Louis University School of Medicine, as described earlier.[98,99] Briefly, Arg93Ala, Arg97Ala, Arg101Ala, Arg126Ala, Arg165Ala, Lys169Ala, Arg173Ala, Arg175Ala, Arg233Ala, Lys235Ala, Lys236Ala, Lys240Ala, Arg93,97Ala, Arg93,101Ala, Arg97,101Ala or Arg93,97,101Ala thrombin were prepared in prothrombin-1 form by PCR mutagenesis and expression in baby hamster kidney cells (BHK) using the pNUT-PL2 expression/purification vector system. The mutants were purified to homogeneity by immunoaffinity chromatography using the Ca^{2+}-dependent monoclonal antibody, HPC4, and activated to thrombin. The active-site concentrations of thrombin mutants were determined by an amidolytic activity assay and stoichiometric titrations with antithrombin.[98,99] These concentrations were within 90–100% of those expected on the basis of their absorbance at 280 nm. Stock solutions of these mutants were prepared in 20 mM sodium phosphate buffer, pH 7.4, containing 100 mM NaCl and 2.5 mM $CaCl_2$.

3.2.3. Michaelis-Menten Kinetics of Substrate Hydrolysis by Thrombin in the Presence of $FDSO_3$.

Several concentrations of Spectrozyme TH (0.5–80 μM) were hydrolyzed by 2 nM wild-type thrombin in presence of fixed concentration of $FDSO_3$ (0.48–2.38 μM). The initial rate of substrate hydrolysis was monitored from the linear increase in A_{405} in 20 mM Tris-HCl buffer, pH 7.4, containing 100 mM NaCl, 2.5 mM $CaCl_2$ and 0.1 % PEG 8000 in PEG 20,000-coated acrylic cuvettes at 25 °C. The data obtained was fitted by the standard Michaelis-Menten equation to calculate the apparent K_M and V_{MAX}.

3.2.4. Competitive Binding Studies with a Hirugen analog HirP, H8 or Porcine Unfractionated Heparin (UFH).

The inhibition effect of $FDSO_3$ on wild-type thrombin was studied in the presence of either HirP, H8 or UFH in a manner similar to that described above for direct thrombin inhibition. Briefly, a solution of $FDSO_3$ (0.24 – 24 μM) and thrombin (4 nM) was mixed at 25 °C with either HirP (0 – 103 nM), H8 (0 – 25 μM) or UFH (0 – 25 μM) in 20 mM Tris-HCl buffer, pH 7.4, containing 100 mM NaCl, 2.5 mM $CaCl_2$ and 0.1 % PEG 8000 in PEG 20,000-coated acrylic cuvettes. Following mixing, hydrolysis of Spectrozyme TH (20 μM) was monitored at 405 nm. The dose-dependence of the fractional residual thrombin activity at each concentration of the competitor was fitted using equation 1 to obtain the apparent concentration of $FDSO_3$ required to inhibit thrombin activity by 50% ($IC_{50,app}$).

$$Y = Y_O + \frac{Y_M - Y_O}{1+10^{(\log[LMWL]_0 - logIC_{50})\times HS}} \qquad \textbf{(equation 1)}$$

In this equation, Y_M and Y_O are the maximum and minimum values of the fractional residual thrombin activity; HS is Hill slope and IC_{50} is the concentration of the inhibitor that results in 50% inhibition of enzyme activity. Sigmaplot 8.0 (SPSS, Inc., Chicago, IL) was used to perform nonlinear curve fitting in which Y_M, Y_O, HS and IC_{50} were allowed to float.

3.2.5. Quantitative Measurement of Wild-type and Mutant Thrombin Inhibition Potential of $CDSO_3$ and $FDSO_3$.

The two polymers inhibition of recombinant wild-type and mutant thrombins was studied in a manner identical to that described earlier for human plasma thrombin. The buffer used for these experiments was 20 mM Tris–HCl buffer, pH 7.4, containing 100 mM NaCl, 2.5 mM $CaCl_2$ and 0.1% PEG 8000 in PEG 20,000-coated acrylic cuvettes. Either Spectrozyme TH or S2238 was used as substrate and the residual thrombin activity was quantified by measuring the initial rate of hydrolysis from the linear increase in absorbance at 405 nm as a function of time under conditions where less than 10% substrate is consumed. Briefly, a solution of 10 µl $CDSO_3$ or $FDSO_3$ at concentrations ranging from 0.1 to 8.6 mM was diluted with 963 µl of buffer and 7 µl of 0.23–1.07 µM thrombin and mixed well. This was followed by addition of 20 µl of either S2238 (0.8 mM) or Spectrozyme Th (2 mM) and the initial rate was rapidly measured. Logistic equation 1 was used to fit the dose dependence of residual thrombin activity to obtain Y_M, Y_O, HS and IC_{50} of inhibition.

3.3. RESULTS

3.3.1. Allosteric Inhibition of Thrombin is a Common Property of Sulfated LMWLs.

Earlier work with $CDSO_3$ inhibition of thrombin has shown that the direct inhibitor reduces the forward rate constant of hydrolysis of a peptide substrate, i.e., Spectrozyme TH, without affecting its Michaelis constant.[48] Structurally, $FDSO_3$ and $CDSO_3$ are oligomers of either 3-methoxy or 3-hydroxy analogs of 4-hydroxy cinnamic acid, respectively (Figure 14). They may be expected to have identical complex structures, however, oligomerization is known to proceed with some selectivity, which induces subtle compositional differences.[100] We reasoned that for identifying the site of binding on thrombin, a prototypic sulfated LMWL is needed.

Earlier we have shown that $CDSO_3$ does not bind in the active site or exosite 1 of thrombin.[48] To assess whether $FDSO_3$ exhibits a similar phenomenon, we studied the Michaelis-Menten kinetics of Spectrozyme TH hydrolysis by wild-type thrombin at pH 7.4 and 25 °C in the presence of $FDSO_3$. Michaelis-Menten constants were derived by non-linear regression analysis of the initial rate *versus* Spectrozyme TH concentration profiles (Figure 15). Table 1 lists the calculated apparent V_{MAX} and K_M values. As the concentration of $FDSO_3$ increased, the K_M was found to essentially remain constant, while the V_{MAX} decreased nearly 2.8-fold. This indicates that the presence of $FDSO_3$ does not affect the affinity of binding of Spectrozyme TH in the active site of thrombin, but induces some changes that significantly reduce the rate of conversion of the Michaelis complex into products. This implies a non-

competitive type of inhibition induced by $FDSO_3$. Thus, the results support the conclusion that allosteric inhibition of thrombin is a common property of sulfated LMWLs.

3.3.2. $FDSO_3$ Does Not Bind in Exosite 1 of Thrombin.

To test whether $FDSO_3$ binds in the exosite 1, we measured the effect of a hirugen analog, [5F]-Hir[54-65](SO_3^-) (HirP), on the IC_{50} of $FDSO_3$ inhibition of thrombin. HirP binds exclusively in exosite 1 of thrombin with an affinity of 4 nM.[85,97] Thus, the apparent IC_{50} of $FDSO_3$ inhibition of thrombin in the presence of HirP was measured in a dose-response assay as described earlier. The presence of HirP did not significantly affect the thrombin inhibition profiles as shown in figure 16. Fitting the dose-response equation 1 to the data indicated that the apparent IC_{50} remained essentially invariant as the HirP concentration increased from 8.8 nM to 103 nM (Table 2). A quantitative comparison of the observed versus the predicted K_D (IC_{50} in our case) assuming ideal competition can be obtained by applying the Dixon-Webb calculation:

$$K_{D,predicted.} = K_D \times \left(1 + \frac{[Competitor]_o}{K_{Competitor}}\right) \quad \textbf{(equation 2)}$$

$K_{competitor}$ refers to the equilibrium dissociation constant of the competitor (HirP) – thrombin complex, which was measured independently under otherwise identical conditions. A visual representation helps to clarify how the IC_{50} is almost unchanging compared to the predicted values obtained from the Dixon–Webb calculation with increasing competitor concentration if the competition was ideal (Figure 17). Likewise, the maximal inhibition induced by $FDSO_3$ in the presence of HirP, i.e., $\Delta Y = Y_M - Y_0$, also did not alter significantly (~60%, see Table 2) with the concentration of the competitor. This suggests that the exosite 1

ligand induces no change in the efficacy of $FDSO_3$ inhibition of thrombin, just as it induces no change in the potency of inhibition. Thus, in a manner similar to $CDSO_3$, $FDSO_3$ also does not appear to bind in the anion-binding exosite 1 of thrombin.

3.3.3. Competition with UFH is a Common Property of Sulfated LMWLs.

Previous studies have indicated that $CDSO_3$ does not interact with the hirudin-binding site (exosite 1) of thrombin, but binds in or near the heparin-binding site, referred to as exosite 2.[48] A wide range of affinities have been reported in literature for polymeric heparin binding to coagulation enzymes. This is primarily because of the heterogeneity present in the heparin preparations. For example, the affinity of FXa, FIIa and FIXa for heparin has been measured in the range of 0.006–10 μM using several reaction conditions,[27,28,86-89,101,102] while that of FXIa has been found to be ~10 nM.[12,103] To probe if $FDSO_3$ displays similar characteristics to $CDSO_3$, the apparent IC_{50} was measured in the presence of porcine unfractionated heparin. Figure 18A shows the dose-response profiles of $FDSO_3$ inhibition of thrombin in the presence of 4.2 to 25 μM porcine heparin. A distinct shift in the profiles is observed as the concentration of the competitor increases suggesting competition between the two ligands for thrombin binding. The apparent IC_{50} increases by 8-fold in the presence of 25 μM heparin (Table 2). This suggests that $FDSO_3$ and full-length heparin compete for binding to exosite 2 of thrombin in an almost ideal manner based on the Dixon-Webb calculations (Figure 19A). Yet, the efficacy of inhibition increases from 56% to 76% as the concentration of UFH changes from 0 to 25 μM, which appears to indicate that the two ligands may be interacting in a partially co-operative manner.

To test whether $FDSO_3$ competes with smaller heparin chains, competitive inhibition studies were performed in the presence of heparin derived octasaccharide H8. As the concentration of H8 increased from 1 to 25 μM, the apparent IC_{50} did not change significantly (Figure 18B, Table 2). This indicates that $FDSO_3$ and H8 do not compete with each other, although both are exosite 2 ligands. The results become more apparent by comparing the obtained values with the Dixon-Webb predicted ones assuming ideal competition (Figure 19B). Interestingly, the presence of H8 increased the maximal inhibition from ~50% to 70% at the highest concentration studied, further supporting the conclusion that $FDSO_3$ and smaller heparin chains may simultaneously bind in exosite 2 and possibly interact in a cooperative way (Table 2). Taken together, these results show that $FDSO_3$ binds in exosite 2 but at a site distinct from the site of H8. Combining these results with other studies,[48,96,104] the experiments show that sulfated LMWLs compete with UFH for recognizing multiple coagulation enzymes. Thus, engaging an exosite 2-like domain in the targeted coagulation proteases appears to be a generic property of these novel inhibitors.

3.3.4. Site-Directed Mutagenesis of Thrombin Exosite 2 Residues Indicates Key Role of Arg93, Arg97 and Arg101 in Recognition of $FDSO_3$.

Exosite 2 of thrombin is a considerably large ellipsoidal region spanning an area of approximately 20×30 $Å^2$. It consists of several basic residues including Arg173, Arg175, Arg101, Arg93, Arg97, Arg126, Lys235, Lys240, Lys236, Arg165, and Lys169. We reasoned that the negatively charged sulfate and carboxylate groups of LMWLs are likely to interact with one or more of these basic residues. Thus, to identify the residues that play important role

in $FDSO_3$ recognition, we studied inhibition of a library of thrombin mutants containing single, double and triple replacement of Arg/Lys to Ala. As a group, the library included all the basic residues present in exosite 2 of thrombin. The preparation and characterization of these thrombins have been described earlier[98,99] and each thrombin mutant was screened for direct inhibition by $FDSO_3$ in a manner similar to that used for wild-type thrombin (Table 3). To ascertain the generality of inhibition properties in key mutants, two chromogenic substrates – Spectrozyme TH and S2238 – were used in these studies.

The dose – response profiles of most of the twelve single mutants studied in this work were essentially identical to the recombinant wild type enzyme. The IC_{50} measured for alanine replacements for Arg93, Lys235, Arg165, Arg175, Arg173, Arg233, Lys240, and Arg236 ranged from 0.79 μM to 1.12 μM, while that measured for the wild-type enzymes was 0.98 μM. Two thrombin mutants – Lys169Ala and Arg97Ala – displayed slightly stronger inhibition potency (2.3–2.6-fold) than the wild-type, while Lys126Ala and Arg101Ala displayed a 1.4–1.6-fold defect (Table 3). The maximal inhibition efficacy of $FDSO_3$ across these thrombin mutants ranged from 40 – 79% in comparison to 47% observed for the recombinant wild-type. These results suggest that single-point mutations appear to not induce major defect in $FDSO_3$ – thrombin interaction.

To test the possibility that multiple point charges may be involved in binding, we evaluated double and triple mutants of 93, 97 and 101 residues. Mutation at those specific residues was reported to alter the binding of some exosite 2 ligands including heparin.[98] We hypothesized, based on the competition of $FDSO_3$ with heparin, that similar alteration of

$FDSO_3$ binding could occur. Replacement of two arginines at these positions – either 93,97 or 97,101 or 93,101 – right shifted the dose-response profile in comparison to the wild-type enzyme (Figure 20). The measured IC_{50} for the 97,101-double mutant was 1.6 μM, while those for 93,97- and 93,101-double mutants were 1.8 and 2.7 μM, which represent 1.6-, 1.8-, and 2.7-fold increases in IC_{50} over corresponding controls (Table 3).

Replacement of all three arginines with alanines introduced a major defect in thrombin inhibition by $FDSO_3$. The IC_{50} measured using Spectrozyme TH hydrolysis was 56 μM suggesting a dramatic defect of 57-fold, while that measured using S2238 hydrolysis indicated a similar defect of 49-fold (Figure 20, Table 3). These results suggest that the three arginines at 93, 97, and 101 positions are collectively critical for interacting with $FDSO_3$. Further, the massive increase in the order of defect upon mutation of all three arginines suggests that the three positive charges appear to work simultaneously (or interchangeably) in recognizing $FDSO_3$. Similar results were obtained when studying the interaction between thrombin and the fibrinogen γ′ chain, where none of the acidic residues in the peptide were found to be critical for the binding, yet an ensemble of three residue mutations led to abolishing the affinity. The authors' conclusion was that the peptide recognized thrombin through electrostatic complementarity with the three residues imposing the specificity of the interaction.[105]

The efficacy of inhibition for the triple mutant (~98%, Table 3) is also considerably enhanced in comparison to all other thrombins studied in this work. The basis for the significant increase is not clear, although it is important to recognize that $FDSO_3$ inhibition of wild-type thrombin appears to be primarily a k_{CAT} effect, which probably arises from conformational

changes induced in the active site. This induced conformational change can be different for each thrombin molecule resulting in variable efficacies of $FDSO_3$ inhibition.

3.3.5. Specific Residues of Thrombin Are Involved in Recognition of $CDSO_3$.

Earlier studies supported the exosite 2-like site as the prime site of $CDSO_3$ recognition. To identify the key residues of exosite 2 that are important for $CDSO_3$ binding, we studied inhibition of the same library of thrombin mutants. Direct inhibition of these mutants by $CDSO_3$ was studied in a manner similar to that used for wild-type thrombin.[48] Alanine replacement at Arg97, Arg101, Lys235, Lys236, or Lys240 positions did not affect the $CDSO_3$ inhibition potency (0.9–1.5-fold effect), while substitutions at the 165, 169, 173 and 233 positions introduced a 2.2–3.7-fold decrease in inhibition potency (Table 4). The measured IC_{50}s for Arg93Ala and Arg175Ala thrombin mutants were 313 and 275 nM, which were 7–8-fold greater than that of the recombinant wild-type thrombin (39 nM) (Table 4, Figure 21). The maximal inhibition efficacy of $CDSO_3$ across these thrombin mutants ranged from 47% to 82% in comparison to 58% observed for the recombinant wild-type form. These efficacies are generally similar to that noted earlier for human plasma thrombin and human plasma plasmin (~80%).[48]

To assess the effect of multiple replacements on $CDSO_3$ inhibition potency, double and triple replacement at the 93, 97, and 101 positions were studied. Replacing arginines at both 93 and 97 positions with alanines shifted the dose–response profile significantly to the right in comparison to both the wild-type enzyme as well as either single-site mutants (Table 4, Figure 22). The measured IC_{50} for the 93,97-double mutant was 679 nM, which indicated an increase

of 17-fold and 2-fold over wild-type and Arg93Ala enzymes, respectively. Introducing alanines for arginines at 93, 97, and 101 positions led to an increase in IC_{50} of 36-fold from the wild-type form (Figure 22). The efficacy of inhibition for the double and triple mutants was again comparable to other thrombins studied in this work (~80%, Table 4).

3.4. DISCUSSION

Sulfated LMWLs were initially designed to mimic the global structural complexity and anticoagulant property of heparins. The novel molecules do mimic the anticoagulant activity, but are proving to be strikingly different from the polysaccharide counterparts in nearly all other respects. Thus, whereas heparins do not directly inhibit thrombin, fXa and other clotting enzymes, sulfated LMWLs were found to potently inhibit thrombin and factor Xa[48] and moderately inhibit plasmin.[96] Nearly all other enzymes of the coagulation cascade as well as trypsin and chymotrypsin are not affected by sulfated LMWLs.[104] This selectivity is interesting because it represents an excellent opportunity for designing macromolecular anticoagulants, a task that is known to be more challenging than designing traditional small molecule anticoagulants. For molecules that can be readily prepared in high yields using simple chemical and enzymatic reactions,[49] the exceptional anti-coagulant activity was striking. Recently, physicochemical studies have highlighted another interesting characteristic of these novel molecules. Sulfated LMWLs appear to possess unusually high solubility in organic solvents despite the presence of a number of anionic groups.[90] These interesting structural, mechanistic, biological and physicochemical properties imply that understanding the molecular aspects of

the interaction of sulfated LMWLs with target proteins may lead to the design of novel anticoagulants that are radically different from all the molecules being pursued to date.

A priori, exosite 2 of thrombin is known to bind highly anionic molecules such as heparin[1,86,99,106] and chondroitin sulfate,[65] while exosite 1 is known to bind anions that are significantly hydrophobic, e.g., hirudin.[107,108] Studies with peptides have suggested that highly anionic peptides prefer exosite 2 in comparison to exosite 1, which prefers less anionic and more hydrophobic peptides.[62] Thus, sulfated LMWLs, which are much less anion-dense and significantly more hydrophobic than LMWH, were expected to recognize exosite 1. It was surprising to observe that $CDSO_3$ prefers interacting with exosite 2 of thrombin.[48] Thus to further understand the basis for thrombin inhibition by sulfated LMWLs, we studied $FDSO_3$ which is also a prototypic inhibitor in this class and the only sulfated LMWL found to date to potently inhibit factor IXa.[104]

This work demonstrates that $FDSO_3$ does not bind in exosite 1 of thrombin and prefers to interact with exosite 2, while chromogenic substrate hydrolysis studies indicate that $FDSO_3$ disrupts the catalytic apparatus in a manner similar to $CDSO_3$. Thus, $FDSO_3$ is also an allosteric inhibitor of thrombin function. A key aspect for the development of this explanation was competition observed with polymeric heparin. UFH is known to interact with Arg93 and Arg101 as well as other residues of exosite 2.[86,109] Most probably, polymeric heparin sterically blocks exosite 2 resulting in competition with sulfated LMWLs. Alternatively, polyanionic UFH may electrostatically protect the exosite too.

The library of exosite 2 residue mutants studied in this work has led to a more refined model of $CDSO_3$ and $FDSO_3$ interaction site on thrombin. Of the twelve electropositive residues constituting exosite 2, three residues – Arg93, Arg97 and Arg101 – were found to collectively play a critical role in $FDSO_3$ inhibition mechanism. All three residues belong to the 99-loop of thrombin and are known to interact with full-length heparin,[86,109] thus explaining its competitive effect. A particularly challenging question to address is the nearly complete lack of inhibition defect when the three critical residues are mutated individually. $FDSO_3$ is a complex preparation consisting of numerous sequences that are structurally distinct.[90] The presence of several types of inter-residue linkages (β-5, β-*O*-4, β-β and others) in $FDSO_3$ preparation probably overcomes a defect created by a single point mutation through compensating sequence(s) that utilize another binding mode. Such alternative sequences and interaction geometries would imply that a functionally defective thrombin inhibition may only be possible if all or most critical residues are mutated.

$CDSO_3$ has different recognition elements. Arg93 and Arg175 showed 7 – 8-fold defect in $CDSO_3$ inhibition. Four other residues which form an arch-like structure surrounding the two key residues (Figure 23) appear to be less important with 2 – 3-fold impaired inhibition. The model suggests a well-defined binding pocket where the $CDSO_3$ chains appear to bind. The differences obtained between $CDSO_3$ and $FDSO_3$ from the mutant library data highlights the fact that despite the common structural features, the two polymeric inhibitors have their differences.

Designed sulfated LMWLs are structurally unique anticoagulants. The molecules are strikingly different from any other class of anticoagulant investigated to-date. The generic allosteric regulation mechanism coupled with identification of the binding site is expected to facilitate the design of molecules based on their scaffold. Another advantage with regard to exosite 2-mediated allosteric regulation of coagulation enzymes is an excellent possibility of an antidote strategy with non-inhibitory sulfated carbohydrates. For example, small oligosaccharides that bind in exosite 2 without inducing direct inhibition, such as sucrose octasulfate, may serve as effective antidotes of sulfated LMWLs-based anticoagulants, which would impart considerable safety to it.

Table 1. Michaelis-Menten kinetics of spectrozyme TH hydrolysis by wild-type thrombin in the presence of $FDSO_3$.[a]

[**$FDSO_3$**]$_O$ *(μM)*	**Spectrozyme TH**	
	K_M *(μM)*	V_{MAX} *(mAU/min)*
0	4.8 ± 1.2[b]	39.0 ± 2.5
0.48	4.1 ± 0.8	27.5 ± 1.4
0.96	2.6 ± 0.6	15.9 ± 0.9
2.38	3.3 ± 1.1	14.1 ± 1.2

[a] K_M and V_{MAX} were measured as described in 'Experimental'.
[b] Error represents ±1 S.E.

Table 2. Inhibition of wild-type thrombin by $FDSO_3$ in the presence of hirugen analog HirP, porcine heparin, or heparin octasaccharide H8.[a]

[Competitor]	IC_{50} (μM)	Y_0	Y_M	ΔY	HS
Hirugen Analog					
8.6 nM	1.3 ± 0.2[b]	38 ± 3	106 ± 6	68 ± 9	1.4 ± 0.3
25.8 nM	1.7 ± 0.1	37 ± 1	104 ± 2	67 ± 3	1.8 ± 0.2
51.6 nM	1.3 ± 0.1	36 ± 2	104 ± 3	68 ± 6	2.1 ± 0.3
103 nM	1.5 ± 0.1	39 ± 2	101 ± 2	62 ± 4	2.1 ± 0.3
Porcine Heparin					
0 μM	0.7 ± 0.2	44 ± 3	109 ± 11	65 ± 11	1.8 ± 0.6
4.2 μM	1.9 ± 0.4	43 ± 3	101 ± 6	58 ± 8	1.7 ± 0.6
12.8 μM	4.4 ± 1.3	26 ± 1	112 ± 6	86 ± 8	0.9 ± 0.3
25 μM	5.7 ± 0.6	24 ± 3	103 ± 3	79 ± 12	1.2 ± 0.2
Heparin Octasaccharide H8					
1 μM	1.2 ± 0.1	53 ± 2	98 ± 3	45 ± 3	2.3 ± 0.5
3 μM	1.6 ± 0.1	46 ± 1	101 ± 2	55 ± 2	1.7 ± 0.2
10 μM	1.8 ± 1.0	31 ± 3	115 ± 6	84 ± 13	0.7 ± 0.3
25 μM	1.2 ± 0.1	50 ± 1	99 ± 3	49 ± 3	2.2 ± 0.4

[a] Inhibition studies were performed in 20 mM Tris-HCl buffer, pH 7.4, containing 100 mM NaCl, 2.5 mM $CaCl_2$ and 0.1 % PEG 8000 in PEG 20,000-coated polystyrene cuvette. Spectrozyme TH was used as substrates and the residual enzyme activity in the presence of $FDSO_3$ was assessed by measuring the initial rate of substrate hydrolysis at 405 nm. Logistic equation 1 was used to fit the dose dependence of the residual enzyme activity to obtain log IC_{50}, Y_0, Y_M and HS values. See Methods for details.

[b] Error represents 1 ±S.E.

Table 3. Inhibition of recombinant wild-type and mutant thrombins by $FDSO_3$.[a]

Thrombin	IC_{50} (μM)	Y_0	Y_M	ΔY[b]	HS
Using Spectrozyme TH as Substrate					
WT	0.98 ± 0.09[c]	54 ± 2	101 ± 2	47 ± 2	2.4 ± 0.4
R93A	0.79 ± 0.09	36 ± 2	93 ± 3	57 ± 5	1.6 ± 0.3
R97A	0.42 ± 0.06	42 ± 1	106 ± 4	63 ± 4	1.2 ± 0.2
R101A	1.58 ± 0.15	28 ± 1	101 ± 1	73 ± 3	0.6 ± 1.3
R126A	1.39 ± 0.06	49 ± 1	102 ± 1	54 ± 2	2.0 ± 0.2
R165A	0.82 ± 0.06	40 ± 1	101 ± 1	61 ± 3	1.6 ± 0.2
K169A	0.38 ± 0.04	41 ± 1	98 ± 2	57 ± 3	1.6 ± 0.2
R173A	0.99 ± 0.16	60 ± 1	100 ± 2	40 ± 2	1.2 ± 0.2
R175A	0.83 ± 0.15	47 ± 3	103 ± 6	56 ± 6	2.4 ± 0.8
R233A	1.00 ± 0.05	37 ± 2	102 ± 2	66 ± 4	2.3 ± 0.3
K235A	0.81 ± 0.07	33 ± 2	101 ± 2	68 ± 5	1.5 ± 0.2
K240A	1.10 ± 0.08	42 ± 2	104 ± 3	61 ± 4	2.3 ± 0.4
R236A	1.12 ± 0.26	23 ± 6	102 ± 4	79 ± 25	0.7 ± 0.1
R93A,R97A	1.79 ± 0.10	37 ± 1	101 ± 1	74 ± 2	1.2 ± 0.1
R101A,R93A	2.73 ± 0.59	49 ± 3	100 ± 2	51 ± 3	1.7 ± 0.5
R101A,R97A	1.63 ± 0.19	28 ± 2	103 ± 2	75 ± 8	0.9 ± 0.1
R101A,R93A,R97A	56.0 ± 2.70[d]	0	101 ± 1[d]	~98[d]	0.9 ± 0.1[d]
Using S2238 as Substrate					
WT	0.85 ± 0.04	43 ± 1	99 ± 1	56 ± 2	2.6 ± 0.3
R93A,R97A	1.38 ± 0.16	38 ± 2	98 ± 2	60 ± 4	1.5 ± 0.2
R101A,R93A	2.51 ± 0.30	48 ± 2	100 ± 2	52 ± 4	1.8 ± 0.4
R101A,R97A	1.21 ± 0.13	35 ± 2	104 ± 2	69 ± 4	1.0 ± 0.1
R101A,R93A,R97A	41.7 ± 4.80[d]	0	99 ± 1[d]	98 ± 1[d]	1.1 ± 0.1[d]

[a] Inhibition studies were performed in 20 mM Tris-HCl buffer, pH 7.4, containing 100 mM NaCl, 2.5 mM $CaCl_2$ and 0.1 % PEG 8000 in PEG 20,000-coated polystyrene cuvettes. Either Spectrozyme TH or S2238 were used as substrates and the residual enzyme activity in the presence of $FDSO_3$ was assessed by measuring the initial rate of substrate hydrolysis at 405 nm. Logistic equation 1 was used to fit the dose dependence of the residual enzyme activity to obtain log IC_{50}, Y_0, Y_M and HS values. See Methods for details.

[b] difference between Y_M and Y_0.

[c] Error represents 1 ± S.E.

[d] values derived from fitting the inhibition profile using $Y_0 = 0$.

Table 4. Inhibition of recombinant wild-type and mutant thrombins by $CDSO_3$.[a]

Thrombin	IC_{50} (nM)	Y_0	Y_M	ΔY[b]	HS
WT	38.92 ± 0.37[c]	47 ± 1	105 ± 3	58 ± 3	1.2 ± 0.2
R93A	313.18 ± 3.13	21 ± 2	103 ± 2	82 ± 9	1.3 ± 0.2
R97A	37.13 ± 0.53	49 ± 2	102 ± 3	53 ± 4	0.8 ± 0.3
R101A	36.45 ± 0.64	33 ± 3	101 ± 4	68 ± 9	0.5 ± 0.2
R165A	144.58 ± 3.93	27 ± 5	95 ± 4	68 ± 16	0.5 ± 0.3
K169A	85.35 ± 1.72	33 ± 3	98 ± 3	65 ± 8	0.5 ± 0.1
R173A	115.35 ± 2.13	52 ± 2	99 ± 2	47 ± 3	0.5 ± 0.2
R175A	275.17 ± 2.93	34 ± 2	100 ± 2	66 ± 5	0.8 ± 0.1
R233A	86.14 ± 2.07	30 ± 5	99 ± 4	69 ± 14	0.5 ± 0.2
K235A	43.90 ± 0.79	32 ± 3	101 ± 4	69 ± 9	0.7 ± 0.2
K240A	57.03 ± 0.82	27 ± 2	103 ± 4	76 ± 9	0.6 ± 0.1
R236A	57.77 ± 0.35	20 ± 1	102 ± 1	82 ± 5	1.0 ± 0.1
R93,R97A	679.36 ± 17.55	25 ± 5	96 ± 5	71 ± 18	0.3 ± 0.3
R93,97,101A	1415.14 ± 20.61	18 ± 3	98 ± 2	80 ± 11	0.6 ± 0.1

[a] Inhibition studies were performed in 20 mM Tris-HCl buffer, pH 7.4, containing 100 mM NaCl, 2.5 mM $CaCl_2$ and 0.1 % PEG 8000 in PEG 20,000-coated acrylic cuvettes. S2238 was used as substrate and the residual enzyme activity in the presence of $CDSO_3$ was assessed by measuring the initial rate of substrate hydrolysis at 405 nm. Logistic equation 1 was used to fit the dose dependence of the residual enzyme activity to obtain log IC_{50}, Y_0, and Y_M values. See Methods for details.

[b] difference between Y_M and Y_0.

[c] Error represents 1 ± S.E.

Figure Legends

Figure 14. Representative structure of the two polymeric chains studied, $CDSO_3$ and $FDSO_3$. The chains shown have β-O-4, β-5, β-β and 5–5 inter-residue linkages (shown shaded). X and Y are substituents at α- and β- positions and may be –H, –OH, or $–OSO_3Na$ and –H or COONa, respectively. R may be either –OH or $–OSO_3Na$ in $CDSO_3$ or $–OCH_3$ in $FDSO_3$. Variations in these substituents, inter-residue linkages and configuration at α- or β- positions generate a large number of sequences.

Figure 15. Michaelis-Menten kinetics of Spectrozyme TH hydrolysis by thrombin in the presence of $FDSO_3$. The initial rate of hydrolysis at various substrate concentrations was measured in pH 7.4 buffer as described in 'Experimental'. Solid lines represent non-linear regressional fits to the data using the Michaelis-Menten equation.

Figure 16. Competitive effect of HirP on the inhibition of wild-type thrombin by $FDSO_3$. Residual thrombin activity was measured through Spectrozyme TH hydrolysis in 20 mM Tris-HCl buffer, pH 7.4, containing 100 mM NaCl, 2.5 mM $CaCl_2$ and 0.1 % polyethylene glycol (PEG) 8000 at 25 ^{O}C in the presence of 0 to 103 nM HirP. Solid lines represent fits using the logistic equation 1 to obtain the apparent IC_{50}, as described in 'Experimental'.

Figure 17. Comparison of the observed (black bars) versus the predicted (white bars) IC_{50} values of $FDSO_3$ inhibition in presence of HirP. The calculations were based on the Dixon-Webb equation 2.

Figure 18. Competitive effect of UFH (A) and octasaccharide H8 (B) on the inhibition of wild-type thrombin by $FDSO_3$. Residual thrombin activity was measured through Spectrozyme TH hydrolysis in 20 mM Tris-HCl buffer, pH 7.4, containing 100 mM NaCl, 2.5 mM $CaCl_2$ and 0.1 % polyethylene glycol (PEG) 8000 at 25 ^{O}C in the presence of 0 to 25 μM UFH (A) and 0 to 25 μM H8 (B). Solid lines represent fits using the logistic equation 1 to obtain the apparent IC_{50}, as described in 'Experimental'.

Figure 19. Comparison of the observed (black bars) versus the predicted (white bars) IC_{50} values of $FDSO_3$ inhibition in presence of A) UFH and B) H8. The calculations were based on the Dixon-Webb equation 2.

Figure 20. Dose-response profile of direct inhibition of multi-point thrombin mutants by $FDSO_3$ in 20 mM Tris-HCl buffer, pH 7.4, containing 100 mM NaCl, 2.5 mM $CaCl_2$ and 0.1 % polyethylene glycol (PEG) 8000 at 25 ^{O}C. Mutants include Arg93,101Ala, Arg93,97Ala, and Arg93,97,101Ala. Inhibition of the thrombin mutants by $FDSO_3$ was followed as described in 'Experimental'. Solid lines represent sigmoidal dose-response fits of equation 1 to obtain values of IC_{50}, HS, Y_0 and Y_M.

Figure 21. Dose-response profile of direct inhibition of thrombin wild-type and mutants by $CDSO_3$ in 20 mM Tris-HCl buffer, pH 7.4, containing 100 mM NaCl, 2.5 mM $CaCl_2$ and 0.1 % polyethylene glycol (PEG) 8000 at 25 ^{O}C. Single point mutants include Arg93Ala and Arg175Ala. Inhibition of the thrombin mutants by $CDSO_3$ was followed as described in 'Experimental'. Solid lines represent

sigmoidal dose-response fits of equation 1 to obtain values of IC_{50}, Y_0, Y_M and HS.

Figure 22. Effect of single site (A) and multi-site (B) replacement of electropositive residues of exosite 2 of thrombin on the direct inhibition potency of $CDSO_3$. The ratio of IC_{50} values of the mutant to that of recombinant wild-type is shown. 'Dbl mut' refers to Arg93,97Ala thrombin, likewise 'Trp mut' refers to Arg93,97,101Ala thrombin. Error bars shown are ± 1 S.E.

Figure 23. The overall structure of thrombin indicating the putative binding site of $CDSO_3$ (PDB ID – 1TB6). The electropositive residues studied in this work are highlighted. The carbon atoms of these residues are color-coded based on the magnitude of the decrease in inhibition by $CDSO_3$ upon mutation to alanine (red: > 7-fold, green: 2 – 3-fold and white: < 2-fold). The protein backbone is shown as a ribbon and the 60-loop (blue), 99-loop (yellow), 170-loop (cyan) and C-terminal region (magenta) are highlighted.

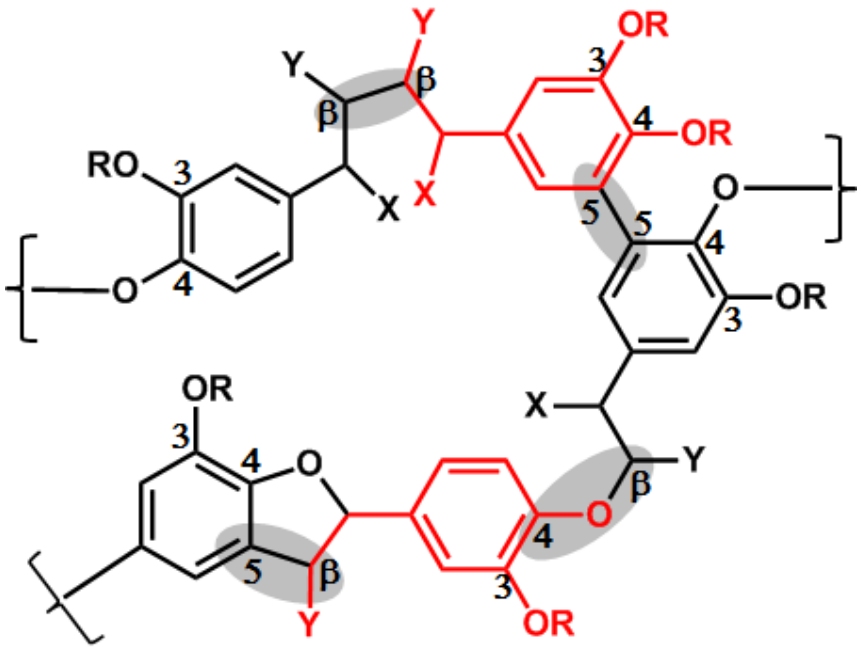

X = H or OH or OSO_3^-

Y = H or COO^-

$CDSO_3$: R = OH or OSO_3^-

$FDSO_3$: R = OCH_3

Figure 14

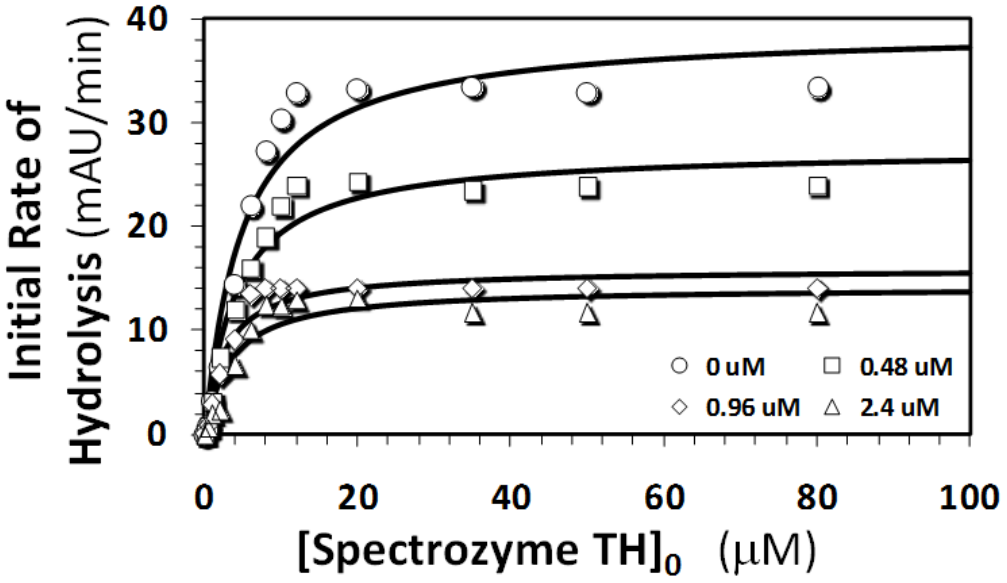
Initial Rate of Hydrolysis (mAU/min)
40
30
20
10
0
0 uM
0.48 uM
0.96 uM
2.4 uM
0
20
40
60
80
100
[Spectrozyme TH]0 (μM)

Figure 15

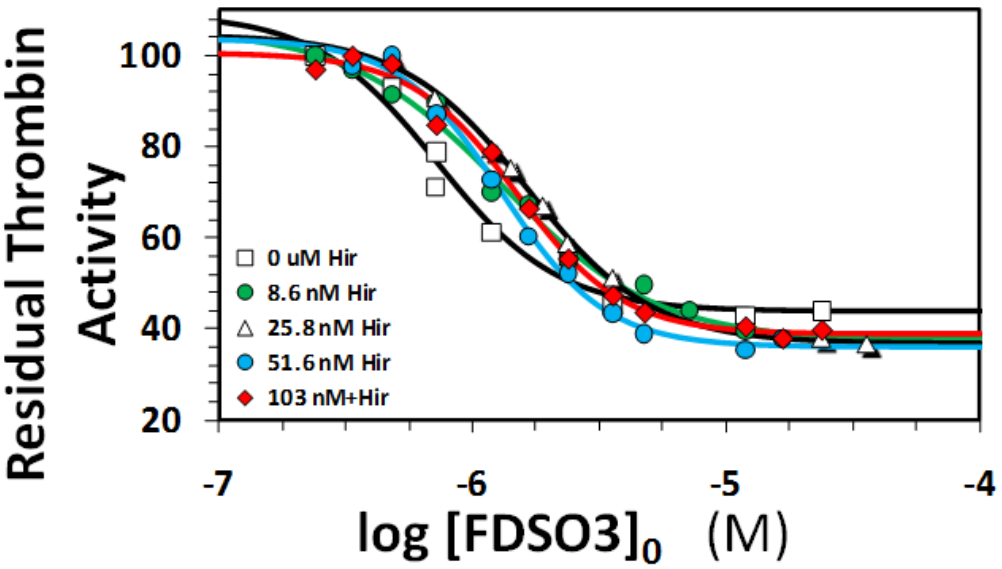
Residual Thrombin Activity
100
80
60
40
20
0 uM Hir
8.6 nM Hir
25.8 nM Hir
51.6 nM Hir
103 nM+Hir
-7
-6
-5
-4
log [FDSO3]0 (M)

Figure 16

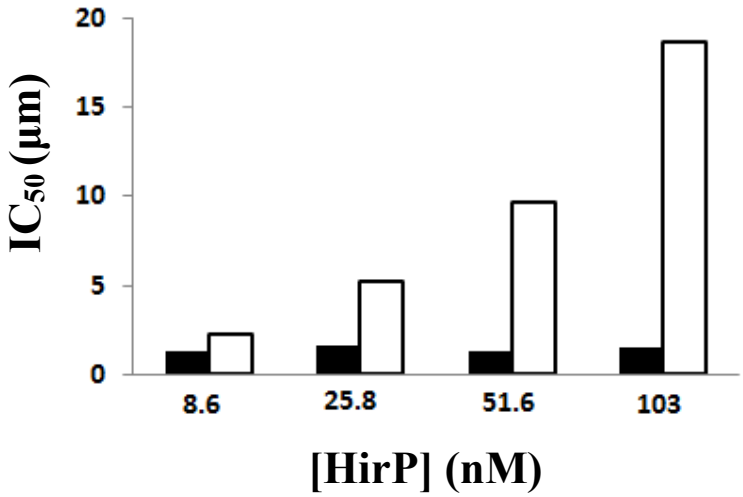

Figure 17

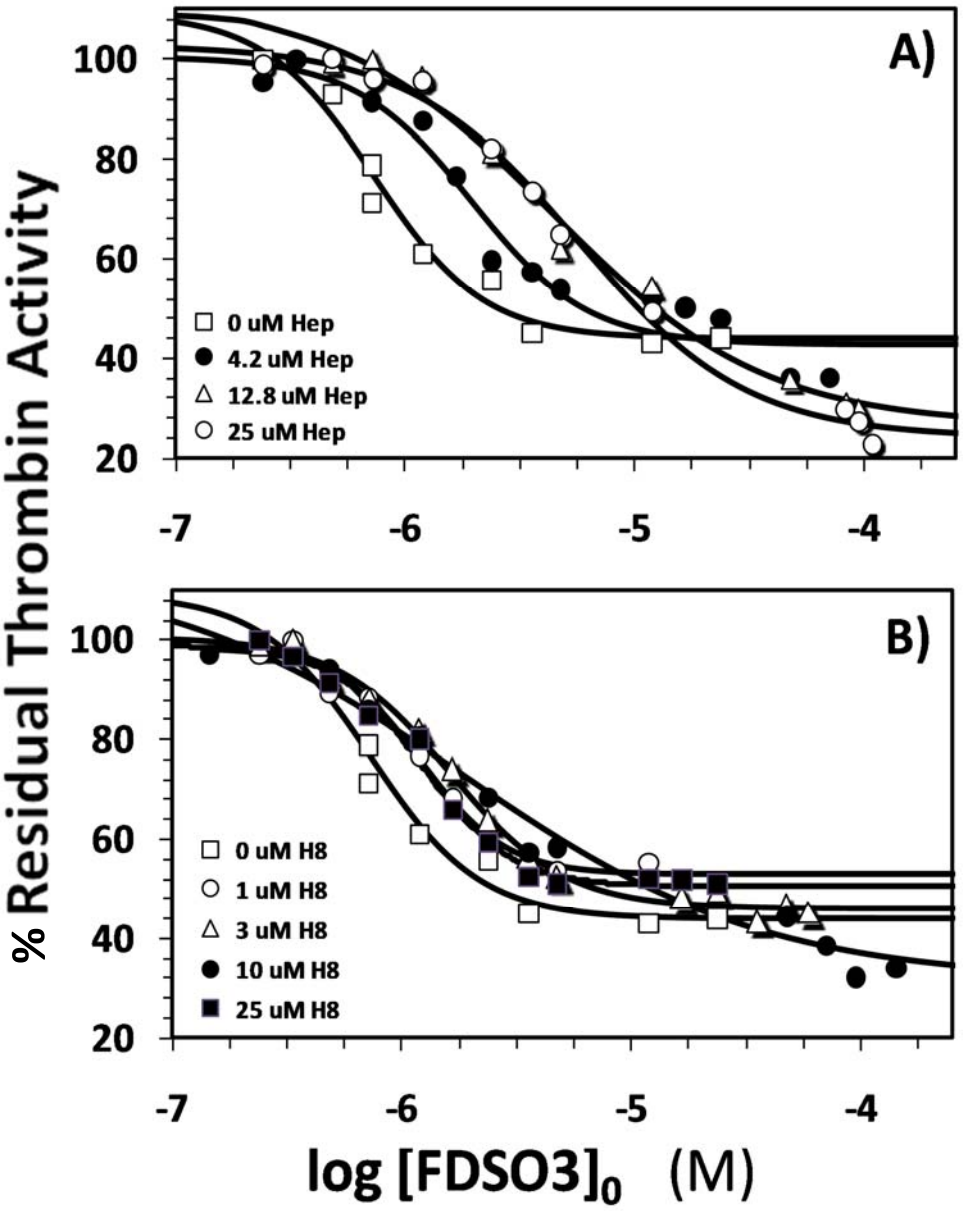
A)
100
80
60
40
20
-7
-6
-5
-4
0 uM Hep
4.2 uM Hep
12.8 uM Hep
25 uM Hep
B)
100
80
60
40
20
-7
-6
-5
-4
0 uM H8
1 uM H8
3 uM H8
10 uM H8
25 uM H8
% Residual Thrombin Activity
log [FDSO3]0 (M)

Figure 18

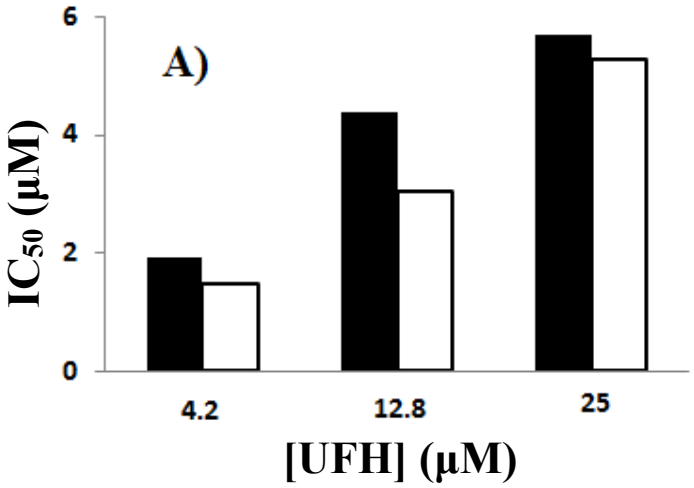

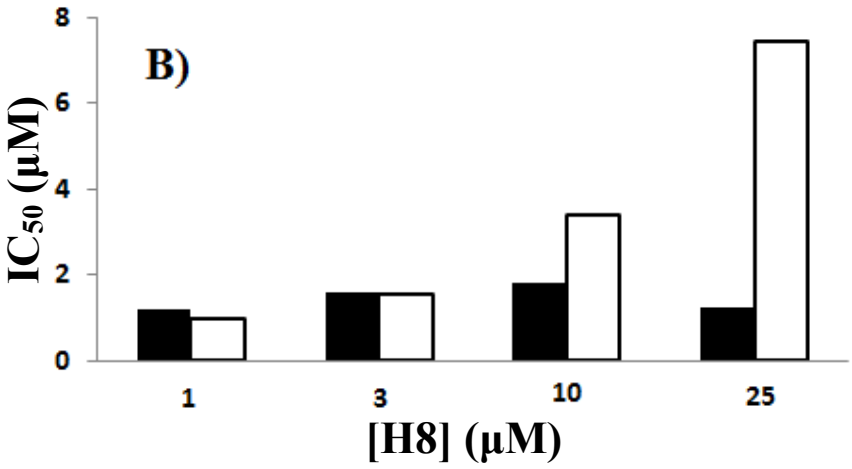

Figure 19

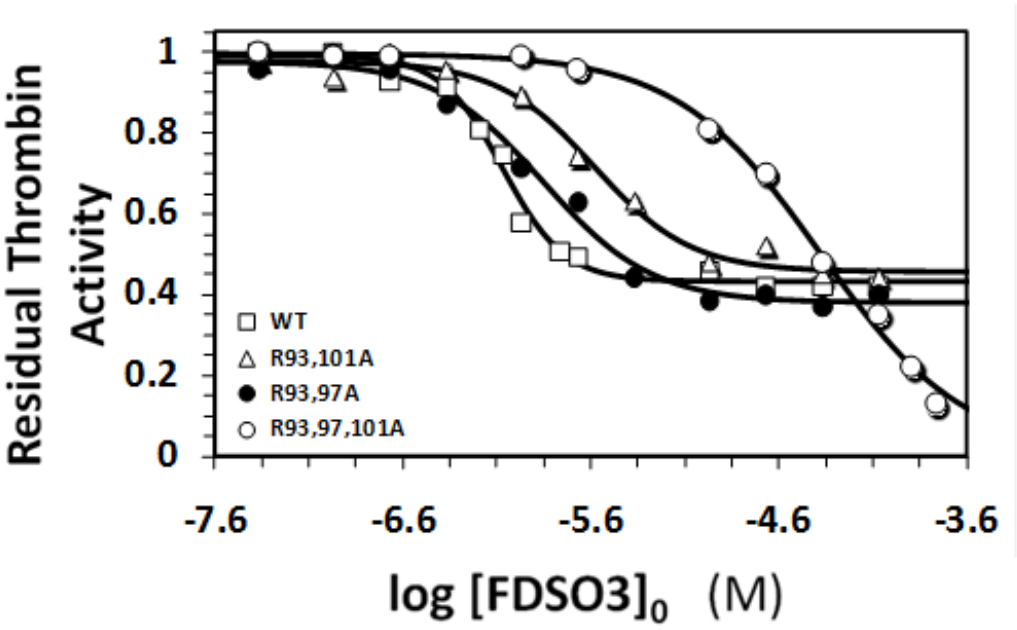
Residual Thrombin Activity
1
0.8
0.6
0.4
0.2
0
WT
R93,101A
R93,97A
R93,97,101A
-7.6
-6.6
-5.6
-4.6
-3.6
log [FDSO3]0 (M)

Figure 20

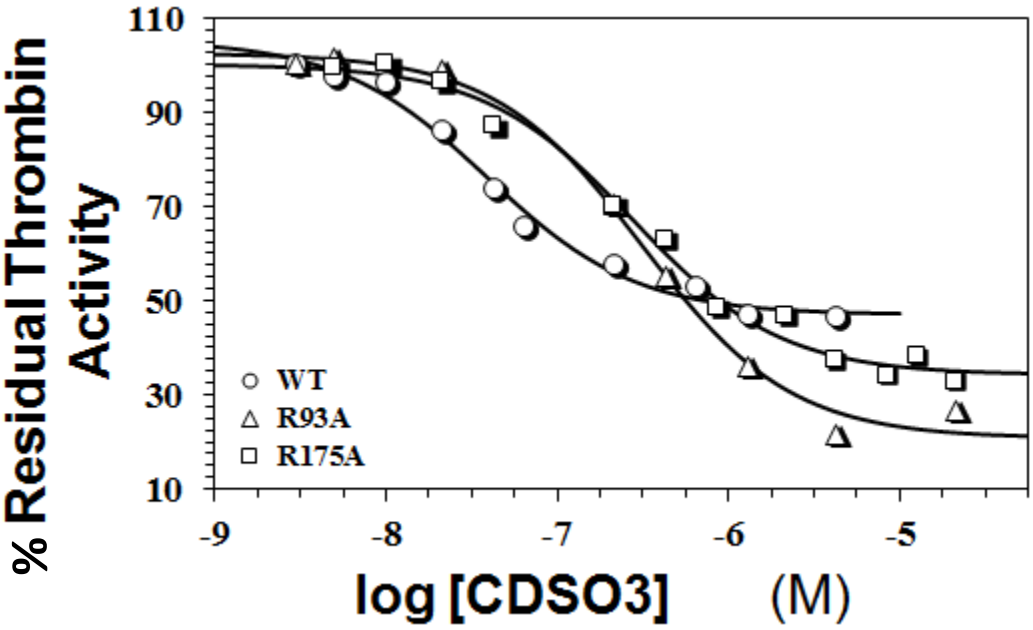
% Residual Thrombin Activity
110
90
70
50
30
10
-9
-8
-7
-6
-5
log [CDSO3] (M)
WT
R93A
R175A

Figure 21

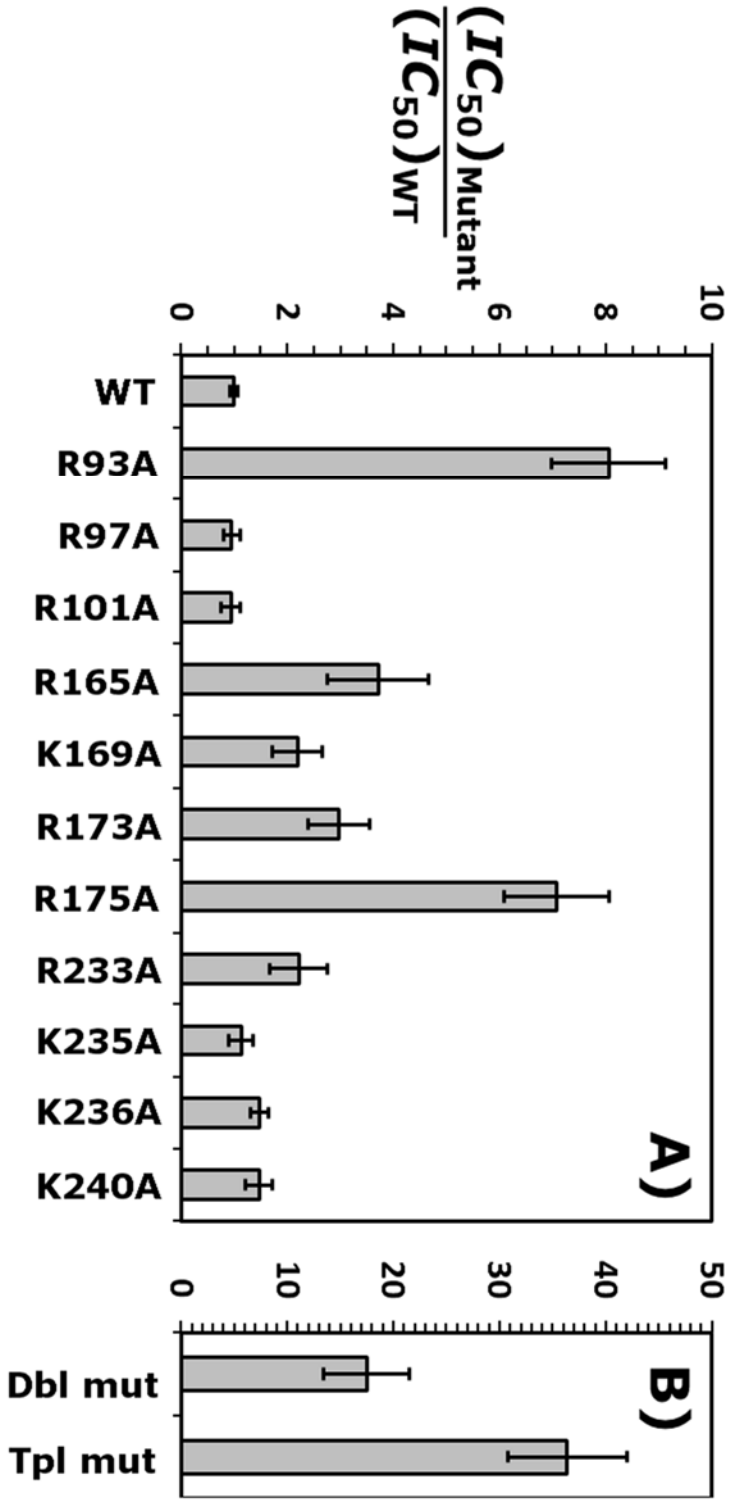
$\frac{(IC_{50})_{Mutant}}{(IC_{50})_{WT}}$
0
2
4
6
8
10
WT
R93A
R97A
R101A
R165A
K169A
R173A
R175A
R233A
K235A
K236A
K240A
A)
0
10
20
30
40
50
Dbl mut
Tpl mut
B)

Figure 22

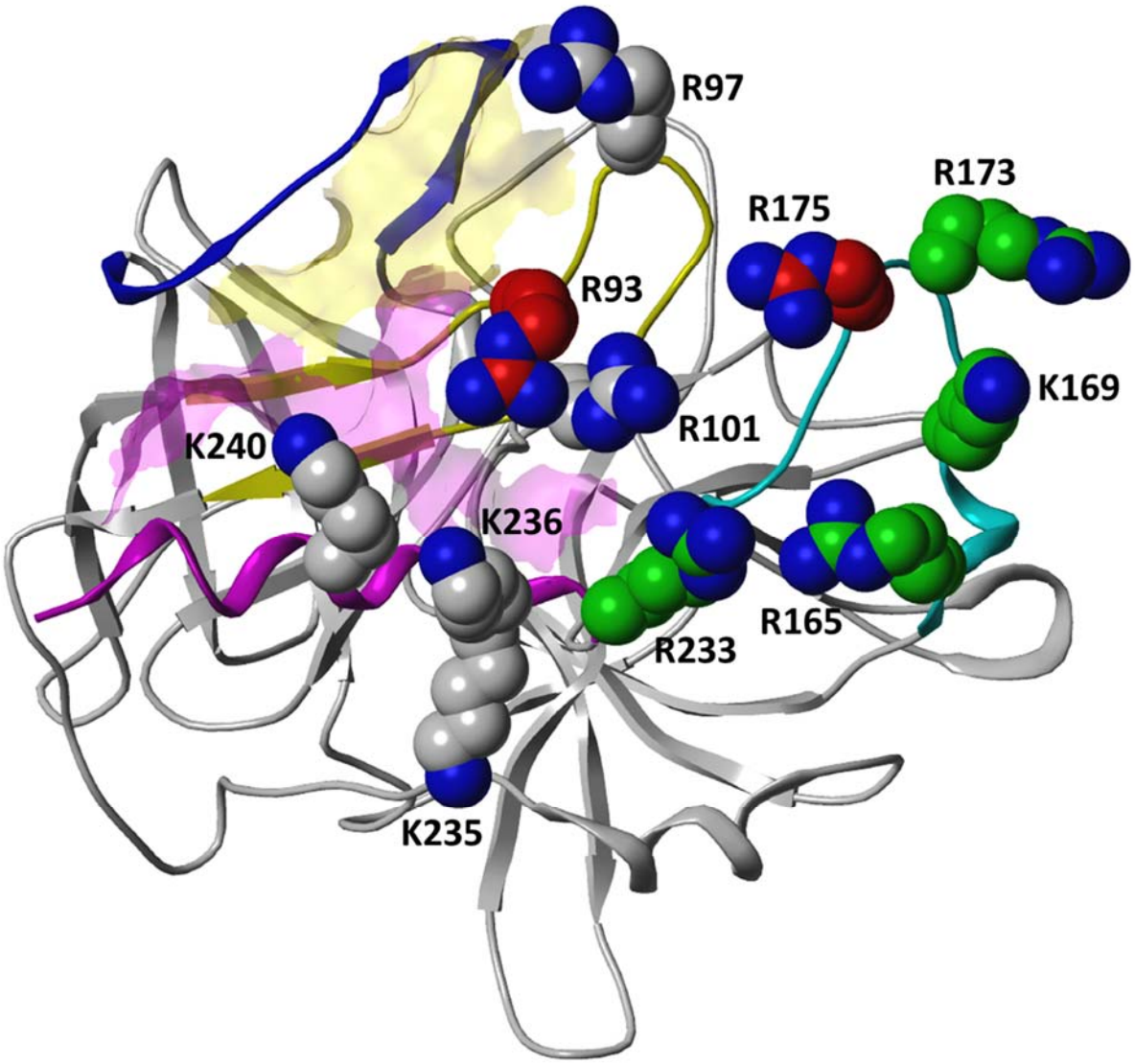

Figure 23

Chapter 4: Identification of the Mechanism of Inhibition, the Binding Site and Key Residues Required for Interaction of Small Molecule Inhibitors with Thrombin

4.1. INTRODUCTION

The coagulation cascade is a rich assembly of homologous serine proteases. Each enzymatic factor of the cascade recognizes a P-1 arginine residue in its target, which sets up possible cross-over reactivity with enzymes of other systems too. Nature avoids this promiscuity, especially of macromolecular substrates, through clever engineering of the environment around the enzyme active sites, known by extended surfaces. For example, thrombin contains the 60-loop, the 149-insertion loop and the bulky Trp215 residue to restrict access to its active site.[53,64,110] Such stringent steric and/or electronic natural 'gating' assists in the design of selective small molecule, active site inhibitors. Yet, the process remains challenging and is threatened by cross-reactivity with closely related enzymes, e.g., factor Xa, or with enzymes that exhibit too broad substrate specificity, e.g., trypsin. In addition to steric or electronic 'gating', an alternative strategy that nature exploits for engineering high selectivity is the use of exosites.

Discovering allosteric modulators of protein function is challenging and yet highly sought after considering that this form of regulation is suggested to offer finer control necessary for therapeutic success, which is difficult to achieve with competitive, active site inhibitors because of the drive to achieve very high potency. At a fundamental level, small molecules may be designed so that the allosteric conformational change can exhibit tailored balance between pro- and anti-coagulant activities that diminishes the current therapeutics side effects. Another advantage of allosteric regulation is the possibility of greater specificity of recognition arising from greater

differences in exosite geometries compared to active sites. In effect, allosteric regulation promises to afford exquisite control over both specificity of recognition and efficacy of inhibition. Despite this expectation, allosteric modulators of cardiovascular enzymes, other than heparin and heparinoids, have not been vigorously pursued.

A classic example of natural allosteric regulation is thrombin cleavage of fibrinogen. In this process, the substrate binds to exosite 1, which then enables its efficient cleavage.[53,64,106,110] Likewise, binding of full-length heparin in exosite 2 enables a much faster inhibition of thrombin by the antithrombin – heparin complex.[10,22] In addition to this exquisite dual recognition, exosites afford a fine opportunity for allosteric modulation of catalytic machinery. Both exosites 1 and 2 of thrombin as well as exosites of many other coagulation enzymes are coupled with the active site. Although the intricate mechanism of this coupling is not fully understood in all cases, it is known that it may involve alteration of structure of the catalytic triad and/or of neighboring residues. For example, sodium binding is known to allosterically alter the conformation of the catalytic triad, shifting thrombin from the slow to the fast form,[111] while heparin binding in exosite 2 is known to change the electrostatics around the active site with minimal change in catalytic activity.[82,112,113] But there are very few examples such as hirugen[114] and bothrojaracin,[115] where these allosteric sites were utilized to inhibit the catalytic activity of thrombin. Those and other allosteric ligands such as heparin, chondroitin sulfate, and haemadin are either long peptides or highly anionic GAG molecules.[66] There has been no report of inhibiting coagulation activity of thrombin allosterically by small, synthetic molecules.

Many heparin mimetics were designed, either polypeptides or polysaccharide fragments derived from heparin, to act clinically as anticoagulants. Heparins are associated with numerous side effects such as narrow therapeutic window, excessive bleeding, and dose response variability

among patients.[116] Other alternatives of smaller oligosaccharides suffer from high production costs and potential toxicity.[117] Thus, the requirement for overcoming the safety problem and regular monitoring requirement drives the research for development of new orally bioavailable, potent and safe antithrombotic agent. To develop such regulators of thrombin, we started with the design of heparin mimetics that are sulfated low molecular weight lignins (LMWLs), which were found to potently inhibit thrombin, factor Xa and plasmin.[48,49,94,96] The oligomeric molecules targeted exosite 2 of thrombin exclusively and were the first molecules in the class of exclusive exosite 2-based allosteric modulators of thrombin.[48] Sulfated LMWLs prevented human blood from clotting in ex-vivo assays with potency comparable to low molecular weight heparins (LMWHs) and thus represented molecules of considerable interest.[94] Yet, the oligomeric nature of these molecules did not bode well for clinical potential.

To address this issue, we designed sulfated benzofuran monomers based on the scaffold of sulfated LMWLs (Figure 24A), which were found to allosterically inhibit thrombin and factor Xa, albeit with poor potency (IC_{50} in mM range).[118] Subsequent advances in the design led to sulfated benzofuran dimers that exhibited a range of inhibition potencies (μM to mM) and efficacies (20 – 60%).[50] A second generation library of trimers containing three linked benzofuran units was synthesized to improve the potency and solubility of the compounds. In this work, we present detailed biochemical studies on the interaction of thrombin with two selected representatives of those molecules, a sulfated benzofuran dimer (SBD) and trimer (SBT), with a goal of identifying the site of binding for further rational structure-based drug design (Figure 24).

4.2. EXPERIMENTAL

4.2.1. Thrombin, Peptides, Chemicals and Reagents.

Human α-thrombin was from Haematologic Technologies (Essex Junction, VT). Stock solutions of thrombin were prepared in 20 mM sodium phosphate buffer, pH 7.4, containing 100 mM NaCl. Chromogenic substrates Spectrozyme TH (H-D-hexahydrotyrosol-Ala-Arg-p-nitroanilide) was purchased from American Diagnostica (Greenwich, CT) and S2238 (H-D-Phe-Pip-Arg–p-nitroanilide) was purchased from ANASPEC (Fremont, CA). Unfractionated porcine heparin (UFH) was purchased from Sigma (St. Louis, MO). Heparin octasaccharide (H8) was purchased from V-Labs (Covington, LA). Tyr63-sulfated hirudin-(54-65) (HirP) was a generous gift from Dr. Paul Bock and its preparation has been described earlier.[97] A peptide corresponding to the 20 amino acids at the carboxyl terminal of γ'-fibrinogen chain (VRPEHPAETE-Y(PO3)-DSL-Y(PO3)-PEDDL) was obtained from Dr. David Farrell.[31] All other chemicals were analytical reagent grade from either Sigma Chemicals (St. Louis, MO) or Fisher (Pittsburgh, PA) and used as such.

4.2.2. Recombinant Thrombin Mutants.

Recombinant wild-type and mutant thrombins were prepared in the Rezaie laboratory, as described earlier.[98,99] Briefly, Arg93Ala, Arg97Ala, Arg101Ala, Arg126Ala, Arg165Ala, Lys169Ala, Arg173Ala, Arg175Ala, Arg233Ala, Lys235Ala, Lys236Ala, Lys240Ala, Arg93,97Ala, Arg93,101Ala, Arg97,101Ala and Arg93,97,101Ala thrombins were prepared in prothrombin-1 form by PCR mutagenesis and expression in baby hamster kidney cells (BHK) using the pNUT-PL2 expression/purification vector system. The mutants were purified to homogeneity by immunoaffinity chromatography using the Ca^{2+}-dependent monoclonal antibody,

HPC4, and activated to thrombin. The active-site concentrations of thrombin mutants were determined by an amidolytic acivity assay and stoichiometric titrations with antithrombin.[98,99] These concentrations were within 90-100% of those expected on the basis of their absorbance at 280 nm.

4.2.3. Inhibition of Thrombin by Chromogenic Substrate Hydrolysis Assay.

Thrombin activity in the presence of inhibitors was studied using chromogenic substrate hydrolysis assay in 20 mM Tris-HCl buffer, pH 7.4, containing 100 mM NaCl, 2.5 mM $CaCl_2$ and 0.1 % polyethylene glycol (PEG) 8000 in PEG 20,000-coated acrylic cuvettes. Spectrozyme TH was used as substrate and the residual thrombin activity was quantified by measuring the initial rate of hydrolysis from the linear increase in absorbance at 405 nm as a function of time as reported earlier. Briefly, a solution of 10 µL of the inhibitors to form final concentrations ranging from 4.5 – 900 µM for SBD and 0.045 – 22.5 µM for SBT was diluted with 970 µL of buffer and 5 µL of 1 µM thrombin (5 nM) and incubated for 10 min for SBD and overnight for SBT. This was followed by addition of 15 µL of 2 mM Spectrozyme TH (30 µM) and the initial rate was rapidly measured. Logistic equation 1 was used to fit the dose dependence of residual thrombin activity to obtain IC_{50}.

$$Y = Y_O + \frac{Y_M - Y_O}{1+10^{(\log[LMWL]_0 - logIC_{50})\times HS}} \qquad \textbf{(equation 1)}$$

In this equation Y is the ratio of residual thrombin activity in the presence of the inhibitor to that in its absence; Y_M and Y_0 are the maximum and minimum possible values of the residual percentage of thrombin activity, respectively; HS is Hill slope and IC_{50} is the concentration of inhibitors that results in 50% inhibition of enzyme activity. Sigmaplot 8.0 (SPSS, Inc. Chicago,

IL) was used to perform non-linear curve fitting in which Y_M, Y_O, HS and IC_{50} were allowed to float.

4.2.4. Michaelis-Menten Kinetics of Substrate Hydrolysis by Thrombin in Presence of SBD or SBT.

The initial rate of Spectrozyme TH hydrolysis by 5 – 10 nM thrombin was monitored from the linear increase in absorbance at 405 nm corresponding to less than 10% consumption of the substrate. The initial rate was measured as a function of various concentrations of the substrate (2 – 600 μM) in the presence of fixed concentration of either SBD (0 – 30 μM) or SBT (0 – 9.9 μM). SBD was incubated with thrombin for 10 min while SBT was incubated either over night at 25 °C or for two hours at 37 °C. The data was fitted by the standard Michaelis-Menten equation to determine K_M and V_{MAX}.

4.2.5. Competitive Studies with Exosite 1 and Exosite 2 ligands.

The inhibition effect of SBD or SBT on wild-type thrombin was studied in the presence of exosite 1 ligand, hirugen, a twelve residue hirudin peptide containing fluorescein at its N-terminus, [5F]-Hir[54-65](SO_3^-). Inhibition experiments were also performed in the presence of exosite 2 ligands, heparin octasaccharide H8, porcine heparin (UFH) and γ'-fibrinogen peptide (FibP) in a manner similar to that described above for direct thrombin inhibition. Briefly, a solution of 10 μL of SBD (0–1000 μM) or SBT (0.045 – 22.5 μM) and 10 μL thrombin (4 – 10 nM) was mixed at 25 °C with 10 μL of the competitor at appropriate stock concentration in 20 mM Tris-HCl buffer, pH 7.4, containing 100 mM NaCl, 2.5 mM $CaCl_2$ and 0.1 % PEG 8000. The solution was incubated for 10 min for SBD and overnight for SBT at 25 °C followed by addition of Spectrozyme TH while monitoring the increase in absorbance at 405 nm. The dose-dependence of the fractional residual

thrombin activity at each concentration of the competitor was fitted using equation 1 to obtain IC_{50}, Y_M, Y_O and HS.

4.2.6. Inhibition of Recombinant Thrombin Mutants.

Direct inhibition of thrombin mutants by SBD or SBT was measured through a chromogenic substrate hydrolysis assay, as reported with wild-type plasma thrombin. The buffer used in these experiments was 20 mM Tris-HCl buffer, pH 7.4, containing 100 mM NaCl, 2.5 mM $CaCl_2$, and 0.1% polyethylene glycol (PEG) 8000. Either Spectrozyme TH or S2238 was used as substrate for SBD and SBT respectively. SBD (2 to 30 μL) at concentrations ranging from 0.25 to 12.5 mM or SBT (0.5 – 150 μL) at 90 μM were diluted with appropriate volume of assay buffer in PEG 20,000-coated acrylic cuvettes at 25 °C. To this solution, 5 μL of thrombin solution was added to give approximately 1.5 – 7.5 nM final concentration. Following addition of thrombin, 20 μL of either 1 mM Spectrozyme TH or 2 mM S2238 was added after the required incubation. The residual thrombin activity was then measured from the initial rate of increase in absorbance at 405 nm. Relative residual thrombin activity at each concentration of the inhibitor was calculated from the ratio of thrombin activity in the presence and absence of inhibitor. Logistic equation 1 was used to fit the dose-dependence of residual proteinase activity to obtain IC_{50}, Y_M, Y_O and HS.

4.3. RESULTS

4.3.1. SBD and SBT Are Allosteric Modulators of Thrombin.

To understand the site of interaction of the inhibitors on thrombin, Michaelis-Menten constants were derived by non-linear regression analysis of the initial rate versus Spectrozyme TH concentration profiles in the presence and absence of the SBD and SBT (Figures 25 and 26, respectively). As the concentration of SBD increased, the V_{MAX} decreased, while K_M stayed

essentially unchanged, which indicates allosteric non-competitive inhibition of thrombin (Table 5). SBT on the other hand caused a decrease in V_{MAX} accompanied by a decrease in K_M as well in both conditions studied (Table 6). This apparent increase in the enzyme's affinity for substrate is considered the hallmark of uncompetitive, allosteric mechanism. Collectively the data indicate that both molecules act allosterically, yet the introduction of a third benzofuran unit in SBT caused it to work with a different inhibition mechanism.

4.3.2. SBD and SBT Do Not Bind in Thrombin Exosite 1.

Considering that anion-binding exosites 1 and 2 of thrombin recognize charged ligands, SBD and SBT were hypothesized to induce inhibition through one of these sites. Sulfated tyrosine-containing hirudin, a 65 amino acid long polypeptide that binds in exosite 1 as well as active site, is known to be the most potent thrombin inhibitor.[114] On the other hand, exosite 2 prefers highly sulfated oligosaccharides,[62,86] molecules that are significantly different in nature from the small molecules studied in this work. This suggested that SBD and SBT may prefer to interact with exosite 1 of thrombin. To test the binding in exosite 1, the inhibition potency of both molecules was measured in the presence of a hirudin-based peptide [5F]-Hir[54-65](SO_3^-), abbreviated as HirP, a molecule known to exclusively engage exosite 1 of thrombin. HirP binds with a dissociation constant of 4 nM as measured independently under similar conditions. Its presence was expected to significantly reduce the potency of the studied inhibitor, if the two molecules competed for the same binding site.

The IC_{50} was measured by quantifying thrombin's hydrolysis of Spectrozyme TH in the presence of fixed concentration of HirP at pH 7.4 and 25 °C, as described earlier.[48] A standard sigmoidal dose-response profile was observed for the inhibition of thrombin for both molecules at all concentrations of HirP (Figures 27, 28), which could be fitted by the logistic equation 1 to

obtain the potency (IC_{50}) and efficacy ($\Delta Y = Y_M - Y_0$) of inhibition. Varying the concentration of HirP from 0 – 30 nM resulted in no apparent change in IC_{50} for both molecules (Tables 7,8). This suggests that HirP and neither SBD nor SBT do not compete with each other for binding in anion-binding exosite 1 of thrombin.

A more quantitative test of competitive binding is the Dixon-Webb relationship (equation 2), which predicts the effect of competition on a measured equilibrium parameter (K_D or IC_{50}).

$$IC_{50,predicted.} = IC_{50} \times \left(1 + \frac{[Competitor]_o}{K_{Competitor}}\right) \qquad \textbf{(equation 2)}$$

In this equation, $K_{competitor}$ is the dissociation constant of thrombin–HirP complex. Figures 27 and 28 show a comparison of the observed and predicted IC_{50} for both molecules at each studied HirP concentration, which clearly points to absence of competition.

4.3.3. SBD Competes Partially with Full-length Heparin and Does Not Compete with a Heparin Derived Octasaccharide.

Highly sulfated polysaccharide chains including heparin octasaccharide H8, low-molecular weight heparin, full-length unfractionated heparin (UFH), γ′ fibrinogen peptide (FibP) and chondroitin sulfate utilize the anion-binding exosite 2 to bind to thrombin.[53,62,110] The major difference in how these polysaccharide ligands recognize thrombin is their span of interaction domain. Whereas H8 recognizes primarily Arg233, Lys235, Lys236 and Lys240, the full-length polymer recognizes a wider area that includes Arg93, Arg101, and Arg165 residues. None of these ligands affects the proteolytic activity of thrombin, which implies that inhibition assays could be used for exosite 2 competitive studies. To assess whether SBD interacts with exosite 2, we first studied competition with UFH. The sigmoidal dose-response profiles displayed a slight shift to the right with increasing concentration of UFH from 0 – 48 μM suggesting a noticeable competitive

phenomenon (Figure 29). The IC_{50} of SBD inhibition of thrombin at pH 7.4 and 25 °C was calculated to increase from 8.8 μM in the absence of UFH to 36.1 μM in the presence of 48 μM UFH (Table 7). This represents a progressive decrease in potency up to 4.1-fold at a UFH concentration ~5-times higher than the K_D of thrombin – heparin complex.[86] Such a decrease in potency is suggestive of inefficient competition, or more appropriately partial competition, as seen from applying the Dixon-Webb relationship (equation 2, Figure 30). This most probably indicates a partial overlap between the binding sites of SBD and UFH on thrombin exosite 2.

Figure 29 shows the dose-response curves of SBD inhibiting thrombin in the presence of H8 at pH 7.4 and 25 °C. As the concentration of H8 was increased from 0 to 10 μM, the IC_{50} of thrombin inhibition increased from 2.7 to 3.7 μM (Table 7). This change in potency was almost negligible when compared to the predicted IC_{50} from the Dixon-Webb relationship (equation 2, Figure 30). Also, no noticeable change in the efficacy of inhibition was observed in the presence of H8. Thus, H8 does not compete with SBD for binding to thrombin, suggesting that it does not recognize Arg233, Lys235, Lys236, or Lys240 known to interact with H8 in exosite 2. This is not too unexpected considering the widely different structural features of the two molecules. H8 is a highly anionic polysaccharide, while SBD is a fairly hydrophobic small molecule with one negative charge.

4.3.4. SBD Competes with γ′-Fibrinogen Peptide for Binding to Thrombin.

The absence of competition for binding to thrombin with H8 eliminated the octasaccharide binding pocket as site of interaction for SBD. By the same token, partial competition observed with UFH suggested recognition of one or more electropositive residues of exosite 2. Yet, exosite 2 of thrombin is a fairly extensive domain with a large number of basic residues, which makes it difficult to find the exact site and mode for the inhibitor interaction. To further reduce the number

of possibilities, competition with γ'-fibrinogen peptide (FibP) was studied. FibP is known to bind in exosite 2 by interacting with residues that bind to H8 (Arg233, Lys235, Lys236 and Lys240),[36] while also interacting with additional residues as demonstrated by NMR studies.[119] In these studies, the C-terminal residues of FibP interact with Arg93, Arg97, Arg173 and Arg175 of exosite 2. This makes FibP an excellent probe for studying interaction with this group of arginines that lie beyond the H8 binding site. Figure 31A shows the dose-response profiles of SBD inhibition of plasma thrombin in the presence of 0 to 6.5 μM FibP. A distinct shift in the inhibition profiles was observed as the concentration of FibP increased suggesting strong competition between the two ligands for thrombin binding. The apparent IC_{50} increased from 7.97 μM in the absence to 118 μM in the presence of 6.5 μM FibP (Table 7). Simultaneously, the efficacy of inhibition increased from ~40% to 55%, which suggests that the two ligands may be interacting in a partially co-operative manner.

The predicted IC_{50} for SBD inhibition of thrombin in the presence of different concentrations of FibP was calculated using the Dixon-Webb relationship (equation 2). Figure 31B shows a comparison of the observed and predicted IC_{50}. Each of the measured values are higher than those predicted for FibP competition, which suggests a strong competitive effect. The reason for the more-than-predicted competitive effect of FibP is not easy to decipher; however, a small change in the affinity of FibP for thrombin under the experimental conditions is likely to significantly alter the predicted IC_{50}. Overall, competition with FibP indicates that SBD binds in exosite 2 in a region away from the H8 binding residues and most probably with one or more of Arg93, Arg97, Arg173 and Arg175.

4.3.5. SBT Binds in Exosite 2 of Thrombin.

The apparent IC_{50} was measured in the presence of the same three exosite 2 binding ligands used with SBD: UFH, H8 and FibP. Figure 32A shows the dose-response profiles of SBT inhibition of thrombin in the presence of 4.2 to 42.6 μM UFH as competitor. A distinct shift in the profiles is observed as the concentration of UFH increases suggesting ideal competition between the two ligands for thrombin binding as predicted by the Dixon-Webb relationship (equation 2, Figure 32B). The apparent IC_{50} increases from 0.68 μM in the absence of heparin to 6.10 μM in the presence of 42.6 μM heparin (Table 8). This indicates that SBT and full-length heparin compete for binding to exosite 2 of thrombin.

Further studies were done to narrow the site of interaction of SBT by testing if it competes with smaller heparin chains or FibP. As the concentration of H8 increased from 1 μM to 20 μM, the apparent IC_{50} did not change significantly (Figure 33A, Table 8). This indicates that SBT and H8 do not share the same binding area on thrombin, although both are exosite 2 ligands. To confirm this observation, the apparent IC_{50} was also measured in the presence of FibP. The peptide is known to interact with thrombin overlapping with H8 binding site, but extending beyond it to reach the boundary of exosite 2. Figure 33B shows the dose-response profiles of SBT inhibition of thrombin in the presence of 0 to 6.5 μM FibP. Again, no shift in the profiles is observed as the concentration of the competitor increases suggesting no competition between the two ligands (Table 8). Using the Dixon-Webb relationship for both H8 and FibP confirmed the absence of competition for both competitors (Figure 34). Taken together, these results show that SBT binds in exosite 2 in a manner similar to full length heparin chains, but at a site distinct from H8 or FibP binding site.

4.3.6. Sulfated Benzofuran SBD Interacts with a Single Arginine of Exosite 2.

To identify the basic residues that might play an important role in the dimer recognition, we studied the inhibition of five thrombin mutants containing single and triple replacement of Arg/Lys to Ala. The preparation of these mutants has been described earlier[98,99] and each thrombin mutant was screened for direct inhibition by SBD in a manner similar to that used for recombinant wild-type thrombin. The rest of the mutant library was excluded from screening based on the absence of competition with H8. The dose – response profiles of three of the four single point mutants studied in this work were essentially identical to the recombinant wild type enzyme (Figure 35). The IC_{50} measured for alanine replacements for Arg175, Lys169, and Lys235 ranged from 5.9 μM to 9.0 μM, while that measured for the wild-type enzyme was 5.5 μM (Table 9). The triple point mutant Arg93,97,101Ala had a comparable IC_{50} of 5.0 μM suggesting none of the three amino acids contribute to SBD binding. This was quite different from our results with macromolecular sulfated LMWLs, which primarily relied on Arg93 and Arg175 for mediating their inhibitory role. Although the above mentioned basic residues do not contribute to SBD recognition, each site-directed thrombin mutant was inhibited more than the wild-type enzyme. For example, the efficacy of SBD inhibition (i.e., ΔY) increased to ~70% for the triple mutant in comparison to ~30% for wild-type enzyme (Table 9).

One particular thrombin mutant, Arg173Ala, was dramatically different. It displayed a 22-fold increase in IC_{50} compared to the wild type enzyme. The efficacy of inhibition for this thrombin mutant was ~55% (Figure 35). This suggested that Arg173 was essential for thrombin binding and inhibition by SBD and related sulfated benzofuran derivatives. It is striking that a single residue, of the 12 electropositive residues present in exosite 2 of thrombin, was identified to be critical for

interaction. It indicates a high level of specificity of recognition, which suggests a strong possibility for development of allosteric thrombin inhibitors based on that scaffold.

4.3.7. Trimer SBT Interacts with Specific Arginines in Exosite 2.

To highlight the basic residues that play a significant role in binding, we studied the inhibition of 12 thrombin mutants containing single replacement of all Arg/Lys in exosite 2 to Ala. Each thrombin mutant was screened for direct inhibition by SBT using a more sensitive substrate, S2238. The activity dropped using this substrate by 2.5-fold to 0.261 μM for wild type thrombin versus Spectrozyme TH. The dose – response profiles of ten of the 12 single point mutants were essentially identical to the recombinant wild type enzyme (Figure 36). The IC_{50} measured ranged from 0.212 μM to 0.308 μM (Table 10). For one single mutant (Arg93Ala), the activity increased by 2-fold with the IC_{50} dropping to 0.169 μM, probably indicating a relief of a steric clash that decreased the inhibition potency in the wild type enzyme. This area of thrombin contains two closely spaced arginines, Arg93 and Arg101, suggesting they might be involved in a more complex manner in the interaction. Only one single mutant, Arg233Ala, showed a 3-fold drop in potency, which is more than any of the double mutants, indicating that Arg 233 is a key residue involved in the binding Most probably the residue forms a salt bridge with the sulfate group in SBT.

This is in accordance with our previous results with the polymeric LMWLs that found Arg 233 to be important for activity, lowering the potency by almost 2.5-fold, albeit with less importance than two other basic residues for the polymer binding, Arg 93 and Arg 175. These finding indicate that the trimeric units of benzofuran are able to bind in a similar fashion to at least some of the active polymeric species. Although the activity of SBT is still almost 10-fold less than the polymer, it offers the advantages of one defined, simple and homogenous structure that could be easily modified to improve potency, selectivity and pharmacokinetic parameters. The binding

site is remarkably different from SBD, which bound mainly to Arg 173 at the edges of exosite 2 and in proximity to the active site. Adding one more unit to form the trimer shifted the binding more towards the center of exosite 2. The polymers ($FDSO_3$ and $CDSO_3$) as well as the small molecules (SBD and SBT) share the same binding site with unfractionated heparin polymers, but unlike heparin they are able to directly inhibit thrombin in an antithrombin independent manner. This makes them a better heparin mimetic than the currently available options as they offer a more controlled safety profile, more selectivity and more specificity of interaction.

Surprisingly, while Arg93Ala showed a 2-fold increase in potency, the double mutant Arg93,101Ala showed 2.5-fold drop in inhibition (Figure 36). This could be attributed to the proximity between Arg 233 on one end and the two basic residues Arg93 and Arg101 on the other end. The sulfate group linked to Arg 233 could form additional hydrogen bond interactions with either of these two basic residues. The triple mutant Arg93,97,101Ala had also 5-fold increase in IC_{50} highlighting again the importance of this constellation of basic residues in anchoring the position of the sulfate group. The same results were obtained with one of the polymeric chains studied ($FDSO_3$), which again points to the resemblance in binding between these two inhibitors.

4.4. DISCUSSION

Similar to heparin, the polymeric LMWLs are a complex mixture of different structures arising from different inter-residue linkages and degrees of sulfation. It is well known that the β-5 linkage is the most abundant linkage present in the natural lignins.[49,90] Based on this assumption and synthetic feasibility, the benzofuran scaffold was chosen due to its scaffold similarity to the β-5 linkage (Figure 24). A series of molecules with dimeric and trimeric units of benzofuran based scaffold were recently synthesized in our lab. No small, drug-like molecules have been designed as yet that function as allosteric modulators of thrombin. SBD and SBT, which were designed as

mimetics of heparin, are the first small hydrophobic molecules that allosterically reduce thrombin's catalytic activity.[118,50] Discovering allosteric modulators is challenging because identifying exosites that are energetically coupled to the active site in an agonistic or antagonistic manner is not routinely possible. More importantly, even if such an exosite was known, designing molecules that fit the site 'snugly' and are able to cause a conformational change is challenging, because the classical, allosteric induced-fit mechanism would require good recognition of both the native and conformationally altered enzyme states.

The advantage with thrombin is that it is a highly pliable enzyme. The presence of multiple exosites in thrombin enhances the likelihood of discovering small molecule allosteric regulators. However, such probabilistic advantage does not imply automatic translation into drug-like molecule design, and thrombin is no exception. The scenario with other coagulation enzymes, such as factors Xa, IXa and XIa, is similar. Yet, allosteric regulation of these enzymes offers phenomenal opportunity to induce tailored conformational change so as to maintain a delicate balance between bleeding and clotting tendencies. With this goal in mind, we designed sulfated LMWLs from which we designed the small molecule dimers and trimers, including SBD and SBT, respectively.[48-50,94,96,118]

This work suggests that SBD and SBT utilize two different sub-sites in exosite 2 to allosterically inhibit thrombin. Although designed as mimetics of heparin, SBD does not engage the traditional exosite 2 residues, including Arg101, Arg126, Lys235, Lys236 and Lys240.[53,62,86,110] The dimer recognizes Arg173, a heparin-binding residue, yet binding seems to occur in a region different from that predicted for sulfated $CDSO_3$, which appears to bind in a linear segment present in exosite 2 on either side of residues Arg93 and Arg175 or $FDSO_3$, which collectively utilizes Arg93, Arg97 and Arg101 for binding. On the other hand, when the same scaffold is extended by

one more benzofuran unit, SBT binds in a different way, more closely related to the polymeric chains. Despite the fact that two of the double mutants had 2 – 2.5-fold defects in binding, the single mutant Arg233 displayed a 3-fold defect (Figure 36), which makes this residue, known to be important for heparin binding, stand out as the major residue for trimer interaction. The triple mutant impaired inhibition proved the importance of the constellation of residues Arg93, Arg97 and Arg101, in regulating the binding of SBT in a manner seen before in FDSO3 polymeric chains.

The mechanism of inhibition changes as well from the non-competitive in the case of SBD to uncompetitive in the case of SBT, which further highlights the difficulty of predicting the behavior of these allosteric modulators using traditional structure-activity relationships. The IC_{50} of SBD for thrombin inhibition at pH 7.4 and 25 °C is approximately 6 μM, which implies a reasonably high affinity interaction. A 1000-fold improvement in potency was found on moving from monomer to dimer SBD, which led us to design the trimer SBT, which had almost another 10-fold improvement in potency over the dimer.

SBD reduces thrombin's catalytic activity approximately 50% (Table 7) in comparison to known inhibitors that target the active site and exosite 1.[119-122] This implies that it does not completely inhibit the pro-coagulant signal. Whereas this could be traditionally considered as a defect of design, considering the problems of over-anticoagulation induced by thrombin inhibitors, the less than perfect reduction in catalytic activity of thrombin may serve to create the fine balance between procoagulant and anticoagulant signals. More importantly, detailed inhibition profiles reveal that SBT exhibits almost 90% efficacy, while for other related dimers and trimers it is between 10 and 20%.[50] The variability in the efficacy of thrombin inhibition suggests that the equilibrium between the native and conformationally altered state is 'tunable' and optimally designed molecule(s) may be effective in treating varying levels of pro-coagulant tendencies.

The discovery of the new allosteric binding pockets and the benzofuran scaffold that is able to bind tightly and regulate thrombin activity raises many questions before a clinically viable candidate can be realized. For example, it is well established that presence of FibP does not affect thrombin-cleavage of fibrinogen,[123] but reduces the cleavage of other thrombin substrates, such as factor V, factor VIII, platelet glycoprotein 1 and PAR-1. Our earlier work has shown that SBD inhibits clotting of human plasma, which implies that presence of this molecule reduces the rate of fibrinogen cleavage by thrombin.[50] But if these molecules also reduce platelet glycoprotein 1 and PAR-1 cleavage, SBD may function as a dual anti-platelet and anti-coagulant agent. This does not necessarily imply a distinct advantage because of the possibility of introducing bleeding risk. Future studies will clarify these involved aspects.

Overall, this work presents two new binding pockets, one near Arg173 and one inside next to Arg233, that are energetically coupled to the active site, and two small, synthetic, hydrophobic molecules that recognize these sites with reasonably high affinity. The allosteric mechanism of thrombin inhibition could prevent the hemorrhagic complications and avoid narrow dosing regimens that are characteristic of thrombin active site inhibitors.[124] Much remains to be learned about these novel binding sites, but structure-based drug design is expected to greatly enhance the 'druggability' of this site. The successful design of allosteric inhibitors of thrombin opens the path for designing the allosteric inhibitors for other upstream proteases of coagulation cascade. The recognition of heparin binding site by these aromatic inhibitors may extend the inhibition activity for other proteases that are known to bind heparin. Exploring the other structural features of lignins, it may be possible to find scaffolds inhibiting other proteases in a highly specific manner.

Table 5. Michaelis-Menten kinetics of Spectrozyme Th hydrolysis by thrombin in presence of SBD.[a]

[SBD] *(μM)*	K_M *(μM)*	V_{MAX} *(mAU/min)*
0	18.9 ± 4.4[b]	100.4 ± 9.3
3	15.5 ± 5.1	106.8 ± 13.0
10.5	15.9 ± 3.8	72.7 ± 11.6
30	15.5 ± 3.4	66.4 ± 5.5

[a] K_M and V_{MAX} were measured as described in 'Experimental'.
[b] Error represents ±1 S.E.

Table 6. Michaelis-Menten kinetics of Spectrozyme Th hydrolysis by thrombin in presence of SBT.[a]

[**SBT**] *(μM)*	***Overnight incubation at 25°C***		***Two hours incubation at 37°C***	
	K_M *(μM)*	V_{MAX} *(mAU/min)*	K_M *(μM)*	V_{MAX} *(mAU/min)*
0	9.50 ± 1.90[b]	80.79 ± 5.13	7.69 ± 2.21	85.76 ± 7.35
0.36	11.14 ± 2.71	79.95 ± 6.51	ND[c]	ND
0.63	7.67 ± 1.27	68.84 ± 3.35	6.73 ± 2.54	72.35 ± 8.68
1.53	ND	ND	2.17 ± 0.80	29.56 ± 1.97
1.80	3.15 ± 0.50	34.71 ± 1.17	ND	ND
3.60	3.07 ± 0.60	18.81 ± 0.77	2.65 ± 0.62	24.74 ± 1.13
9.90	ND	ND	1.92 ± 0.65	14.71 ± 0.87

[a] K_M and V_{MAX} were measured as described in 'Experimental'.
[b] Error represents ±1 S.E.
[c] ND: not determined

Table 7. Inhibition of thrombin by SBD in presence of hirugen analog HirP, porcine heparin, heparin octasaccharide or γ'fibrinogen peptide.[a]

	IC_{50} (μM)	Y_M	Y_0	ΔY	HS
[HirP] nM					
0	5.3 ± 0.03[b]	0.99 ± 0.02	0.59 ± 0.01	0.40 ± 0.01	2.3 ± 0.3
3	7.8 ± 0.05	0.99 ± 0.01	0.45 ± 0.04	0.54 ± 0.05	2.1 ± 0.3
5	4.0 ± 0.04	1.02 ± 0.05	0.39 ± 0.07	0.63 ± 0.14	2.2 ± 0.6
15	3.1 ± 0.03	1.02 ± 0.05	0.44 ± 0.04	0.58 ± 0.08	2.2 ± 0.6
30	3.4 ± 0.03	1.03 ± 0.04	0.48 ± 0.04	0.55 ± 0.07	2.6 ± 0.7
[H8] μM					
0	2.7 ± 0.01	0.98 ± 0.01	0.50 ± 0.02	0.48 ± 0.02	8.4 ± 2.0
1	2.8 ± 0.01	0.98 ± 0.01	0.56 ± 0.01	0.42 ± 0.01	5.1 ± 0.9
3	3.4 ± 0.02	1.0 ± 0.02	0.55 ± 0.03	0.45 ± 0.03	3.4 ± 0.8
10	3.7 ± 0.03	0.99 ± 0.02	0.52 ± 0.03	0.47 ± 0.04	1.9 ± 0.3
[UFH] μM					
0	8.8 ± 0.2	0.99 ± 0.01	0.52 ± 0.01	0.47 ± 0.02	2.7 ± 0.4
4.8	10.6 ± 0.4	1.00 ± 0.03	0.56 ± 0.03	0.44 ± 0.03	2.4 ± 0.8
11.2	21.8 ± 0.4	0.95 ± 0.03	0.46 ± 0.05	0.49 ± 0.07	1.7 ± 0.6
20.6	26.3 ± 0.2	0.98 ± 0.02	0.50 ± 0.03	0.48 ± 0.03	2.1 ± 0.4
48	36.1 ± 0.2	0.95 ± 0.02	0.41 ± 0.04	0.54 ± 0.06	2.7 ± 0.7
[FibP] μM					
0	8.0 ± 0.4	1.04 ± 0.06	0.63 ± 0.03	0.41 ± 0.05	2.9 ± 1.2
0.2	39.2 ± 0.8	1.01 ± 0.02	0.69 ± 0.04	0.32 ±0.02	1.6 ± 0.4
0.65	65.6 ± 0.4	0.99 ± 0.01	0.55 ± 0.02	0.44 ± 0.02	8.0 ± 1.5
2	84.9 ± 0.2	1.00 ± 0.01	0.54 ± 0.01	0.46 ± 0.01	3.5 ± 0.4
6.5	117.8 ± 0.2	0.97 ± 0.02	0.44 ± 0.04	0.53 ± 0.06	3.1 ± 0.8

[a]The IC_{50}, HS, Y_M, Y_O values were obtained following non-linear regression analysis of direct inhibition of human thrombin in 20 mM Tris-HCl buffer, pH 7.4, containing 100 mM NaCl, 2.5 mM $CaCl_2$, and 0.1% polyethylene glycol (PEG) 8000 at 25 °C. Inhibition was monitored through spectrophotometric measurement of residual thrombin activity (see 'Experimental').

[b]Errors represent ± 1 S. E.

Table 8. Inhibition of thrombin by SBT in presence of hirugen analog HirP, porcine heparin, heparin octasaccharide or γ'fibrinogen peptide.[a]

[Competitor]	IC_{50} (μM)	Y_0	Y_M	ΔY[b]
0 μM	0.68 ± 0.01[c]	13 ± 4	110 ± 4	97 ± 6
Hirugen Analog				
3 nM	0.76 ± 0.02	46 ± 5	109 ± 5	63 ± 7
5 nM	0.63 ± 0.01	47 ± 3	108 ± 4	61 ± 5
15 nM	0.56 ± 0.02	51 ± 3	111 ± 7	60 ± 8
Porcine Heparin				
4.2 μM	1.00 ± 0.02	19 ± 6	110 ± 5	91 ± 8
12.8 μM	2.44 ± 0.04	6 ± 5	107 ± 4	101 ± 6
25.0 μM	4.70 ± 0.07	2 ± 5	105 ± 3	103 ± 6
42.6 μM	6.10 ± 0.09	3 ± 5	104 ± 2	101 ± 5
Heparin Octasaccharide H8				
1.0 μM	1.71 ± 0.04	24 ± 7	105 ± 3	81 ± 8
3.0 μM	1.31 ± 0.03	33 ± 6	105 ± 5	72 ± 8
10 μM	1.55 ± 0.04	40 ± 4	107.3 ± 5	67 ± 6
20 μM	2.24 ± 0.07	35 ± 7	105 ± 4	70 ± 8
γ'Fibrinogen peptide				
0.2 μM	1.31 ± 0.03	6 ± 8	108 ± 4	102 ± 9
0.65 μM	1.03 ± 0.02	16 ± 5	107 ± 5	91 ± 7
2 μM	0.92 ± 0.03	23 ± 5	114 ± 9	91 ± 10
6.5 μM	0.90 ± 0.03	29 ± 4	119 ± 11	90 ± 12

[a] Inhibition studies were performed in 20 mM Tris-HCl buffer, pH 7.4, containing 100 mM NaCl, 2.5 mM $CaCl_2$ and 0.1 % PEG 8000 in PEG 20,000-coated acrylic cuvette. Spectrozyme TH was used as substrates and the residual enzyme activity in the presence of the trimer was assessed by measuring the initial rate of substrate hydrolysis at 405 nm after overnight incubation. Logistic equation 1 was used to fit the dose dependence of the residual enzyme activity to obtain log IC_{50}, Y_0, and Y_M values whereas HS were fixed to 1. See Methods for details.

[b] difference between Y_M and Y_0.

[c] represents 1 ± S.E.

Table 9. Inhibition parameters for SBD inhibiting recombinant wild-type and mutant thrombins at pH 7.4 and 25 °C.[a]

Thrombin Mutants	IC_{50} (μM)	Y_M	Y_0	ΔY	HS
WT	5.5 ± 0.02[b]	1.01 ± 0 .02	0.73 ± 0.01	0.27 ± 0.01	6.4 ± 1.3
R93,97,101A	5.0 ± 0.09	1.01 ± 0.06	0.28 ± 0.05	0.73 ± 0.17	2.1 ± 0.9
R169A	6.1 ± 0.04	1.00 ± 0.01	0.68 ± 0.01	0.32 ± 0.01	3.3 ± 0.8
R173A	121 ± 1.2	1.01 ± 0.02	0.47 ± 0.03	0.55 ± 0.05	2.8 ± 0.7
R175A	5.9 ± 0.02	1.00 ± 0.01	0.60 ± 0.01	0.40 ± 0.01	6.3 ± 1.0
K235A	9.0 ± 0.04	0.99 ± 0.01	0.64 ± 0.02	0.35 ± 0.02	6.6 ± 1.9

[a]The IC_{50}, HS, Y_M, Y_O values were obtained following non-linear regression analysis of direct inhibition of human thrombin in 20 mM Tris-HCl buffer, pH 7.4, containing 100 mM NaCl, 2.5 mM $CaCl_2$, and 0.1% polyethylene glycol (PEG) 8000 at 25 °C (see 'Experimental').
[b]Errors represent ± 1 S. E.

Table 10. Inhibition parameters for SBT of S2238 hydrolysis by recombinant wild-type and mutant thrombins at pH 7.4 and 25 °C.[a]

Thrombin Mutants	IC_{50} (μM)	Y_M	Y_0	Δ Y[b]
WT	0.261 ± 0.08[c]	108 ± 5	40 ± 4	68 ± 6
R93A	0.169 ± 0.03	109 ± 4	31 ± 3	78 ± 5
R97A	0.243 ± 0.10	116 ± 9	44 ± 5	72 ± 10
R101A	0.212 ± 0.03	105 ± 4	38 ± 3	67 ± 5
R126A	0.222 ± 0.07	108 ± 5	28 ± 4	80 ± 6
R165A	0.249 ± 0.06	105 ± 4	42 ± 2	63 ± 5
K169A	0.235 ± 0.07	119 ± 7	36 ± 3	83 ± 8
R173A	0.292 ± 0.10	110 ± 7	23 ± 7	87 ± 10
R175A	0.286 ± 0.13	110 ± 9	52 ± 4	58 ± 10
R233A	0.789 ± 0.2	103 ± 2	37 ± 4	66 ± 5
K235A	0.294 ± 0.06	105 ± 3	42 ± 3	63 ± 4
K236A	0.247 ± 0.09	119 ± 9	40 ± 3	79 ± 10
K240A	0.308 ± 0.08	107 ± 3	41 ± 4	66 ± 5
R93,97A	0.190 ± 0.01	120 ± 10	32 ± 5	88 ± 21
R93,101A	0.641 ± 0.01	113 ± 7	38 ± 3	75 ± 11
R97,101A	0.472 ± 0.01	106 ± 5	26 ± 3	80 ± 13
R93,97,101A	3.470 ± 0.07	103 ± 2	31 ± 7	72 ± 18

[a]The IC_{50}, Y_M, and Y_O values were obtained following non-linear regression analysis of direct inhibition of S2238 hydrolysis by human thrombin in 20 mM Tris-HCl buffer, pH 7.4, containing 100 mM NaCl, 2.5 mM $CaCl_2$, and 0.1% polyethylene glycol (PEG) 8000 at 25 °C and overnight incubation whereas HS were fixed to 1. (see 'Experimental').
[b] difference between Y_M and Y_0.
[c] represents 1 ± S.E.

Figure Legends

Figure 24. Structure of sulfated benzofuran dimers and trimers. **A)** Concept behind designing small molecule benzofuran-based inhibitors from polymeric LMWLs. **B)** SBD and SBT studied in this work.

Figure 25. Michaelis-Menten kinetics of Spectrozyme TH hydrolysis by human thrombin in presence of SBD. The initial rate of hydrolysis at various substrate concentrations was measured spectrophotometrically in pH 7.4 buffer after 10 min incubation. Solid lines represent non-linear regressional fits to the data by the standard Michaelis-Menten equation to yield K_M and V_{MAX}.

Figure 26. Michaelis-Menten kinetics of Spectrozyme TH hydrolysis by human thrombin in presence of SBT. The initial rate of hydrolysis at various substrate concentrations was measured spectrophotometrically in pH 7.4 buffer after **(A)** Overnight incubation at 25°C and **(B)** Two hours incubation at 37 °C with different trimer concentrations. Solid lines represent non-linear regressional fits to the data by the standard Michaelis-Menten equation to yield K_M and V_{MAX}.

Figure 27. Competitive effect of the hirudin peptide HirP on the inhibition of human plasma thrombin by SBD. **(A)** Residual thrombin activity was measured through Spectrozyme TH hydrolysis in 20 mM Tris-HCl buffer, pH 7.4, containing 100 mM NaCl, 2.5 mM $CaCl_2$ and 0.1 % polyethylene glycol (PEG) 8000 at 25 °C in the presence of 0 to 48 nM of HirP. Solid lines represent fits using the logistic equation 1 to obtain the apparent IC_{50}, as described in 'Experimental'. **(B)** Graphical comparison of the predicted (shaded bars) and observed (unshaded bars) $IC_{50,app}$ obtained from Dixon-Webb relationship (equation 2) for HirP and SBD competition.

Figure 28. Competitive effect of HirP on the inhibition of human thrombin by SBT. **(A)** Residual thrombin activity was measured through Spectrozyme TH hydrolysis in 20 mM Tris-HCl buffer, pH 7.4, containing 100 mM NaCl, 2.5 mM $CaCl_2$ and 0.1 % polyethylene glycol (PEG) 8000 at 25 ^{O}C and overnight incubation in the presence of 0 – 15 nM of HirP. Solid lines represent fits using the logistic equation 1 to obtain the apparent IC_{50} and ΔY, while HS was fixed to 1 as described in 'Experimental'. **(B)** Graphical comparison of the predicted (shaded bars) and observed (unshaded bars) $IC_{50,app}$ obtained from the Dixon-Webb relationship (equation 2) for HirP and SBT competition.

Figure 29. Competitive effect of heparin octasaccharide H8 **(A)** and unfractionated heparin UFH **(B)** on the inhibition of human plasma thrombin by SBD in 20 mM Tris-HCl buffer, pH 7.4, containing 100 mM NaCl, 2.5 mM $CaCl_2$ and 0.1 % polyethylene glycol (PEG) 8000 at 25 ^{O}C and 10 min incubation in the presence of 0 to 10 μM H8 and 0 to 48 μM UFH. Solid lines represent fits using the logistic equation 1 to obtain the apparent IC_{50}, as described in 'Experimental'.

Figure 30. Graphical comparison of the predicted (shaded bars) and observed (unshaded bars) $IC_{50,app}$ obtained from Dixon-Webb relationship (equation 2) for both **(A)** H8 and **(B)** UFH competition with SBD.

Figure 31. **(A)** Competitive effect of the γ'-fibrinogen peptide (FibP) on the inhibition of human plasma thrombin by SBD in 20 mM Tris-HCl buffer, pH 7.4, containing 100 mM NaCl, 2.5 mM $CaCl_2$ and 0.1 % polyethylene glycol (PEG) 8000 at 25 ^{O}C in the presence of 0 to 6.5 μM of the peptide. Solid lines represent fits using the logistic equation 1 to obtain the apparent IC_{50}, as described in 'Experimental'. **(B)** Comparison of the

predicted (shaded bars) and observed (unshaded bars) $IC_{50,app}$. Obtained from the Dixon-Webb relationship (equation 2) for FibP and SBD competition.

Figure 32. (A) Competitive effect of UFH on the inhibition of human plasma thrombin by SBT in 20 mM Tris-HCl buffer, pH 7.4, containing 100 mM NaCl, 2.5 mM $CaCl_2$ and 0.1 % polyethylene glycol (PEG) 8000 at 25 ^{O}C in the presence of 0 – 42.6 μM UFH after overnight incubation. Solid lines represent fits using the logistic equation 1 to obtain the apparent IC_{50} and ΔY while HS was fixed to 1, as described in 'Experimental'. **(B)** Graphical comparison of the predicted (shaded bars) and observed (unshaded bars) $IC_{50,app}$ obtained from the Dixon-Webb relationship (equation 2) for UFH and SBT competition.

Figure 33. Competitive effect of H8 **(A)** and FibP **(B)** on the inhibition of human plasma thrombin by SBT in 20 mM Tris-HCl buffer, pH 7.4, containing 100 mM NaCl, 2.5 mM $CaCl_2$ and 0.1 % polyethylene glycol (PEG) 8000 at 25 ^{O}C and overnight incubation in the presence of 0 – 20 μM H8 or 0 – 6.5 μM FibP. Solid lines represent fits using the logistic equation 1 to obtain the apparent IC_{50} and ΔY while HS was fixed to 1, as described in 'Experimental'.

Figure 34. Graphical comparison of the predicted (shaded bars) and observed (unshaded bars) $IC_{50,app}$ obtained from the Dixon-Webb relationship (equation 2) for both **(A)** H8 and **(B)** FibP competition with SBT.

Figure 35. Dose-response profiles for SBD inhibition of recombinant wild type and mutant thrombins in 20 mM Tris-HCl buffer, pH 7.4, containing 100 mM NaCl, 2.5 mM $CaCl_2$ and 0.1 % polyethylene glycol (PEG) 8000 at 25 ^{O}C. Solid lines represent sigmoidal dose-response fits of equation 1.

Figure 36. Effect of alanine scanning of the basic residues in thrombin exosite 2 on the direct inhibition potency of SBT. The ratio of IC_{50} values of the mutant to that of recombinant wild-type is shown. Inset shows the dose-response profiles for SBT inhibition of recombinant wild type compared to Arg233Ala and Arg93,97,101Ala mutants using S2238 as substrate in 20 mM Tris-HCl buffer, pH 7.4, containing 100 mM NaCl, 2.5 mM $CaCl_2$ and 0.1 % polyethylene glycol (PEG) 8000 at 25 ^{O}C. Solid lines represent sigmoidal dose-response fits of equation 1 to obtain the apparent IC_{50} and ΔY while HS was fixed to 1, as described in 'Experimental'.

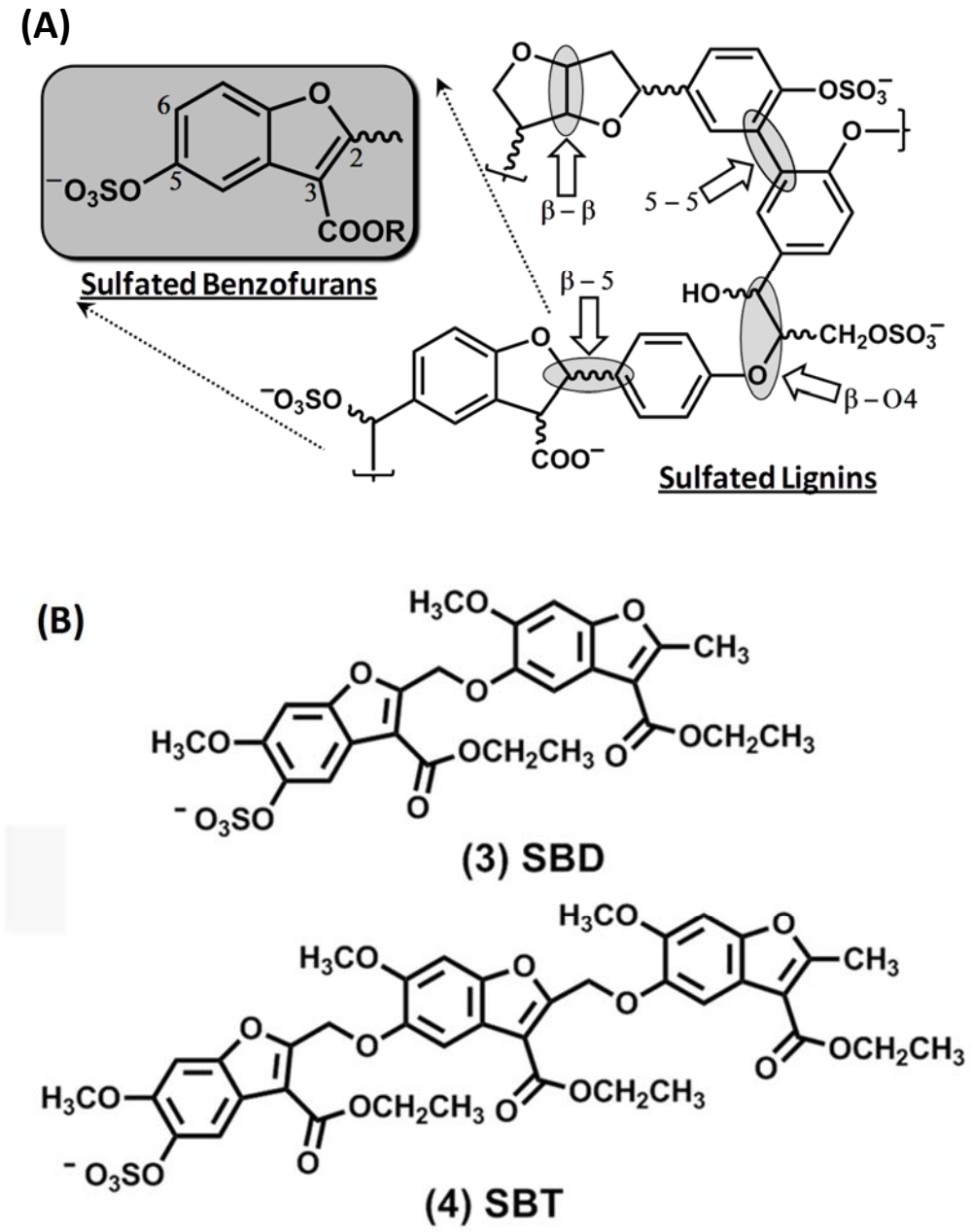
(A)
Sulfated Benzofurans
Sulfated Lignins
β – β
5 – 5
β – 5
β – O4
(B)
(3) SBD
(4) SBT

Figure 24

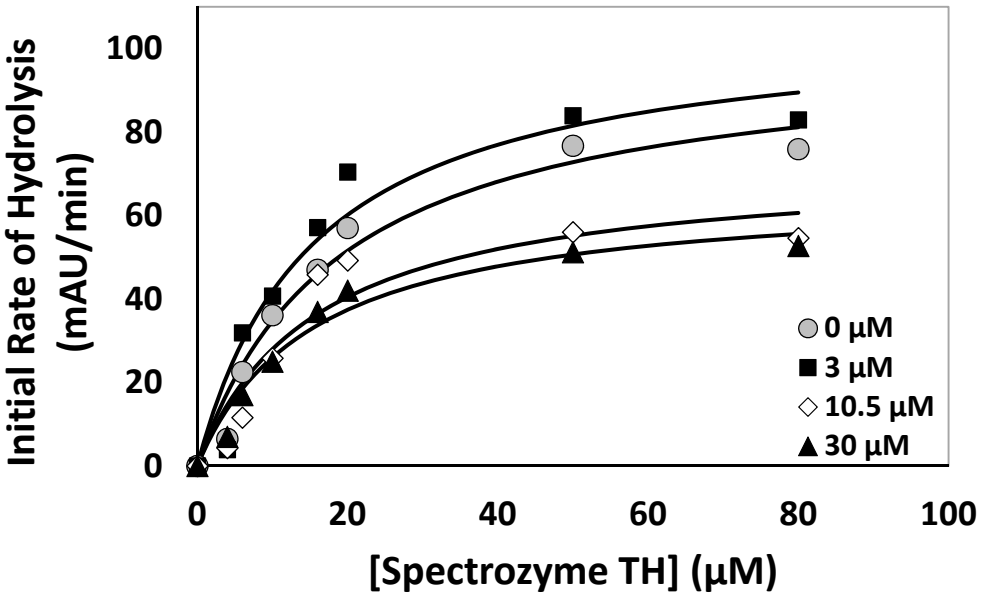
Initial Rate of Hydrolysis (mAU/min)
100
80
60
40
20
0
0
20
40
60
80
100
[Spectrozyme TH] (µM)
0 µM
3 µM
10.5 µM
30 µM

Figure 25

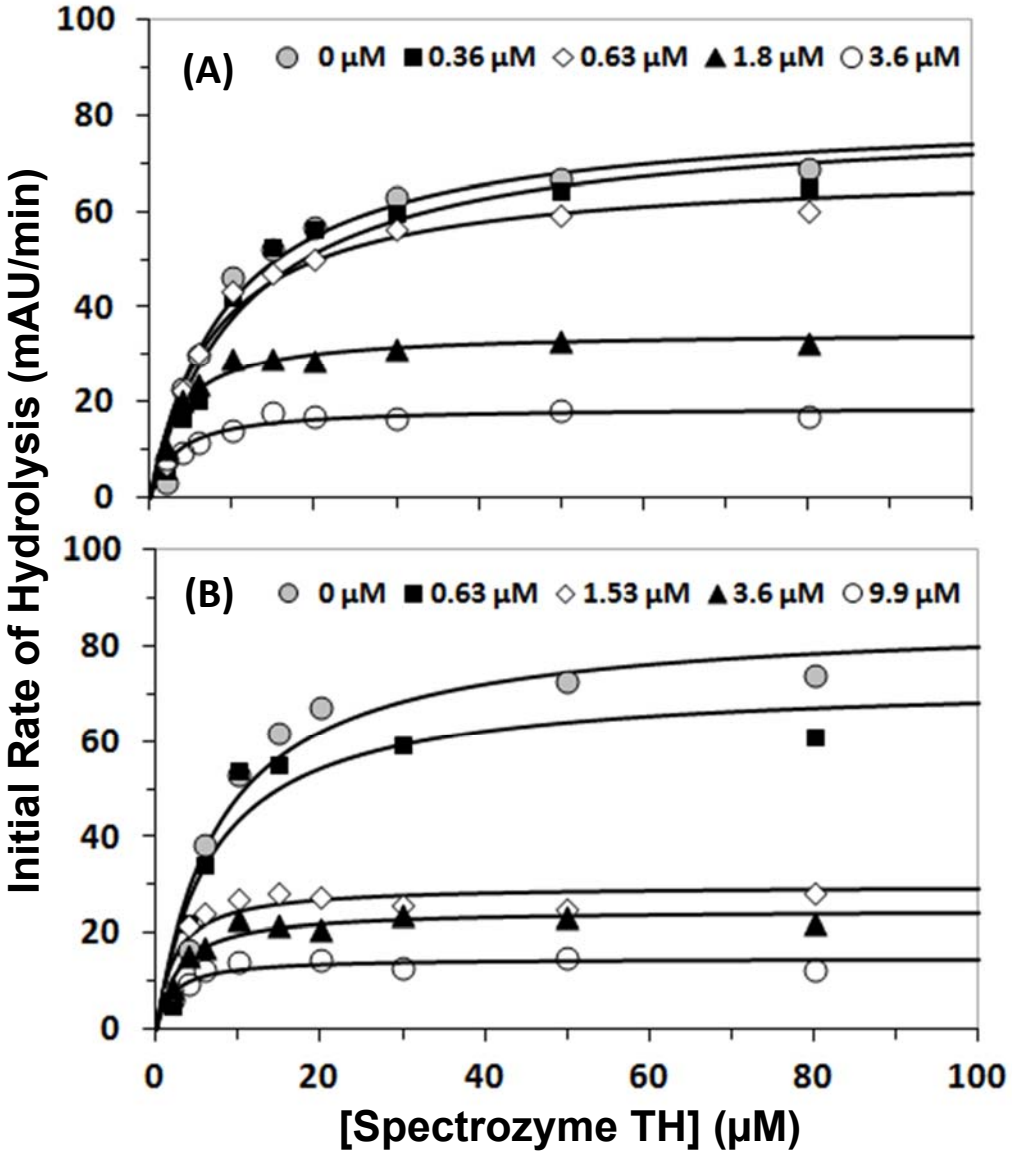
(A)
0 µM
0.36 µM
0.63 µM
1.8 µM
3.6 µM
(B)
0 µM
0.63 µM
1.53 µM
3.6 µM
9.9 µM
Initial Rate of Hydrolysis (mAU/min)
[Spectrozyme TH] (µM)
0
20
40
60
80
100

Figure 26

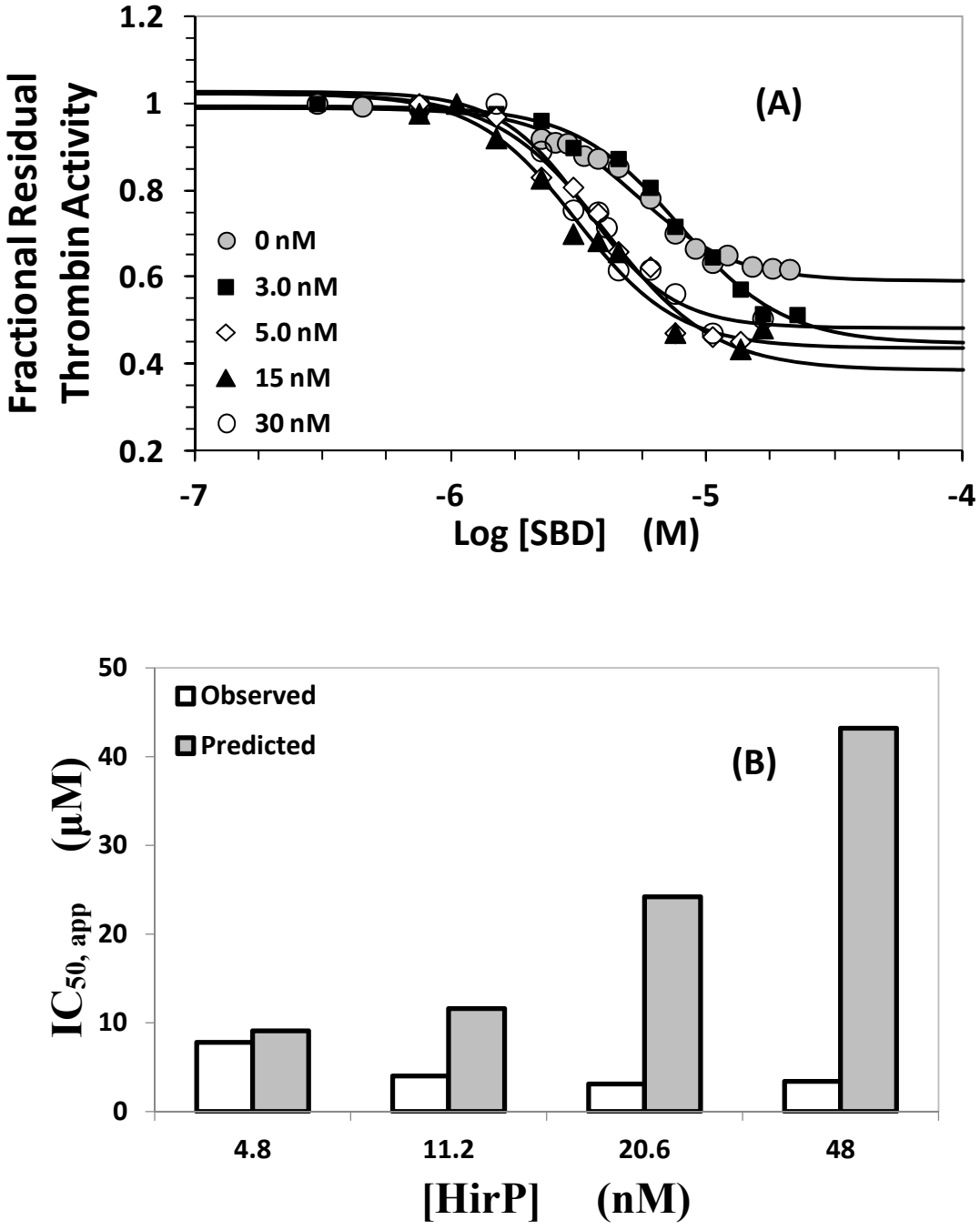
Fractional Residual Thrombin Activity
1.2
1
0.8
0.6
0.4
0.2
(A)
0 nM
3.0 nM
5.0 nM
15 nM
30 nM
-7
-6
-5
-4
Log [SBD] (M)
50
40
30
20
10
0
(B)
Observed
Predicted
IC50, app (μM)
4.8
11.2
20.6
48
[HirP] (nM)

Figure 27

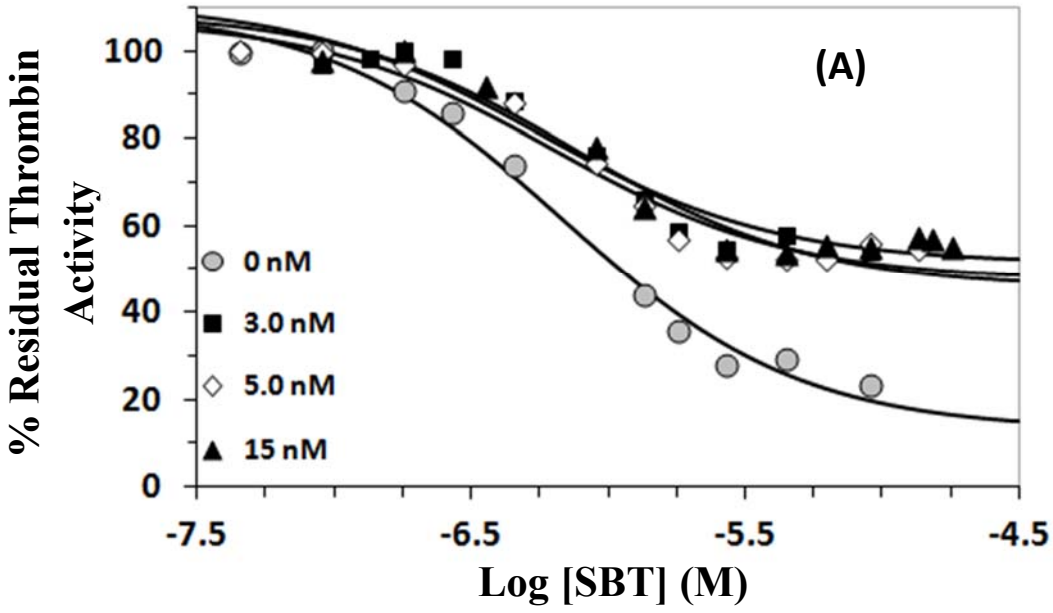
% Residual Thrombin Activity
100
80
60
40
20
0
(A)
0 nM
3.0 nM
5.0 nM
15 nM
-7.5
-6.5
-5.5
-4.5
Log [SBT] (M)

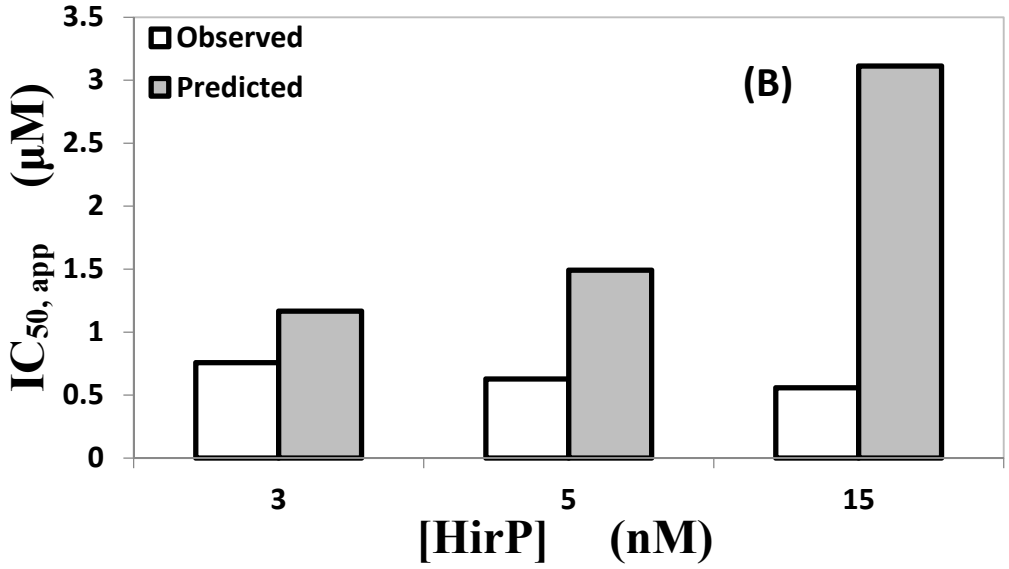
3.5
3
2.5
2
1.5
1
0.5
0
Observed
Predicted
(B)
IC50, app (μM)
3
5
15
[HirP] (nM)

Figure 28

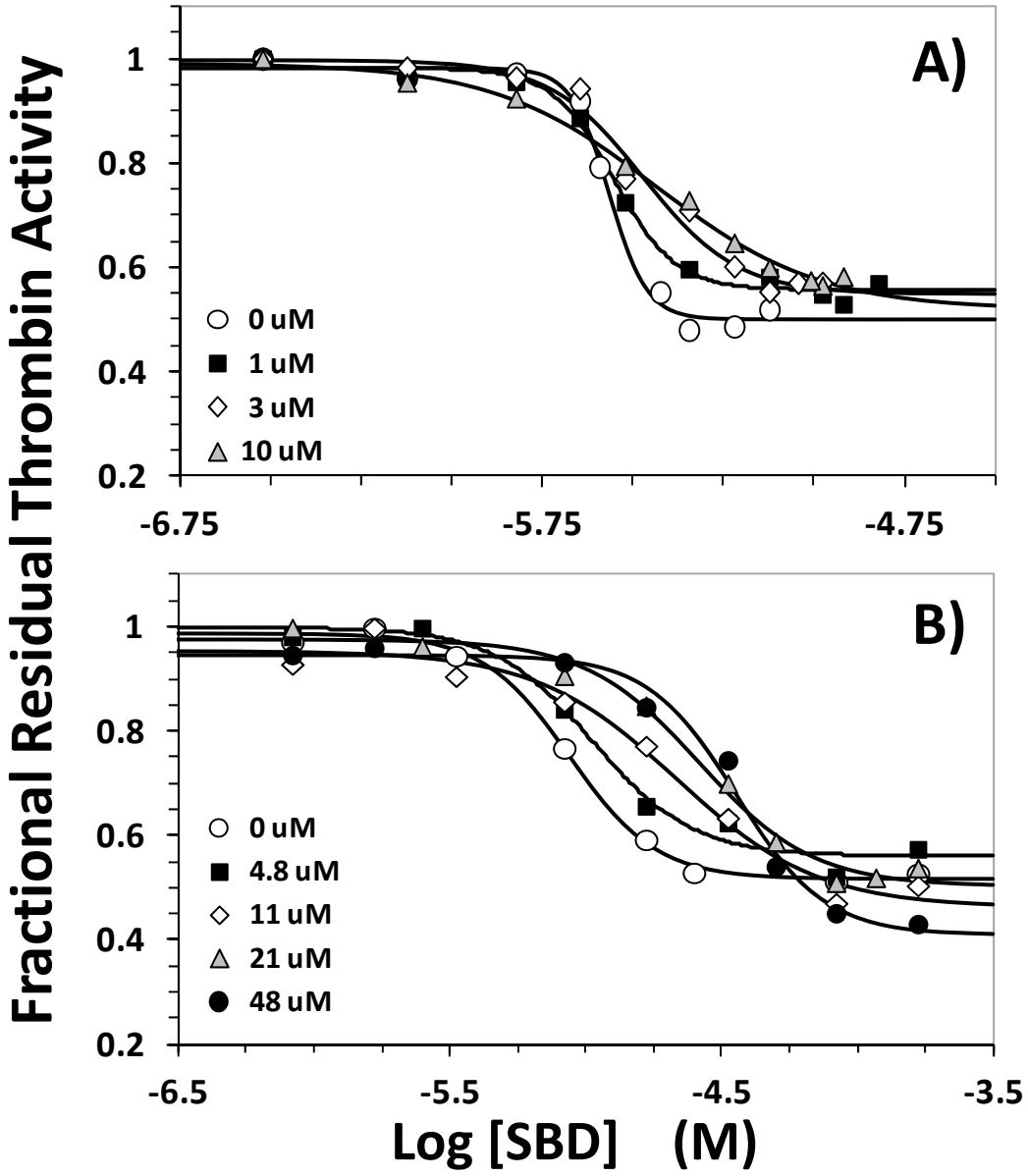
A)
B)
Fractional Residual Thrombin Activity
1
0.8
0.6
0.4
0.2
0 uM
1 uM
3 uM
10 uM
-6.75
-5.75
-4.75
0 uM
4.8 uM
11 uM
21 uM
48 uM
-6.5
-5.5
-4.5
-3.5
Log [SBD] (M)

Figure 29

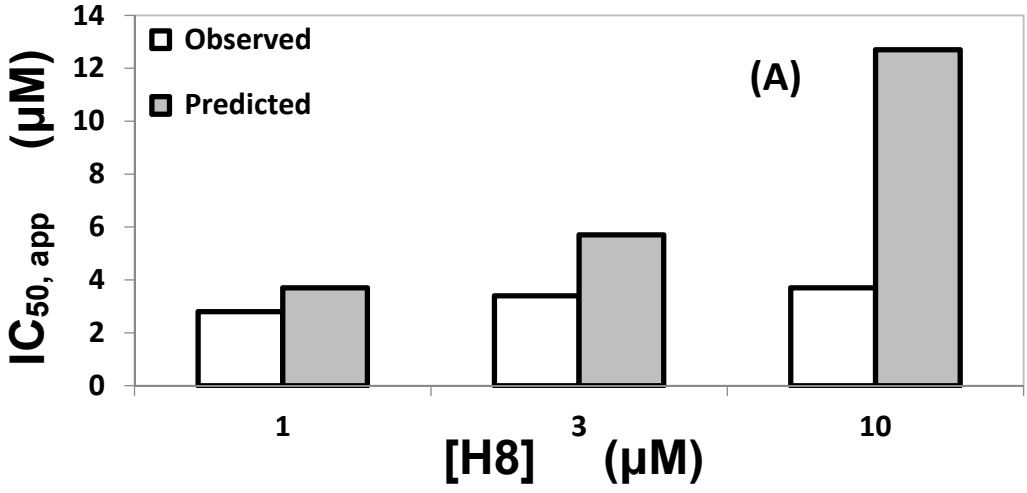
Observed
Predicted
(A)
$IC_{50, app}$ (μM)
14
12
10
8
6
4
2
0
1
3
10
[H8] (μM)

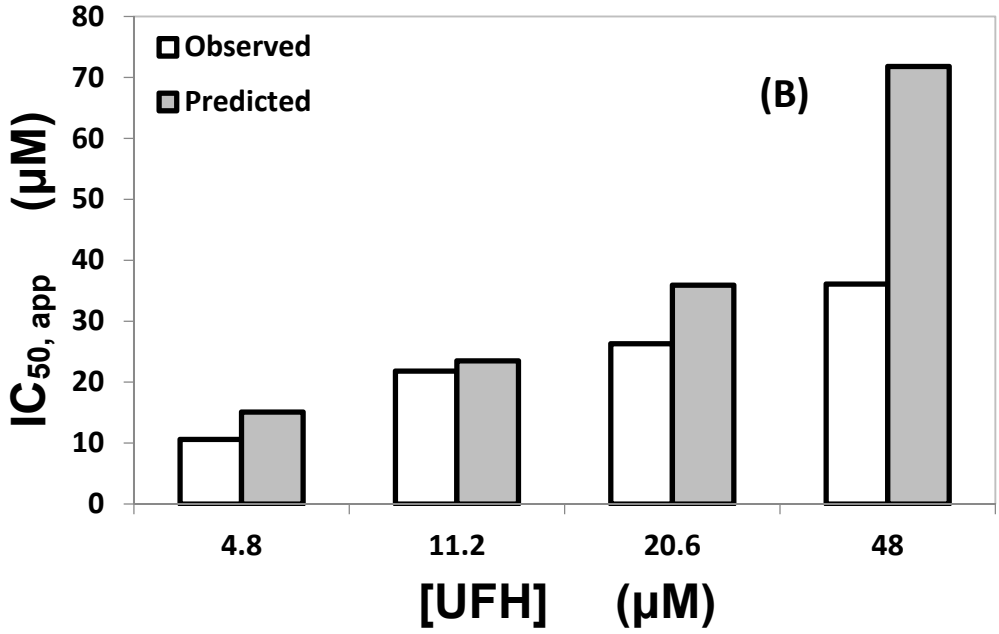
Observed
Predicted
(B)
$IC_{50, app}$ (μM)
80
70
60
50
40
30
20
10
0
4.8
11.2
20.6
48
[UFH] (μM)

Figure 30

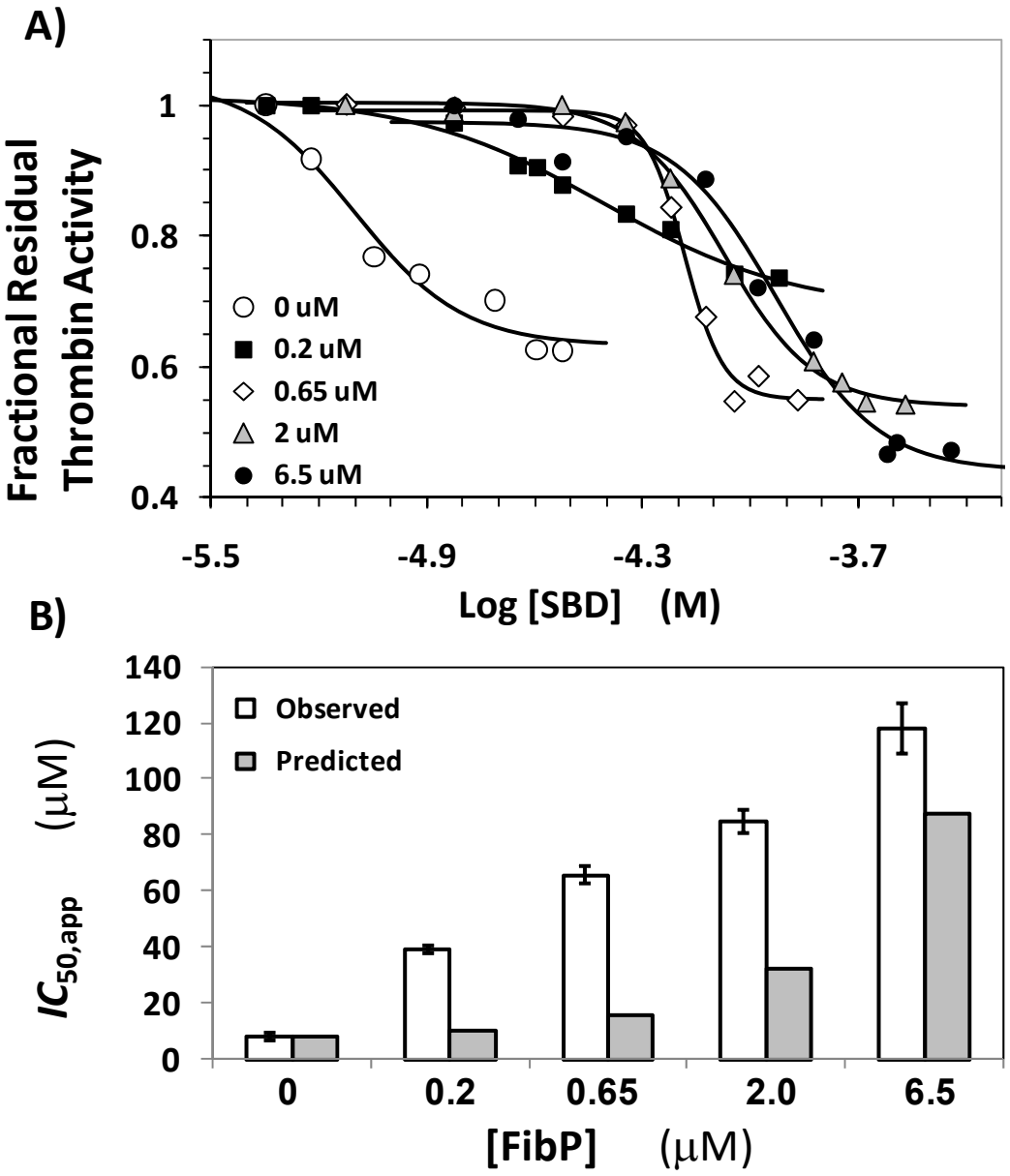
A)
Fractional Residual Thrombin Activity
1
0.8
0.6
0.4
0 uM
0.2 uM
0.65 uM
2 uM
6.5 uM
-5.5
-4.9
-4.3
-3.7
Log [SBD] (M)
B)
$IC_{50,app}$ (μM)
140
120
100
80
60
40
20
0
Observed
Predicted
0
0.2
0.65
2.0
6.5
[FibP] (μM)

Figure 31

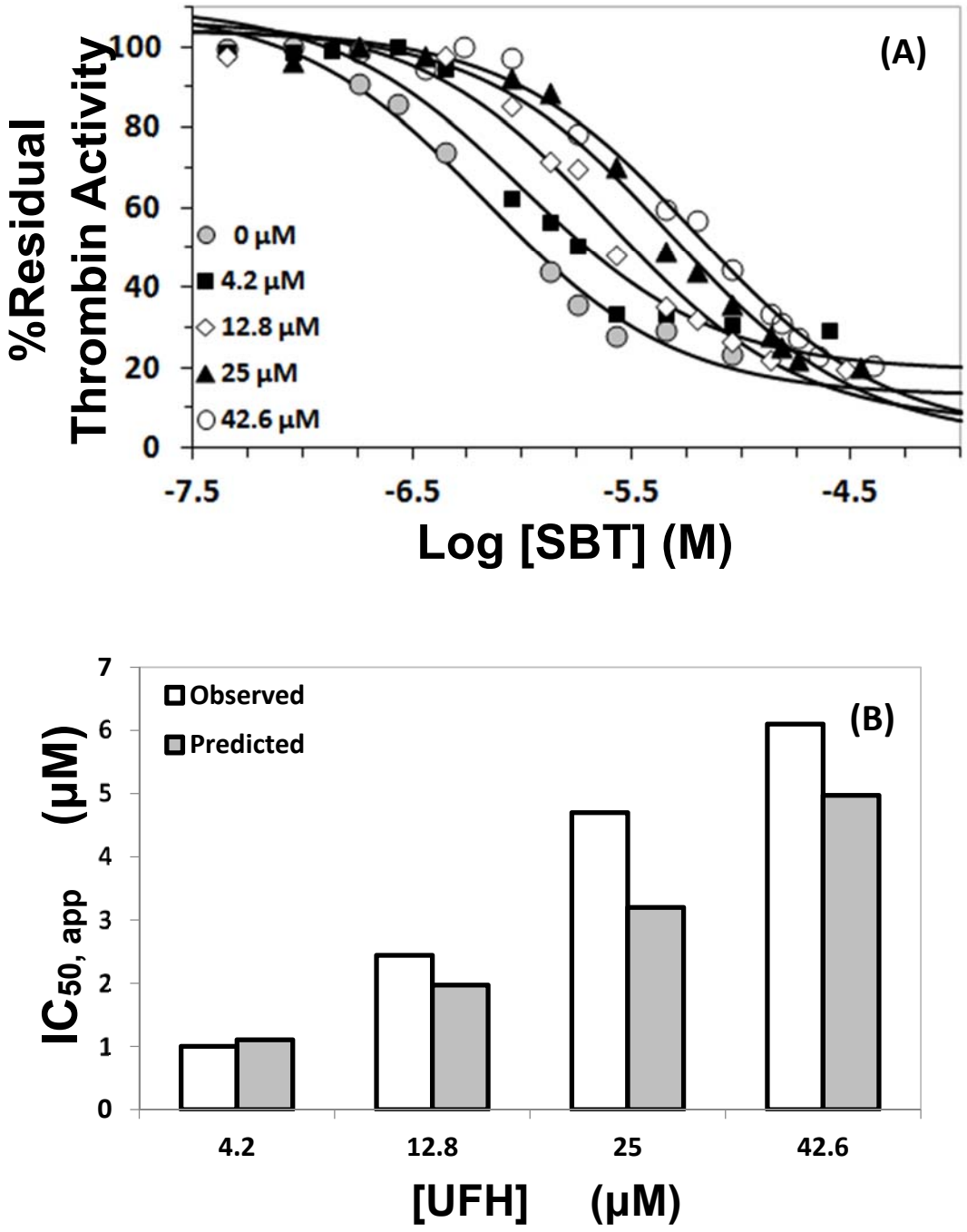
(A)
%Residual Thrombin Activity
100
80
60
40
20
0
0 µM
4.2 µM
12.8 µM
25 µM
42.6 µM
-7.5
-6.5
-5.5
-4.5
Log [SBT] (M)
(B)
Observed
Predicted
IC50, app (µM)
7
6
5
4
3
2
1
0
4.2
12.8
25
42.6
[UFH] (µM)

Figure 32

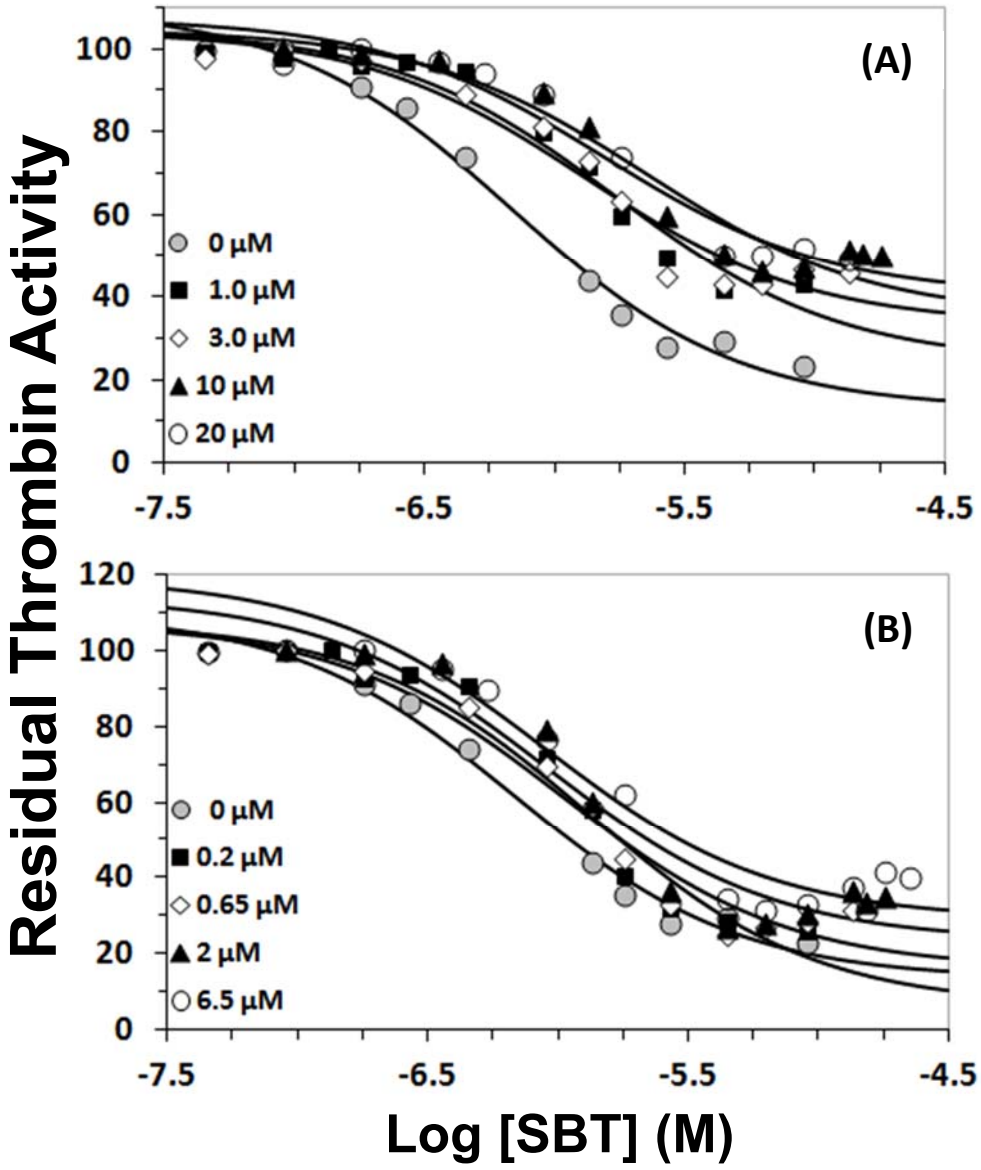
(A)
100
80
60
40
20
0
0 µM
1.0 µM
3.0 µM
10 µM
20 µM
-7.5
-6.5
-5.5
-4.5
(B)
120
100
80
60
40
20
0
0 µM
0.2 µM
0.65 µM
2 µM
6.5 µM
-7.5
-6.5
-5.5
-4.5
Residual Thrombin Activity
Log [SBT] (M)

Figure 33

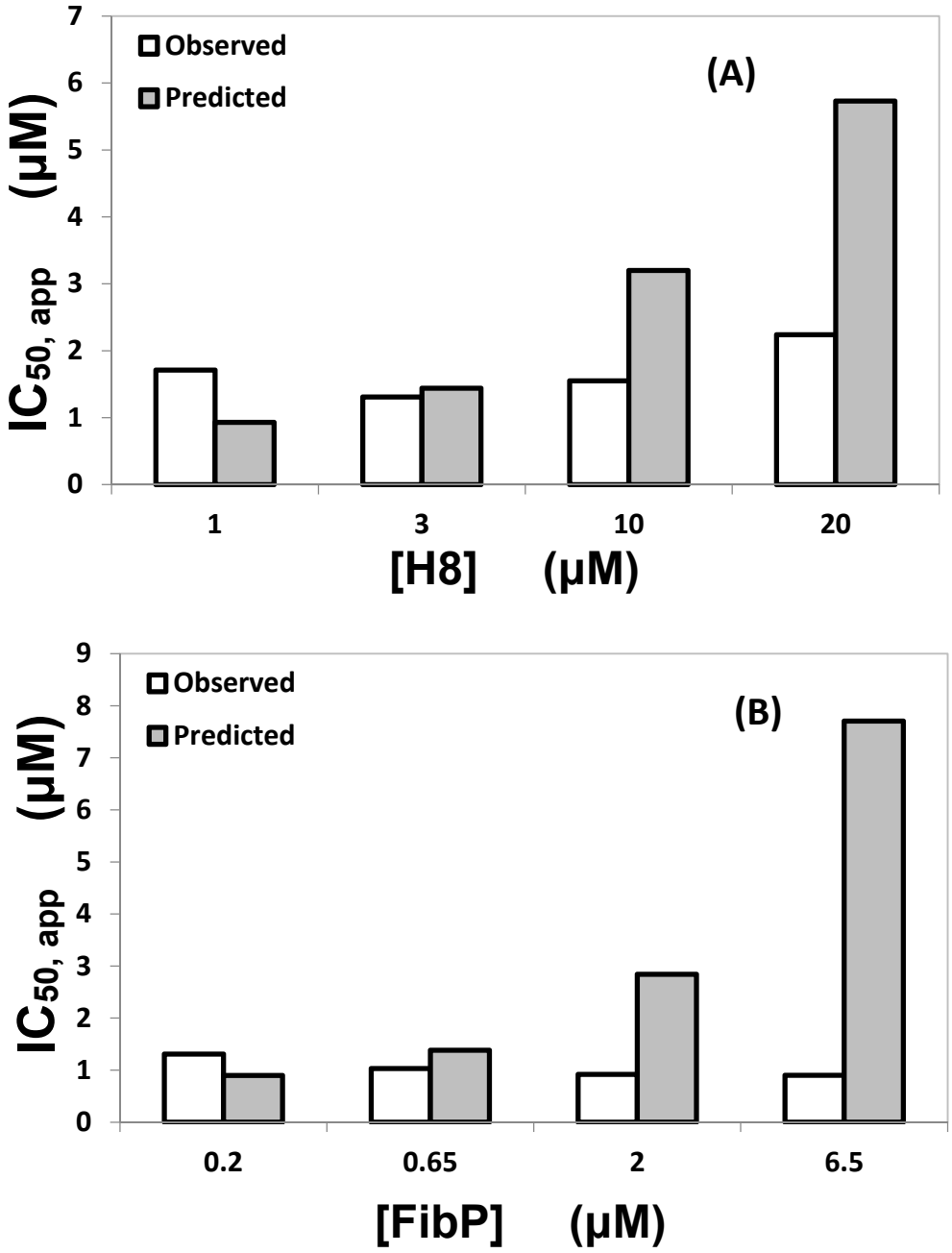
Observed
Predicted
(A)
$IC_{50, app}$ (μM)
0
1
2
3
4
5
6
7
1
3
10
20
[H8] (μM)
Observed
Predicted
(B)
$IC_{50, app}$ (μM)
0
1
2
3
4
5
6
7
8
9
0.2
0.65
2
6.5
[FibP] (μM)

Figure 34

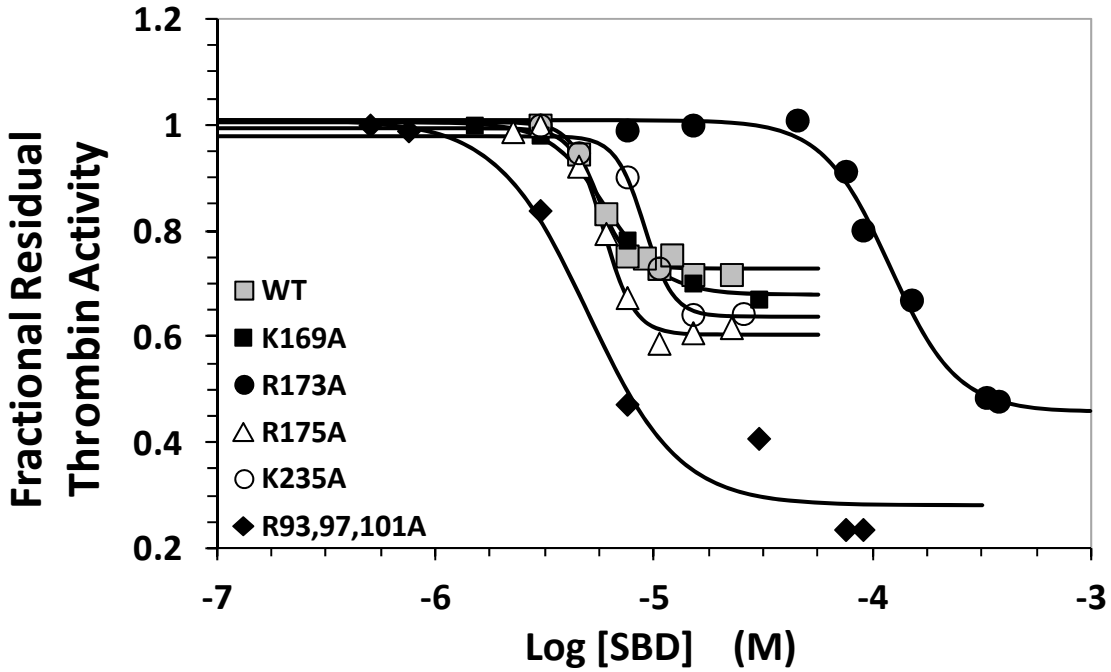
Fractional Residual Thrombin Activity
1.2
1
0.8
0.6
0.4
0.2
WT
K169A
R173A
R175A
K235A
R93,97,101A
-7
-6
-5
-4
-3
Log [SBD] (M)

Figure 35

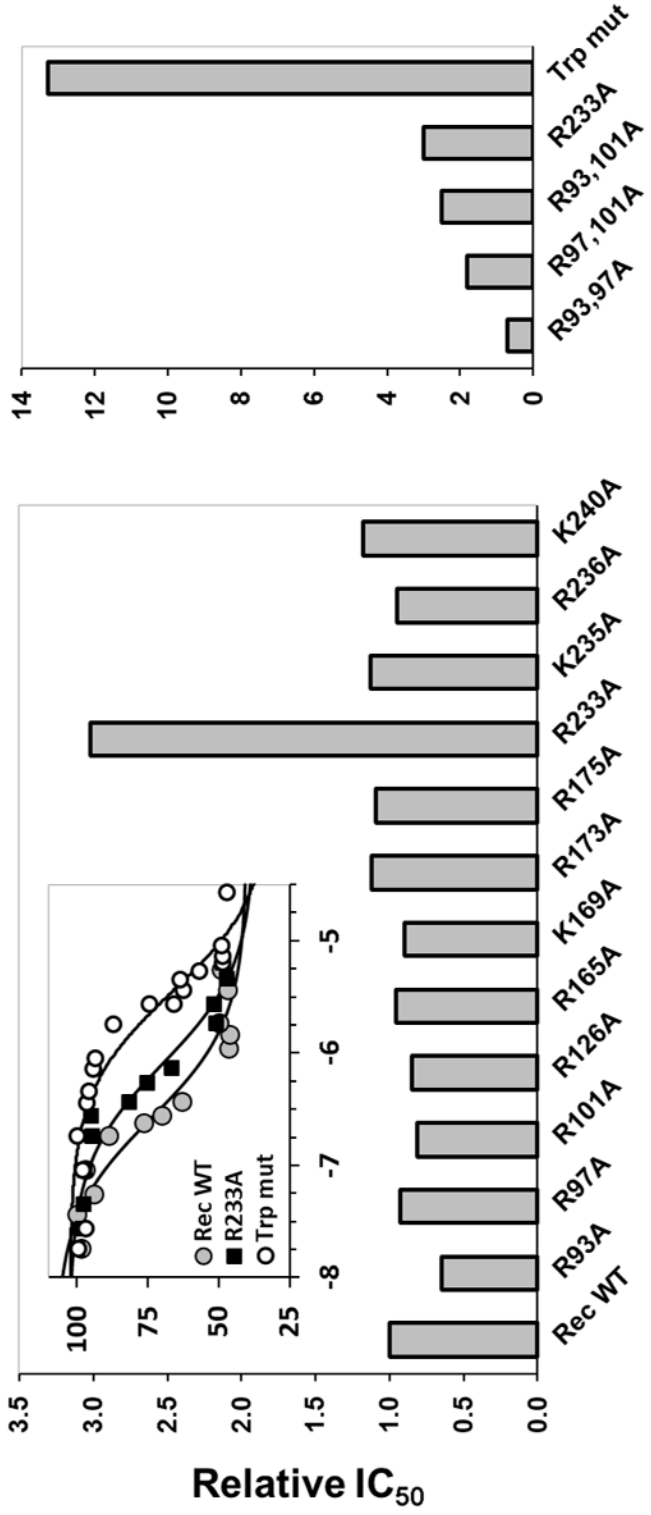
Trp mut
R233A
R93,101A
R97,101A
R93,97A
14
12
10
8
6
4
2
0
K240A
R236A
K235A
R233A
R175A
R173A
K169A
R165A
R126A
R101A
R97A
R93A
Rec WT
Rec WT
R233A
Trp mut
100
75
50
25
-5
-6
-7
-8
3.5
3.0
2.5
2.0
1.5
1.0
0.5
0.0
Relative IC50

Figure 36

Chapter 5: Detailing the Nature of Molecular Interaction between Low Molecular Weight Lignins and Thrombin

5.1. INTRODUCTION

Macromolecules are known by the complex nature of their interactions. Characterizing their binding to proteins, crystallizing their complexes and understanding their binding on the molecular level is more complicated than small drug-like molecules. While some macromolecules have been successfully co-crystalized with thrombin, understanding the way they interact is far less investigated. Taking thrombin as our focus, new theories are introduced each day that prove the intricacy involved in its interactions. Another complication is the presence of the two anion-binding exosites that engage different ligands, some of which bind to both sites. For example, the GpIb receptor present on the platelet surface interacts with exosite 2. However a recent study has shown that the receptor binds to thrombin in a model where each of the two exosites are involved in binding a different GpIb molecule.[67] The energetic linkage between the two exosites when ligands bind is also a well-known controversial issue. For thrombin there are studies that support strongly linked binding[85] and other studies proving that their binding is mutually exclusive.[83]

LMWLs are no exception. As the first macromolecules to inhibit thrombin in an allosteric way by exclusively engaging exosite 2, it was important to understand how they evoke their action. The polymeric nature of these molecules complicates the process of co-crystallizing them with thrombin. This makes it difficult to understand the nature of their interaction from structural data. A way to work around this obstacle is to obtain insight about their binding from other biochemical techniques. Heparin is a good model whose interaction is well characterized by such studies. It

also serves as a good example due to the fact that sulfated LMWLs were initially designed as heparin mimetics.

A multi-disciplinary approach with three major aspects was designed to dissect the interactions of two LMWLs, $CDSO_3$ and $FDSO_3$, with thrombin. The first aspect is to characterize the electrostatics of binding using salt-dependency studies so as to understand the involvement of ionic and non-ionic interactions in the binding. Ionic interactions mainly invoke charge pairs and salt bridges, while non-ionic ones involve hydrophobic interactions and hydrogen bond formation. The two LMWLs are fairly similar in origin and structure, yet analysis of the physicochemical properties showed that $FDSO_3$ had a higher charge density than $CDSO_3$, which offers a better chance for $FDSO_3$ to form ionic interactions.[90] Another difference is the presence of a hydroxyl group in caffeic acid, the monomeric unit for $CDSO_3$, that is replaced by a methoxy group in ferulic acid, the building block for $FDSO_3$. This difference may allow $CDSO_3$ to better hydrogen bond with thrombin. Detailed analysis of the contribution of these forces would elaborate more on the nature of the interaction of these molecules and their similarity to heparin.

The second goal is to characterize the thermodynamic profile of these molecules. Heparin itself is not well characterized in this regard and it would be interesting to compare the behavior of the three polymers. The emerging significance of thermodynamics in drug discovery and more importantly in lead optimization has received considerable attention in literature.[125] The binding of a ligand to its target occurs spontaneously only when the free energy of binding (ΔG) is favorable. This energy is the sum of two terms, enthalpic ΔH and entropic $-T\Delta S$, which can have similar or opposite signs, potentially leading to different thermodynamic signature for each binding event. The binding can be either enthalpy-driven or entropy-driven. Understanding the

contribution of each term to the binding affinity allows their optimization to obtain better ligands with higher affinity and/or specificity to their targets.

The last aspect is to understand the linkage between sodium and LMWLs binding to thrombin. Sodium is well-documented to shift the enzyme to a fast (proteinase-like) form. Removal of sodium has been shown to shift the equilibrium back to the slow (zymogen-like) form.[77] One of the reasons that LMWLs inhibit thrombin could be the displacement of sodium and the concomitant shift to the catalytically less efficient thrombin. Yet, little is known about how the activation of thrombin by sodium affects exosite 2. Studying the effects of changing sodium concentration on the binding affinity of LMWLs may also point out the novelty of these molecules as probes for investigating the binding in thrombin exosite 2.

The three aspects are different in methodology, yet they draw one broad picture about the nature of interaction of these molecules with thrombin. They will be handled individually in the following sections, then a general conclusion for all the results will be presented at the end of the chapter.

5.2. Electrostatics of Binding of LMWLs and Thrombin

Heparin and related molecules follow the polyelectrolyte theory of binding for charged polymers.[126,127] The theory postulates that interaction of charged polymers with proteins results in displacement of large numbers of counter-ions. This leads to an increase in entropy that has a significant contribution to the free energy of binding. Thus, the increase in the ionic strength or salt concentration in the medium leads to weakening of the binding. This phenomena was used extensively for studying heparin interactions.[126-130] The nature of LMWLs as polyelectrolytes makes it feasible to use the same theory for studying their interaction with thrombin. Unfortunately, changing the concentration of sodium in the medium has another important effect on thrombin that can affect the results obtained from such studies. It is well established now that sodium binding activates thrombin catalytic efficiency, while it also leads to conformational changes that have global effects on the enzyme structure,[23,27,28,131,132] which may lead to changing the binding affinity of LMWLs.

To avoid the structural and catalytic side effects of changing sodium concentration on thrombin, we resorted to an active site labeled, inhibited form of the enzyme. Using a fluorescein labeled inhibitor D-Phe-Pro-Arg-CH_2Cl (FPR) that irreversibly alkylates His57 of the catalytic triad achieves two important goals. First, the fluorescence dye reports any structural changes that occur near the environment of the active site. As our molecules bind to exosite 2, they are postulated to induce a conformational change in the active site that the dye will be able to report, and from which the K_D can be calculated. The second goal is that inhibiting thrombin locks the structure of the enzyme in one conformation and thus preventing sodium from changing the structure of the enzyme as it would do with the free form. This will restrict the effects of increasing the sodium concentration in the medium to only the electrostatic disturbance of LMWLs binding.

The same technique was applied before for studying the salt dependancy of thrombin – thrombomodulin interaction.[133]

5.2.1. EXPERIMENTAL

5.2.1.1. Proteins, LMWLs, Chemicals and Reagents.

Sulfated dehydropolymers $CDSO_3$ and $FDSO_3$ (Figure 37) were synthesized in two steps from 4-hydroxycinnamic acid monomers, caffeic acid and ferulic acid, using chemo-enzymatic synthesis.[49] Active site inhibited thrombin labeled with fluorescein (*f*FPR-Th) was purchased from Haematologic Technologies (Essex Junction, VT). Stock solutions of thrombin were prepared in 20 mM Tris-HCl buffer (pH 7.4). All other chemicals were analytical reagent grade from either Sigma Chemicals (St. Louis, MO) or Fisher (Pittsburgh, PA) and used as such.

5.2.1.2. Thrombin – LMWLs Binding Study.

*f*FPR-Th was freshly prepared from stock solution to get a final concentration of 50 nM in 20 mM Tris-HCl buffer, pH 7.4, containing 150 mM NaCl, 2.5 mM $CaCl_2$ and 0.1 % polyethylene glycol (PEG) 8000 at 25 °C in a fluorescence quartz cuvette. Experiments were done using a QM4 fluorometer (Photon Technology International, Birmingham, NJ) thermostated with a Lauda-Brinkmann circulating water bath. Equilibrium dissociation constants (K_D) for either $CDSO_3$ or $FDSO_3$ – thrombin complex were determined by titrating the polymer into a solution of *f*FPR-Th and monitoring the decrease in the fluorescence at $\lambda_{emission}$ = 525 nm ($\lambda_{excitation}$ = 490 nm). The studied molecules did not have any absorbance at the emission wavelength to interfere with the readings (Figure 38). The slit widths on the excitation and emission side were 1 and 2 mm, respectively. The decrease in fluorescence signal upon complex formation was fit to the quadratic equilibrium binding equation 3 to obtain the K_D of interaction:

$$\frac{\Delta F}{F_o} = \frac{\Delta F_{max}\, Q - \sqrt{Q^2 - 4 \times [fFPR - Th]_o \times [LMWL]_o}}{F_o \qquad\qquad 2 \times [fFPR - Th]_o}$$

$$Q = [fFPR - Th]_o + [LMWL]_o + K_D \qquad \textbf{(equation 3)}$$

where ΔF is the change in fluorescence due to formation of the complex following each addition of inhibitor $[LMWL]_o$ from the initial fluorescence F_o, and ΔF_{max} represents the maximum change in fluorescence observed on saturation of *f*FPR-Th. A binding stoichiometry of 1:1 was assumed for the interaction.

5.2.1.3. Salt Dependence of LMWLs – Thrombin Interaction.

The contribution of ionic and non-ionic binding energies to thrombin – LMWLs interaction was determined by measuring the $K_{D,obs}$ of the binding in buffers with increasing salt concentration. NaCl was added to 20 mM Tris-HCl buffer, pH 7.4, containing 2.5 mM $CaCl_2$ and 0.1 % polyethylene glycol (PEG) 8000 in concentrations ranging from 100 – 300 mM using 50 nM *f*FPR-Th. The plot of log $K_{D,obs}$ versus log $[Na^+]$ yields a linear relationship (equation 4) that can be used to analyze the ionic and non-ionic forces involved in binding. The equation also determines the number of ionic interactions formed between the protein and the polyelectrolyte:

$$\log K_{D,obs} = \log K_{D,NI} + Z\psi \log[Na^+] \qquad \textbf{(equation 4)}$$

where $K_{D,obs}$ is the recorded equilibrium dissociation constant, which is a summation of ionic and non-ionic forces, $K_{D,NI}$ is the equilibrium dissociation constant for the non-ionic component of binding (at 1 M Na^+), Z is the actual number of ionic interactions formed between the protein and the polyelectrolyte during binding and ψ is the fraction of counter-ions attached to each charge on the polyelectrolyte and released to solution after binding to protein. The value of ψ for heparin has been experimentally determined to be ~0.8,[23,132] and the same value was used for LMWLs.[28] Thus,

the straight line obtained will have a slope of $Z\psi$ and an intercept of log $K_{D,NI}$ from which the free energy component of non-ionic interaction can be determined according to Gibbs free energy (ΔG) relationship,

$$\Delta G = - RT \ln K_A \qquad \textbf{(equation 5)}$$

where R is the gas constant, T is absolute temperature and K_A is the equilibrium association constant.

5.2.2. RESULTS

5.2.2.1. LMWLs Bind Thrombin with High Affinity and Cause a Conformational Change in Thrombin Active Site.

Binding of $CDSO_3$ and $FDSO_3$ with *f*FPR-Th resulted in a decrease in fluorescence to ~30% of the initial value (Figure 39). This reflects the changes happening in the active site environment, where the label is covalently attached after LMWLs bind at exosite 2. The decrease in fluorescence could be fitted to the quadratic equation 3 to obtain the affinity of interaction. The K_D was found to be 75 nM for $CDSO_3$ and 300 nM for $FDSO_3$ at pH 7.4, 25 °C, and I = 0.15. This corresponds to binding energies of -9.75 kcal/mol for $CDSO_3$ and -8.93 kcal/mol for $FDSO_3$. This is a significantly high affinity for sulfated non-carbohydrate polymers interacting with proteins, which renders these molecules potent thrombin ligands.[134-136]

5.2.2.2. $CDSO_3$ and $FDSO_3$ Show Different Contributions of Ionic and Non-ionic Binding Energies.

The dissociation constants for both polymers were studied under variable salt concentrations using spectrofluorometric titration of the enzyme solution with the ligands. The $K_{D,obs}$ was found to increase with increasing sodium concentration for $CDSO_3$ and $FDSO_3$ (Table

11, Figure 40) as observed before for heparin and heparin pentasaccharide interaction with antithrombin.[23,132] According to the polyelectrolyte theory, the non-ionic component of the binding $K_{D,NI}$ can be obtained from the intercept of the linear plot of log K_D versus log $[Na]^+$ (Figure 41), while the slope can be used to calculate Z, the actual number of ion pair interactions involved in the complex formation.

The slopes of the lines for $CDSO_3$ and $FDSO_3$ plots were 1.66 and 3.65, respectively. This was the first major difference between the two polymers. Assuming ψ to be 0.8, the slopes indicate that $CDSO_3$ forms only 2 ion-pair interactions, while $FDSO_3$ forms 4-5 ionic interactions with thrombin. This result shows that $FDSO_3$ behaves more like heparin in having multiple ionic interactions with thrombin.[28] The intercept for $CDSO_3$ came at a large value of -5.78, which corresponds to a large $K_{D,NI}$ of 1.66 μM. Using equation 5 to estimate the ΔG_{NI} gives a value of 7.91 kcal/mol which is almost 81% of the total binding energy of the complex formation, highlighting the importance of non-ionic forces in $CDSO_3$ interaction with thrombin. On the other hand, $FDSO_3$ had an intercept of -3.35, which represented a $K_{D,NI}$ of 445.76 μM. This translates to ΔG_{NI} of -4.59 kcal/mol which represents 51% of the total binding energy and indicates that $FDSO_3$ enjoys a balanced ionic and non-ionic contributions to its binding to thrombin.

5.2.3. DISCUSSION

LMWLs are structurally and mechanistically distinct from any thrombin inhibitor known to date. Although they were initially designed as heparin mimetics, the molecules were found to inhibit thrombin directly in an antithrombin independent manner. Moreover, it was found that these polymers act allosterically through interacting with exosite 2. The affinity of those polymers was found to be in the nanomolar range, which is quite potent compared to similar non-carbohydrate sulfated ligands interacting with coagulation enzymes and serpins.[134-136] Measuring the affinity

using labeled active site inhibited thrombin puts the enzyme in a locked conformation that is not affected by the variation in sodium concentration used to assess the salt dependency. The change in fluorescence after LMWLs – thrombin complex formation indicates a change in the environment of the active site that is arising from a conformational change induced by the inhibitors' binding and leads to impairing the catalytic efficiency of the enzyme.

Plotting log $K_{D,app}$ versus log [Na^+] displayed a linear relationship, which proves that LMWLs follow the polyelectrolyte theory. From the intercept and slope of the line it was clear that $CDSO_3$ and $FDSO_3$ have distinct profiles of binding energies. While $CDSO_3$ formed only 2 ion-pair interactions with thrombin and the majority of the affinity (~80%) came from non-ionic forces, $FDSO_3$ had more significant salt dependence of K_D that resembled the heparin profiles.[28] The plot indicated that 4 – 5 ion pairs are formed during its complex formation with thrombin and that the polymer enjoyed balanced ionic and non-ionic forces for binding.

The results are expected based on the structural differences between the two related polymers. $CDSO_3$ had side chains of hydroxyl groups that are probably involved in hydrogen bond formation with the basic residues in exosite 2, which would significantly increase the non-ionic contribution to ΔG. This is also corroborated by site-directed mutagenesis data obtained earlier for both polymers. $CDSO_3$ had only two key residues important to its binding, Arg93 and Arg175, and mutating them to Ala led to reducing the inhibition potency by 7 – 8 fold. The formation of only 2 ion-pairs during complex formation reaffirms that fewer ionic interactions may generate high affinity for thrombin and points to Arg93 and Arg175 as the two residues involved in the ion-pair formation. On the other hand, $FDSO_3$ inhibition was not affected by any single point mutation of all arginines and lysines in exosite 2. Double and triple mutants showed progressively impaired inhibition that reached almost 50-fold with triple mutant Arg93,97,101Ala. This highlights the fact

that $FDSO_3$ makes multiple ionic interactions with exosite 2 residues such that knocking down one residue at a time had no effect on its affinity. The results were clarified with the salt dependency data that showed 4 – 5 ion pairs formed in $FDSO_3$ – thrombin complex.

Table 11. The salt dependency of K_D of $CDSO_3$ and $FDSO_3$ was monitored by measuring the K_D using fluorescence titration of *f*FPR-Th in buffers of increasing sodium concentrations.

$[Na^+]$ (M)	K_D (M)[a]	
	$FDSO_3$	$CDSO_3$
0.100	0.12×10^{-6}	ND
0.150	0.30×10^{-6}	0.76×10^{-7}
0.200	1.36×10^{-6}	1.09×10^{-7}
0.250	3.18×10^{-6}	1.60×10^{-7}
0.300	ND[b]	2.40×10^{-7}

[a]The K_D was obtained following analysis of binding to 50 nM fFRP-Th in 20 mM Tris buffer, pH 7.4, containing 100 - 300 mM NaCl, 2.5 mM $CaCl_2$, and 0.1% polyethylene glycol (PEG) 8000 at 25 °C (see 'Experimental').
[b] ND: not determined.

Figure Legends

Figure 37. The two polymeric chains studied, $CDSO_3$ and $FDSO_3$, with possible linkage types shown shaded. Main structural difference in substitution R which may be either –OH or $–OSO_3Na$ in $CDSO_3$ or $–OCH_3$ in $FDSO_3$.

Figure 38. Emission scan of $CDSO_3$ (1 μM), $FDSO_3$ (1 μM) and *f*FPR-Th (200 nM) in 20 mM Tris-HCl buffer (pH 7.4) at 25 °C. Excitation was set at 490 nm and emission scanned from 500 – 600 nm.

Figure 39. Binding of *f*FPR-Th to $CDSO_3$ and $FDSO_3$, where the fluorescence of 50 nM enzyme was monitored in 20 mM Tris buffer, pH 7.4, containing 150 mM NaCl, 2.5 mM $CaCl_2$ and 0.1 % polyethylene glycol (PEG) 8000 as it was titrated by a stock solution of 5 μM LMWLs at 25 °C in a fluorescence quartz cuvette. Solid lines represent fits using equation 3 to obtain the apparent K_D as described in 'Experimental'.

Figure 40. Salt dependency of LMWLs interaction with *f*FPR-Th. The fluorescence of 50 nM enzyme was monitored in 20 mM Tris buffer, pH 7.4, containing increasing concentrations of NaCl (100 – 300 mM), 2.5 mM $CaCl_2$ and 0.1 % polyethylene glycol (PEG) 8000 as it was titrated by a stock solution of 5 μM $CDSO_3$ **(A)** or $FDSO_3$ **(B)** at 25 °C in a fluorescence quartz cuvette. Solid lines represent fits using equation 3 to obtain the apparent K_D as described in 'Experimental'.

Figure 41. A plot for $CDSO_3$ and $FDSO_3$ where data of log K_D obtained from fluorescence titrations where used versus log $[Na]^+$. Solid lines represent linear fits using equation 4 to obtain the $K_{D,NI}$ and Z as described in 'Experimental'.

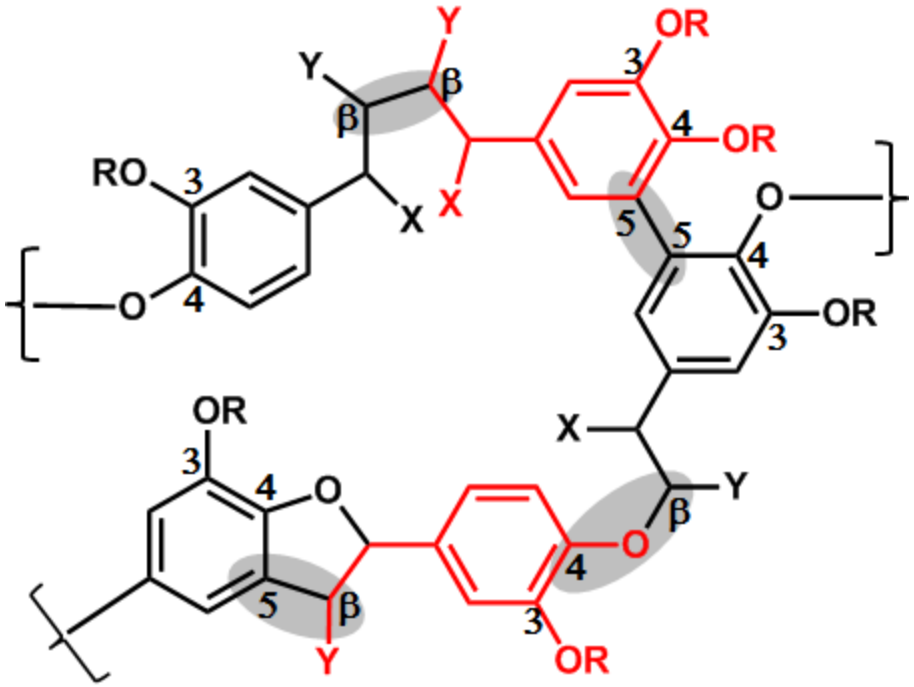

$X = H$ or OH or OSO_3^-

$Y = H$ or COO^-

$CDSO_3$: $R = OH$ or OSO_3^-

$FDSO_3$: $R = OCH_3$

Figure 37

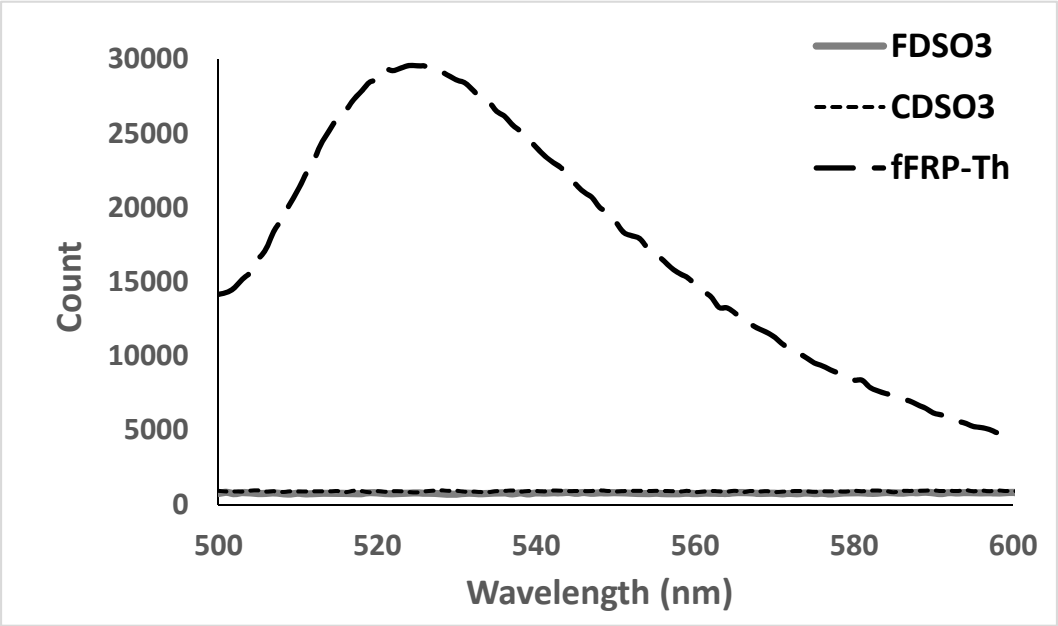
FDSO3
CDSO3
fFRP-Th
30000
25000
20000
15000
10000
5000
0
Count
500
520
540
560
580
600
Wavelength (nm)

Figure 38

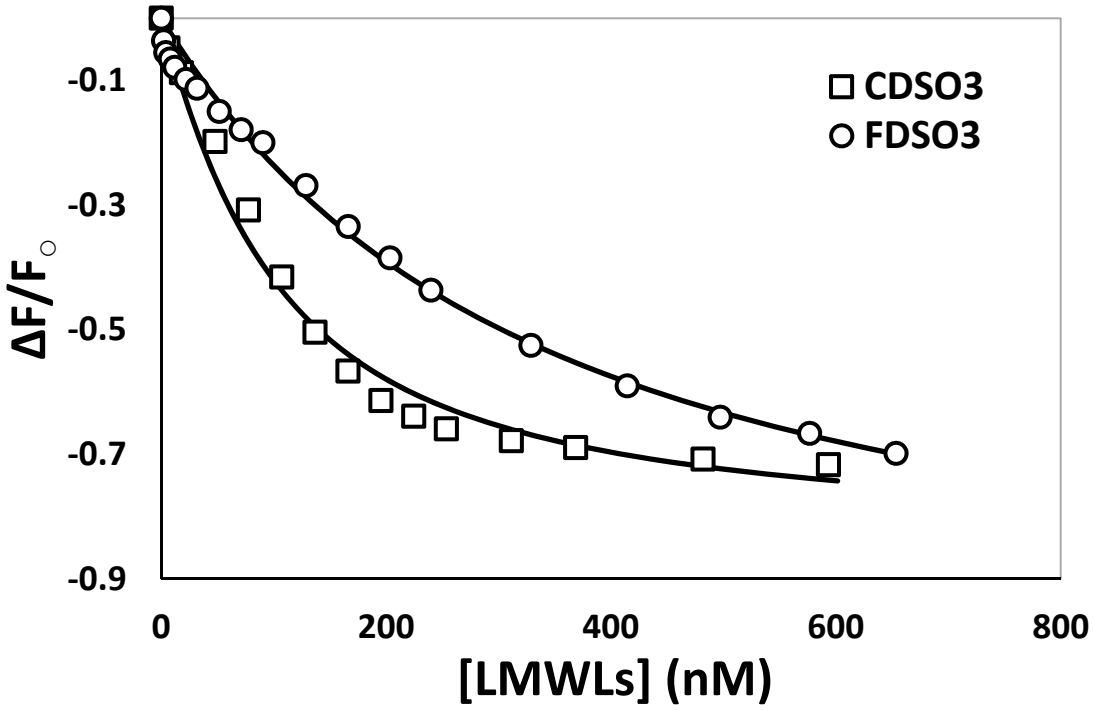

Figure 39

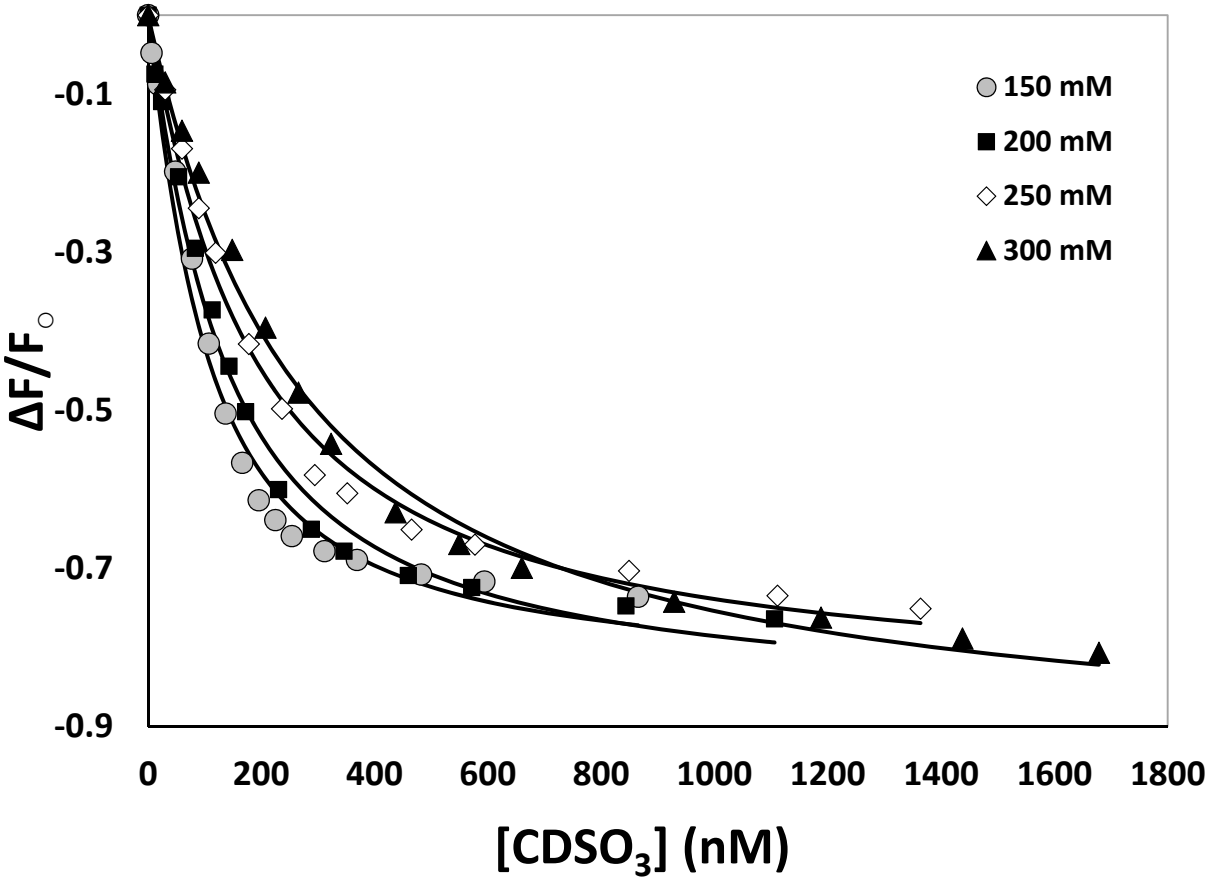
150 mM
200 mM
250 mM
300 mM
-0.1
-0.3
-0.5
-0.7
-0.9
ΔF/F○
0
200
400
600
800
1000
1200
1400
1600
1800
[CDSO3] (nM)

Figure 40A

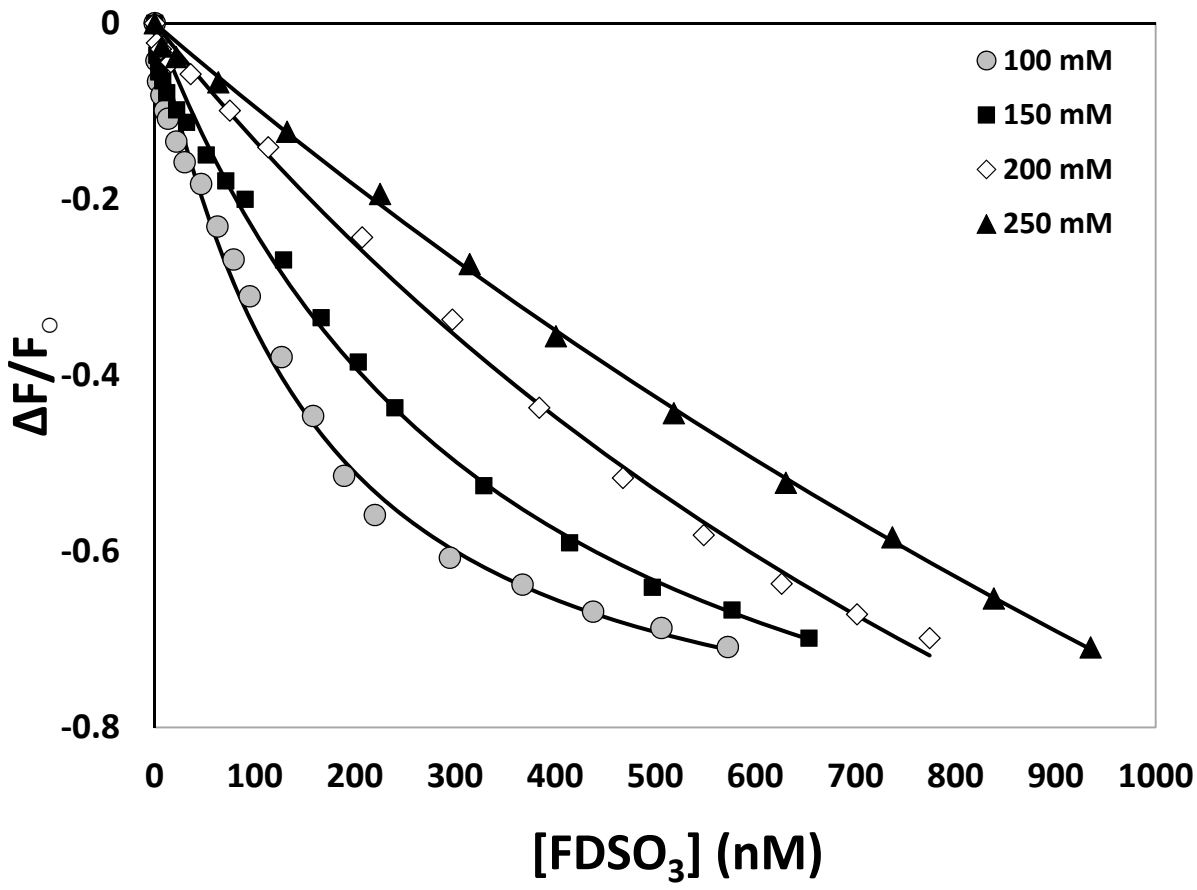
0
-0.2
-0.4
-0.6
-0.8
ΔF/F○
0
100
200
300
400
500
600
700
800
900
1000
[FDSO3] (nM)
100 mM
150 mM
200 mM
250 mM

Figure 40B

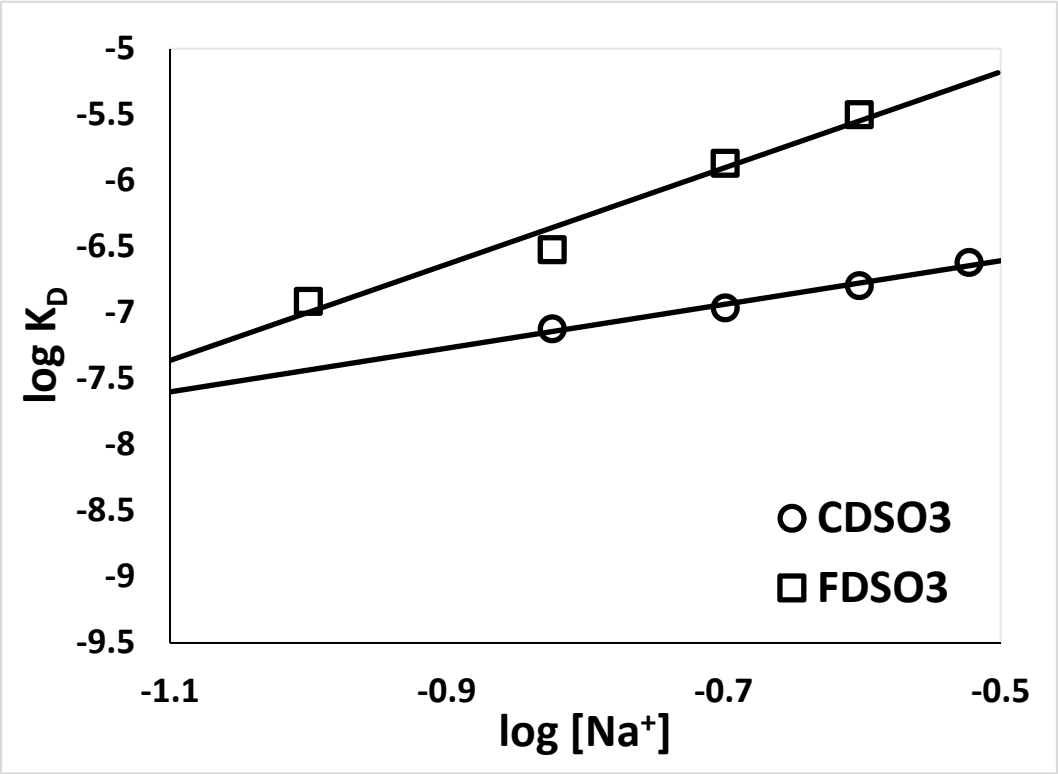

Figure 41

5.3. Thermodynamics of Binding of LMWLs and Thrombin

Acquiring thermodynamic parameters is done using three major methods, either directly through isothermal titration calorimetry (ITC), differential scanning calorimetry (DSC) or indirectly through thermodynamic calorimetry, which does not use a calorimeter.[137] DSC measures heat capacity (Cp) changes as a function of temperature, while ITC is the most comprehensive tool since it measures the heat uptake/release during molecular interaction. This gives a direct measure of the enthalpy of binding (ΔH). It also measures the amount of free or bound ligand, which is used to determine the equilibrium binding constant K_A (inverse of the dissociation constant K_D). From that information, ΔG and other thermodynamic binding parameters like entropy (ΔS) are estimated, and if done at different temperatures, allow the calculation of ΔCp.

Heat capacity is one of the lesser understood, yet rich in information, thermodynamic parameters. With more than a dozen definitions, the most general one (equation 6) would be the amount of heat energy the protein requires to raise its temperature:

$$Cp = \frac{dH}{dT} \quad \textbf{(equation 6)}$$

Other commonly used equation is:

$$Cp = T\ \frac{dS}{dT} = -T^2\ \frac{d^2G}{dT^2} \quad \textbf{(equation 7)}$$

Integrating these equations assuming constant heat capacity gives rise to the modified Gibbs-Helmholtz, or the integrated van't Hoff equation:

$$\Delta G = -RT\ lnK_A = \Delta H - T\Delta S = \Delta Cp\ (T - T_H - T\ ln\frac{T}{T_S}) \quad \textbf{(equation 8)}$$

T_H and T_S are specific temperature values, where the binding enthalpy and entropy vanishes, respectively. T_H in particular is the absolute temperature where the equilibrium dissociation constant assumes its minimum value. This equation has been applied before to thrombin interactions with several of its natural substrates like hirudin and thrombomodulin, and in multiple other biological systems as well, yet it has seldom been used to analyze a protein – polyelectrolyte interaction.[138-141]

Heat capacity changes in protein interactions received significant attention almost 40 years ago. The interpretation of the magnitude and sign of ΔCp is a complex process that implicates protein folding/unfolding and binding to small ligands as well as macromolecules. This is simply the difference between the heat capacity of the complex and heat capacity of its individual components. If the unreacted partners require more heat energy to raise their temperature (i.e., high heat capacity) compared to the complex formed, then the difference (ΔCp) will be negative. The sign of ΔCp could be positive or negative according to the type of interaction between the protein and its binding partner, whether a macromolecule or a small ligand. Protein folding, for example, shows a large negative ΔCp.[137]

Heat capacity changes are attributed to changes in the ordered molecular water layer around the protein and its partner, which have lower kinetic energy than bulk water, allowing it to absorb more heat energy without raising its temperature. When, for example, two hydrophobic surfaces are buried in the binding process, the surface area covered by water in the complex is less than the individual partners, this is known as the hydrophobic effect. This lower number of water molecules can thus absorb less heat energy and the complex as a whole will have lower heat capacity. This is why negative ΔCp is often noted as the hallmark of hydrophobic interactions.[142]

In this work we used thermodynamic calorimetry where we calculate the thermodynamic parameters of LMWLs interaction with thrombin by studying the dependence of the binding on temperature. This technique tracks the changes in K_D at different temperatures using fluorescence. Fitting the data to the integrated van't Hoff equation, one can obtain ΔCp of binding, and calculate ΔH and ΔS at each studied temperature. The electrostatic forces governing the binding of these polyelectrolytes are not common in protein – protein or protein – ligand interactions that mainly involve burial of hydrophobic surfaces and negative heat capacity change (ΔCp). Few cases of polyelectrolyte thermodynamic investigation have been documented in the literature,[27] so unfractionated heparin was also studied under the same conditions as a prototypic example.

5.3.1. EXPERIMENTAL

5.3.1.1. Proteins, LMWLs, Chemicals and Reagents.

Sulfated dehydropolymers $CDSO_3$ and $FDSO_3$ were synthesized in two steps from 4-hydroxycinnamic acid monomers, caffeic acid and ferulic acid, using chemo-enzymatic synthesis.[49] Unfractionated porcine heparin (UFH) was purchased from Sigma (St. Louis, MO). Active site inhibited thrombin labeled with fluorescein (*f*FPR-Th) was purchased from Haematologic Technologies (Essex Junction, VT). Stock solutions of thrombin were prepared in 20 mM Tris-HCl buffer (pH 7.4). All other chemicals were analytical reagent grade from either Sigma Chemicals (St. Louis, MO) or Fisher (Pittsburgh, PA) and used as such.

5.3.1.2. Thermodynamics of LMWLs–Thrombin Interaction.

The thermodynamic parameters of interaction were determined by measuring the K_A of the binding at different temperatures (5 – 45 °C) in 20 mM Tris-HCl buffer, pH 7.4, containing 100 mM NaCl, 2.5 mM $CaCl_2$ and 0.1 % polyethylene glycol (PEG) 8000 in a fluorescence quartz

cuvette. Experiments were done using a QM4 fluorometer (Photon Technology International, Birmingham, NJ) thermostated with a Lauda-Brinkmann circulating water bath. Equilibrium dissociation constants (K_D) for either $CDSO_3$, $FDSO_3$ or the UFH–thrombin complex were determined by titrating the ligand into a solution of *f*FPR-Th and monitoring the decrease in the fluorescence at 525 nm (λ_{ex} = 490 nm) upon complex formation. The studied molecules did not have any absorbance at the emission wavelength to interfere with the readings. The slit widths on the excitation and emission side were 1 and 2 mm, respectively. The decrease in fluorescence of the complex signal was fit to the quadratic equilibrium binding equation 3 to obtain the K_D of interaction at different studied temperatures from which K_A was calculated. The integrated van't Hoff equation 8 was rearranged to

$$\ln K_A = \frac{\Delta C_p^o}{R}\left[\frac{T_H}{T} - \ln\left(\frac{T_S}{T}\right) - 1\right] \quad \textbf{(equation 9)}$$

A plot of K_A versus 1/T yields a non-linear curve; fitting the curve to equation 9 will allow the determination of ΔCp, T_H and T_S. Sigmaplot 8.0 (SPSS, Inc. Chicago, IL) was used to perform non-linear curve fitting in which ΔCp, T_H and T_S were allowed to float. Equation 8 was again rearranged to obtain ΔH and ΔS at each studied temperature, where

$$\Delta S^o = \Delta C_p^o ln\left(\frac{T}{T_S}\right) \quad \textbf{(equation 10)}$$

$$\Delta H^o = \Delta C_p^o (T - T_H) \quad \textbf{(equation 11)}$$

5.3.2. RESULTS

5.3.2.1. Heparin and LMWLs – Thrombin Interactions Follow an Electrostatic Binding Model with a Characteristic Positive ΔC_p.

The thermodynamic parameters for $CDSO_3$, $FDSO_3$ and UFH interaction with thrombin were measured using thermodynamic calorimetry. In this technique the K_D of binding is measured using fluorescence at different temperatures (5 – 45 °C). Active site inhibited thrombin labeled with fluorescein (*f*FPR-Th) was used in the measurements. The decrease in fluorescence due to the complex formation was used to obtain the K_D for either $CDSO_3$, $FDSO_3$ or UFH binding to thrombin at each temperature (Figure 42). This would yield the K_D of interaction at different studied temperatures, from which K_A was calculated (Table 12). Using this information, a plot of ln K_A versus 1/T was plotted and found to have a characteristic U-shaped curve (Figure 43). The integrated van't Hoff equation 9 was used to calculate ΔC_p as well as T_H and T_S for each of the three studied complexes (Table 13). ΔCp of interaction had a positive sign for all interactions ranging between 0.98 – 1.26 kcal/K mol. The positive sign indicates that the complex formation involves burial of a polar surface area on protein, i.e. exosite 2.

The enthalpy and entropy of the interaction at each temperature was estimated using equations 10 and 11, respectively, for each ligand. There was a large dependence of ΔH and ΔS on the temperature of the interaction for all three polymers that caused the values to change signs across the temperature range (Table 14). The data show that for $CDSO_3$ and UFH the interaction is enthalpically driven only at 5 °C and entropically driven at higher temperatures. $FDSO_3$, on the other hand, does not show this inflection except at 30 °C, indicating more favorable enthalpy than the other two ligands. At physiological conditions, the interactions for all three polymers are

entropically driven. The UFH – antithrombin interaction was shown before to be controlled by entropy, linear fitting of van't Hoff equation was applied to obtain the results.[134]

5.3.3. DISCUSSION

The majority of protein–protein interactions and most of the protein–small ligand interactions involve the burial of hydrophobic surface area, which resembles protein folding and warrants a negative sign for ΔCp. Very few protein–protein interactions are dominated by electrostatic and/or hydrogen bonds, which accompany the burial of polar surfaces of the protein. Those reported interactions have a positive ΔCp, like the interaction between xanthine oxidase and superoxide dismutase, which reaches almost 3 kJ/mol.K, and was found to be mediated mainly by hydrogen bond interactions.[144] Likewise, the tetramerization of phosphofructokinase shows a similar behavior.[145] The same applies for protein – DNA/RNA interactions, such as the binding of the translation initiation factor eIF4E to mRNA with ΔCp of 2 kJ/mol.K.[146,147] Some ligands, including polyelectrolytes like heparin, bind to macromolecules with a similar thermodynamic signature, such as heparin binding to cationic cell penetrating peptides (11-89 cal/mol.K)[148] or with brain natriuretic peptide (1 kcal/mol).[149] Heparan sulfate binding to HIV-1 *trans*-acting activator of transcription has similar positive ΔCp value of 135 cal/mol.K[150], while the small molecules inhibitors of HIV-1 protease had a larger value of 3.2 kcal/mol.K.[151]

Another phenomena also complicates the thermodynamic scene, the involvement of water in the binding process, which is known to have an important role especially in carbohydrate – protein complexes.[152-154] Some studies investigating the hydrophobic component of binding found, surprisingly, that it was enthalpically driven.[155-157] This contradicts the classic view of the hydrophobic effect, which predicts that bringing together two hydrophobic partners during binding releases the water at the interface to the bulk solvent and renders the whole process entropic. The

researchers attributed this behavior to the nature of the binding protein surface that was poorly hydrated, thus the enthalpic penalty of breaking the bonds of the few water molecules was overcome by the newly formed ligand–protein interactions and resulted in a large enthalpic gain.[142,156,158]

On the other hand, the release of tightly bound water molecules from the protein binding pockets to bulk solvent is accompanied by a favorable entropic gain estimated to be up to 2 kcal/mol.K at 300 K.[159] Thus, in a well hydrated binding surface, the enthalpic loss due to breaking of multiple bound water molecules is not compensated by the gain from the newly formed interactions with the ligand. This was established using two models in recent literature, thrombin active site binding to a series of inhibitors[160] and selectins binding to the tetrasaccharide sialyl lewis X.[161] The ligand in the former study was termed a "water oligomer" owing to its numerous hydroxide groups, yet it was still incapable of compensating for the enthalpic penalty of water release resulting in an unfavorable ΔH. It logically follows that the bigger and more polar the binding surface, the more hydrated it will be and the larger the enthalpic penalty of binding.

Another contribution of water is through the formation of internal water networks or channels inside the core of the protein that are assumed to transfer allosteric signals between distal sites. One such channel was proposed to exist in thrombin connecting the sodium binding site and the active site 15 A° apart. Binding of sodium is said to organize the water molecules inside the channel leading to signal transmittance that activates thrombin. The ordering of water molecules in the channel was suggested to be the reason behind the large negative ΔCp associated with sodium binding to thrombin.[75] This unexpected thermodynamic signature does not correlate with the size of the pocket where sodium binds, and cannot be explained by the burial of hydrophobic surface area. Similar behavior was seen in sodium interaction with other serine proteases.[76]

The results obtained here prove that the studied polyelectrolytes $CDSO_3$, $FDSO_3$ and UFH have a positive ΔCp and the interaction is indeed entropically driven under physiological conditions. The difference between the two studied inhibitors is also clear. While $CDSO_3$ has favorable enthalpy only at very low temperatures, $FDSO_3$ has enthalpically driven interaction up to 30 °C. This concurs with the fact that $FDSO_3$ had 4 – 5 ion pair interactions formed with thrombin versus only 2 for $CDSO_3$, which means it has better bond formation, i.e., more negative enthalpy.

Table 12. The temperature dependence of the K_D of $CDSO_3$, $FDSO_3$ and UFH measured by fluorescence titration using *f*FPR-Th at different temperatures (5 – 45 °C).

Temp (K)	K_D (M)[a]		
	$CDSO_3$	$FDSO_3$	UFH
278	3.06×10^{-8}	0.38×10^{-8}	6.80×10^{-8}
283	ND[b]	0.70×10^{-8}	9.82×10^{-8}
288	4.67×10^{-8}	2.02×10^{-8}	ND
293	5.15×10^{-8}	2.98×10^{-8}	10.91×10^{-8}
298	3.22×10^{-8}	6.35×10^{-8}	8.75×10^{-8}
303	2.51×10^{-8}	5.11×10^{-8}	4.76×10^{-8}
308	ND	4.11×10^{-8}	ND
313	1.57×10^{-8}	ND	2.26×10^{-8}
318	0.53×10^{-8}	3.30×10^{-8}	ND

[a]The K_D was obtained following analysis of binding to 50 nM fFRP-Th in 20 mM Tris buffer, pH 7.4, containing 100 mM NaCl, 2.5 mM $CaCl_2$, and 0.1% polyethylene glycol (PEG) 8000 at variable temperatures (278 – 318 K) (see 'Experimental').
[b] ND: not determined.

Table 13. The values for K_D, K_A and ΔG at 25 °C and the ΔCp, T_H and T_S for $CDSO_3$, $FDSO_3$ and UFH

Ligand	K_D (M)	K_A (M)	ΔG (kcal/mol)	ΔCp (kcal/K mol)	T_H (K)	T_S (K)
$CDSO_3$	3.22×10^{-8}	3.11×10^{7}	-10.28	0.98	289	279
$FDSO_3$	6.35×10^{-8}	1.58×10^{7}	-9.88	1.26	305	297
UFH	8.75×10^{-8}	1.14×10^{7}	-9.69	1.03	289	280

The K_D, K_A and ΔG are the values previously determined at 25 °C while ΔCp, T_H and T_S were obtained following analysis of K_D previously obtained versus 1/T after applying equation 9 (see 'Experimental).

Table 14. Temperature dependence of thermodynamic parameters of thrombin interaction with $CDSO_3$, $FDSO_3$ and UFH

Temperature (K)	$CDSO_3$		$FDSO_3$		UFH	
	ΔH (kcal/mol)	TΔS (kcal/K mol)	ΔH (kcal/mol)	TΔS (kcal/K mol)	ΔH (kcal/mol)	TΔS (kcal/K mol)
278	-10.92	-1.33	-33.86	-23.02	-11.21	-2.05
288	-1.12	8.60	-21.26	-11.02	-0.91	8.36
293	3.78	13.69	-14.96	-4.86	4.24	13.70
298	8.68	18.86	-8.66	1.41	9.39	19.12
303	13.58	24.12	-2.36	7.79	14.54	24.64
310	20.44	31.62	6.46	16.89	21.75	32.50
318	28.28	40.37	16.54	27.54	29.99	41.68

ΔH and ΔS were obtained after previous determination of ΔCp, T_H and T_S after applying equations 10 and 11 (see 'Experimental').

Figure Legends

Figure 42. The temperature dependence of K_D for **A)** $CDSO_3$, **B)** $FDSO_3$ and **C)** UFH, using 50 nM *f*FPR-Th for $CDSO_3$ and $FDSO_3$ or 200 nM *f*FPR-Th for UFH in 20 mM Tris buffer, pH 7.4, containing 100 mM NaCl, 2.5 mM $CaCl_2$, and 0.1% polyethylene glycol (PEG) 8000 at variable temperatures (278 – 318 K) (see 'Experimental').

Figure 43. The temperature dependence of ln K_A of binding for $CDSO_3$, $FDSO_3$ and UFH studied using fluorescence titration of *f*FPR-Th in 20 mM Tris buffer, pH 7.4, containing 100 mM NaCl, 2.5 mM $CaCl_2$, and 0.1% polyethylene glycol (PEG) 8000 at variable temperatures (278 – 318 K) (see 'Experimental'). Solid lines represent regressional fit to equation 9 where ΔCp, T_H and T_S were allowed to float.

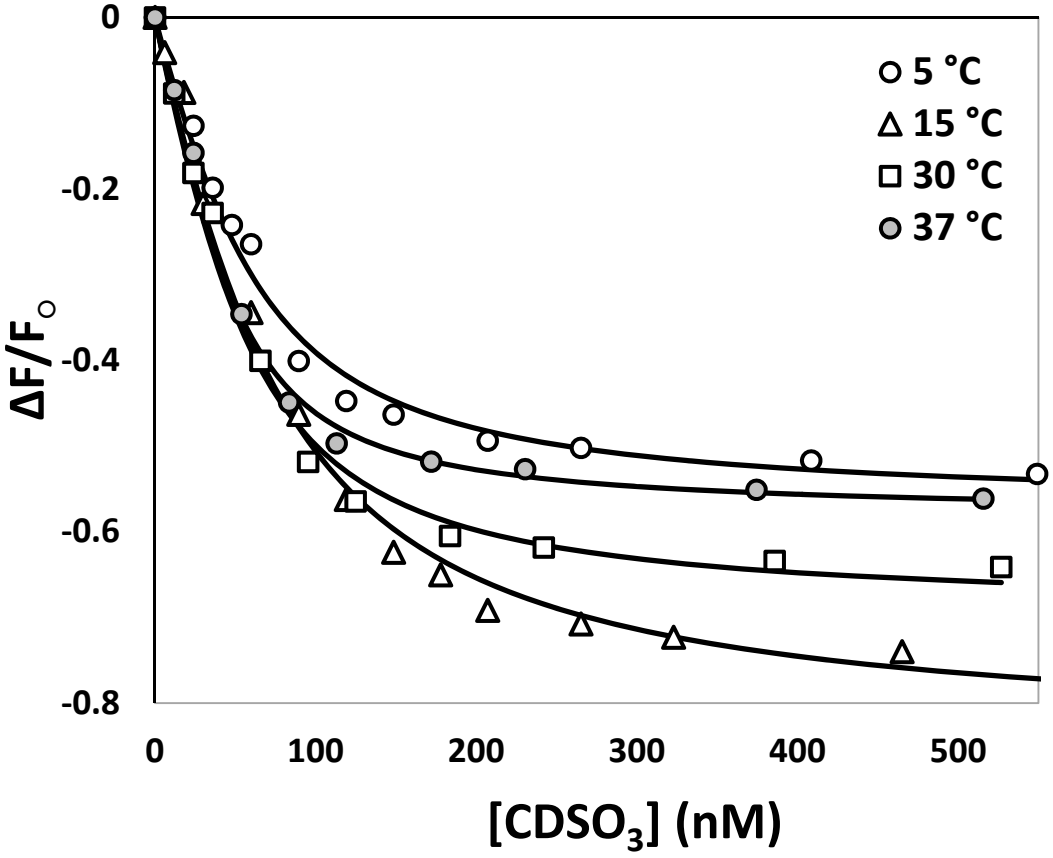

Figure 42A

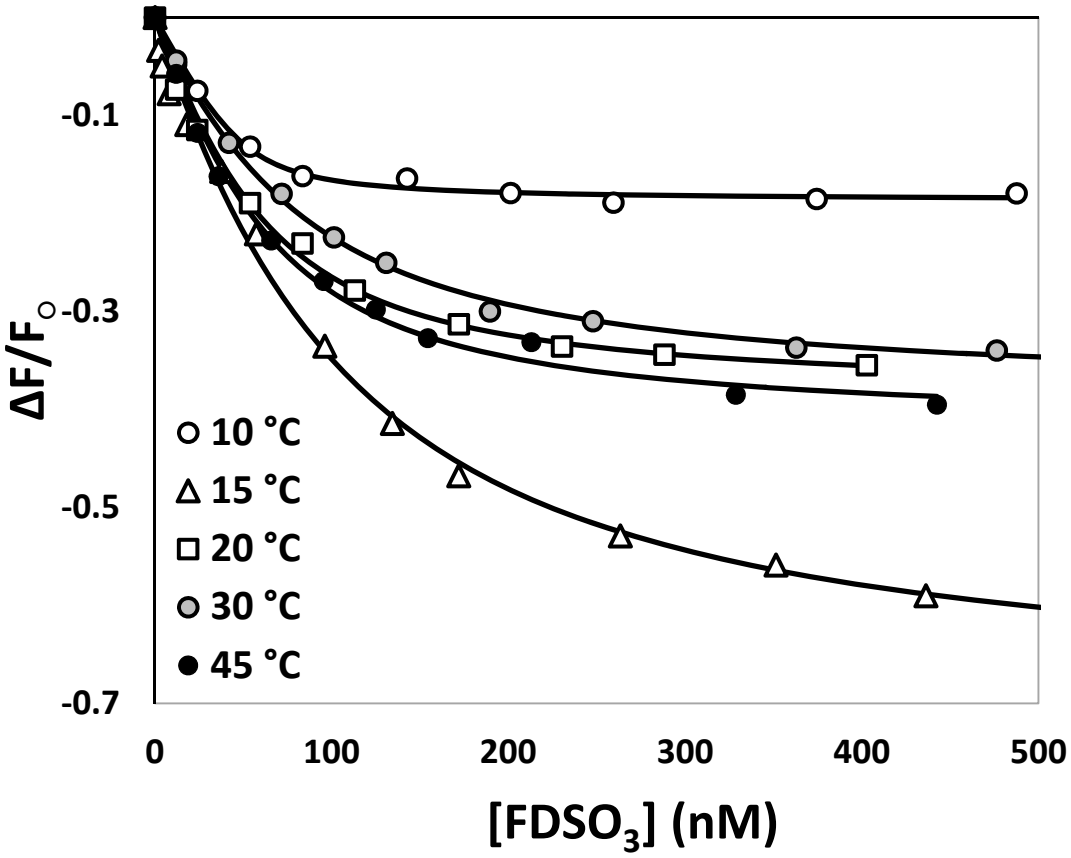

Figure 42B

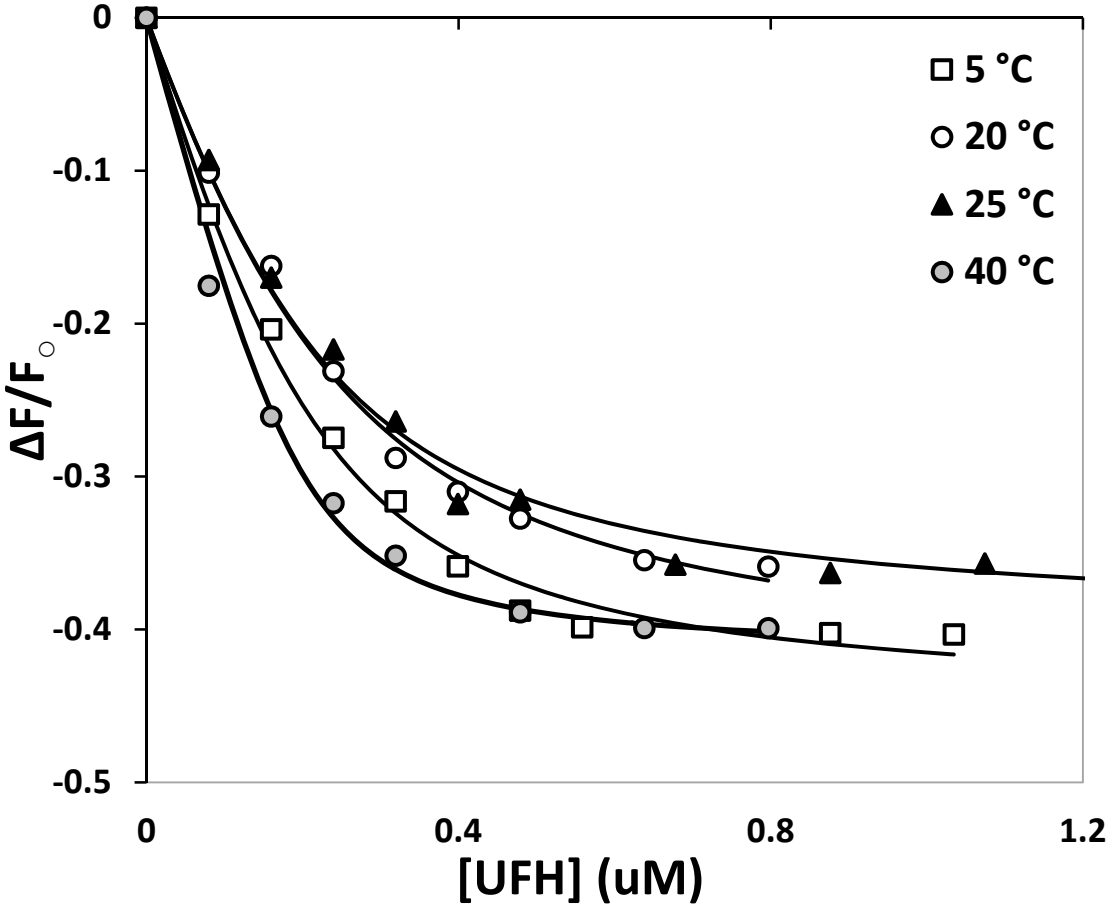

Figure 42C

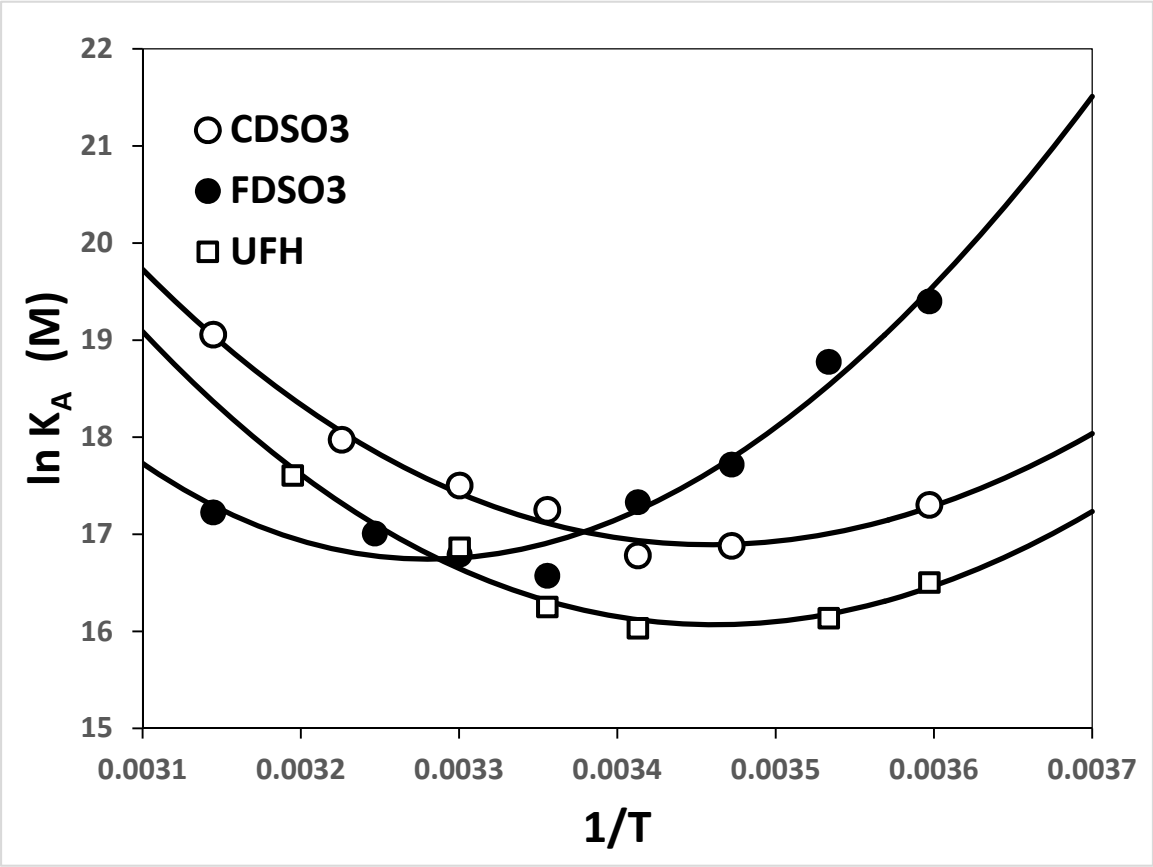
22
21
20
19
18
17
16
15
ln K_A (M)
CDSO3
FDSO3
UFH
0.0031
0.0032
0.0033
0.0034
0.0035
0.0036
0.0037
1/T

Figure 43

5.4. Energetic Linkage between Sodium Binding Site and Exosite 2 of Thrombin

Sodium is well known as an allosteric effector for thrombin. It is not a cofactor since the enzyme is catalytically active in its absence. Yet, the activity increases significantly after sodium binds.[54-56,71] This has led to the now famous designation of "slow" and "fast" thrombins.[53,60] Fast thrombin mainly acts on fibrinogen and PARs, while in the sodium-free form it is better geared towards protein C activation.[60] Hence, sodium promotes the pro-coagulant functions of thrombin, while in its absence, the enzyme initiates its anticoagulant role. Sodium binding has a global effect on the structure of the enzyme. The change in intrinsic fluorescence of thrombin was used to study the effects of sodium binding. All the nine tryptophans of thrombin were mutated one at a time to phenylalanine. Each mutant experienced a change in the fast phase of fluorescence increase, which represents the kinetics of Na^+ binding to thrombin. This indicated that the conformational change is not only restricted to the active site, but it is extended to affect the entire enzyme.[72] Similar effects were induced by hirudin binding to exosite 1, even in absence of sodium. It was postulated that occupancy of either sodium binding site or exosite 1 stabilizes the enzyme, yet to shift thrombin to the fully active conformation, both sites need to be occupied.[81]

The linkage between sodium binding and the active site, and that between sodium binding and exosite 1, or between exosite 1 and the active site is discussed in a number of papers.[60,65,78-81] Contradictory studies were published regarding the connection between exosites 1 and 2, ranging from strong linkage[85] to mutually exclusive binding.[83] Yet, very few studies discuss the interplay of exosite 2 with any of these domains. This can be attributed to the fact that beside GAGs, few ligands were known to interact with this domain, none of which affected the catalytic efficiency of thrombin.

A recent publication reported an exosite 2 ligand (F12 fragment) that shows preferred binding to the thrombin zymogen-like form. Increasing sodium concentration to the physiological level shifts thrombin to the proteinase (fast) form and dramatically decreases the binding of this ligand. Thrombin was shown to be almost 80% saturated with sodium under physiological conditions, which means that it is mostly found in the fast form in blood.[77] Our lab has been working on developing allosteric direct inhibitors for thrombin that target exosite 2. The hypothesis that exosite 2 ligands prefer the slow form of thrombin would make those inhibitors clinically less relevant.

To test this hypothesis, experiments were designed to assess $FDSO_3$ affinity for thrombin under different sodium concentrations. This was done by directly measuring K_D using surface plasmon resonance (SPR). Thrombin was fixed to a gold chip using a standard amine coupling technique. The calculated kinetic parameters are used to estimate the binding affinity according to the equation:

$$K_D = \frac{k_{off}}{k_{on}} \quad \textbf{(equation 12)}$$

A series of buffers with varying concentration of sodium chloride were used as the running buffer, keeping the ionic strength constant using choline chloride. This prevents the electrostatic interference arising from variation in the salt content and focuses on the structural consequences of varying sodium concentration.

5.4.1. EXPERIMENTAL

5.4.1.1. Proteins, LMWLs, Chemicals and Reagents.

The sulfated dehydropolymers $CDSO_3$ and $FDSO_3$ were synthesized in two steps from 4-hydroxycinnamic acid monomers, caffeic acid and ferulic acid, using chemo-enzymatic

synthesis.[49] Mixed, self-assembled monolayer of alkanethiolates generated from the combination of polyethylene glycol-terminated alkanethiol (90%) and COOH-terminated alkanethiol (10%) slides were purchase from Reichert Technologies (Buffalo, NY). Human α-thrombin was purchased from Haematologic Technologies (Essex Junction, VT). Stock solutions of thrombin were prepared in 10 mM sodium acetate buffer (pH 5.2). All other chemicals were analytical reagent grade from either Sigma Chemicals (St. Louis, MO) or Fisher (Pittsburgh, PA) and used as such.

5.4.1.2. Measuring the Affinity of $FDSO_3$ – Thrombin Interaction Using Surface Plasmon Resonance (SPR).

The affinity of $FDSO_3$ binding to thrombin was determined using 10 mM HEPES buffer (pH 7.4) containing 2.5 mM $CaCl_2$, 0.1 % PEG 8,000 as the running buffer. Thrombin was attached to mixed, self-assembled monolayer sensor chips using a standard amine coupling technique. In the coupling process, the surface of the slide is initially activated by injecting a solution of 1-ethyl-3-[3-dimethylaminopropyl]carbodiimide (EDC) and N-hydroxysuccinimide (NHS), mixed right before the injection, for 20 min at a flow rate of 10 µl/min. This was followed by injecting 100 µM thrombin at a flow rate of 10 µl/min for 20 min to load the enzyme on one channel only on the chip surface (sample channel). The loading was monitored by the increase in response unit that indicate thrombin attachment. The other channel was kept unchanged (reference channel). After loading thrombin, the remaining activated surface on the sample channel as well as the reference channel was treated twice with 1M ethanolamine (pH 8.5) for 20 min at 10 µl/min flow rate, repeating this step is essential to ensure blockage of the remaining active groups on the chip that can lead to non-specific binding. A serial dilution of $FDSO_3$ (20 – 2,400 nM) was injected at a flow rate of 50 µl/min on the two channels of the loaded chip, each concentration was allowed 3 min

for association, this was followed by buffer flow for 6 min at 50 µl/min to allow dissociation. The surface of the slide was regenerated in-between the injections using 20 mM NaOH for 15 sec at 50 µl/min. The reading from the reference chip as well as three blank injections were used to account for any non-specific binding or baseline drift. Data obtained was processed using Scrubber 2 software®.

5.4.2. RESULTS

5.4.2.1. $FDSO_3$ Binding and Inhibition Is Improved by Increasing Sodium Concentration.

The study was performed in constant ionic strength buffers (0.2 M) to ensure the electrostatic component of $FDSO_3$ binding will remain the same with varying Na^+ concentration. As the concentration of sodium increased, there was a decrease in the K_D, which indicates an improved affinity of binding (Figure 44, Table 15). The affinity increased from 49.2 nM to 1.29 nM as sodium concentrations increased from 0 – 200 nM. The K_D values were used as a signal to estimate the affinity of sodium binding to thrombin (Figure 45) using standard binding equation:

$$f = B_o + \frac{B_{max}\,[Na]^+}{(K_D + [Na]^+)} \qquad \textbf{(equation 13)}$$

The K_D was calculated to be 1.9 ± 0.4 mM, which is in good agreement with the most recent published data of 4 mM.[77] The data show clearly that, unlike the reported F12 fragment that binds at exosite 2, $FDSO_3$ binding is improved with higher sodium concentrations. This essentially means that it binds preferentially to the "fast" proteinase thrombin, which is the prevalent and clinically relevant form.

5.4.3. DISCUSSION

Unlike all known exosite 2 ligands, our molecules were shown to inhibit thrombin in a direct, antithrombin-independent manner. A recent study postulated that a series of species or conformations of thrombin exists between the activated proteinase-like and zymogen-like states.[77] Lower affinities were reported for an exosite 2 binding ligand (F12 fragment) when the sodium concentration was increased. To determine if increasing sodium concentrations will decrease the affinity of $FDSO_3$, the K_D was measured with increasing sodium concentrations using SPR.The ionic strength was kept constant at 0.2 M using complementary concentrations of choline chloride. As the sodium concentration increased in the running buffer, $FDSO_3$ showed increased affinity for exosite 2. The affinity increased from 50 nM in absence of sodium to ~2 nM in presence of 0.2 M sodium (Table 15). This indicated that unlike the reported exosite 2 ligand, our molecules show preference for binding to the proteinase form of thrombin that prevails under physiological levels of sodium.

Previous publications showed that energetic linkages exist between active site, sodium binding site and exosite 1. This work presents a proof that the energetic linkage between sodium binding site and exosite 2 is direct and effector-dependent. $FDSO_3$ shows increased binding and inhibition with increased sodium concentration, unlike the F12 fragment reported to have lower affinity with sodium binding. The data offers a more comprehensive view of the allosteric network of thrombin, where signaling can be bidirectional and ligand dependent. Na^+ binding is needed for stabilizing the conformation of thrombin and our results show that this leads to better binding for exosite 2 ligands.

Table 15. The salt dependency of K_D of $FDSO_3$ was monitored by measuring the k_A and k_D using SPR in buffers of increasing sodium concentrations (0 – 200), ionic strength was kept constant using complementary concentrations of chloride.

$[Na]^+$ (mM)	$[Choline]^+$ (mM)	$FDSO_3$ K_D (nM)[a]
200	0	1.29
150	50	5.79
50	150	7.32
20	180	8.96
7.5	192.5	11.4
5	195	13.4
3	197	24.2
0	200	49.2

[a]K_D was measured using Scrubber® software by fitting the association and dissociation rate constants obtained directly from SPR to equation 12 (see experimental section).

Figure Legends

Figure 44. Binding isotherms for binding of $FDSO_3$ to the immobilized thrombin using surface plasmon resonance. Increasing concentrations of $FDSO_3$ (80, 160, 240, 320, 400 nM) were bound to thrombin at 25 °C in either 150 mM (black lines) or 5 mM (grey lines) of NaCl complemented by 50 or 195 mM choline chloride, respectively. Injections were done to allowing association (3 minutes) then buffer flowed for dissociation (6 minutes). Scrubber software was used to calculate affinity based on a 1:1 binding model, fit is shown in thick lines versus thin lines for actual data.

Figure 45. K_D determined by SPR used as a signal to calculate the affinity of sodium binding to thrombin. Solid lines represent the regressional fit to equation 13 in which K_D, B_o and B_{max} were allowed to float.

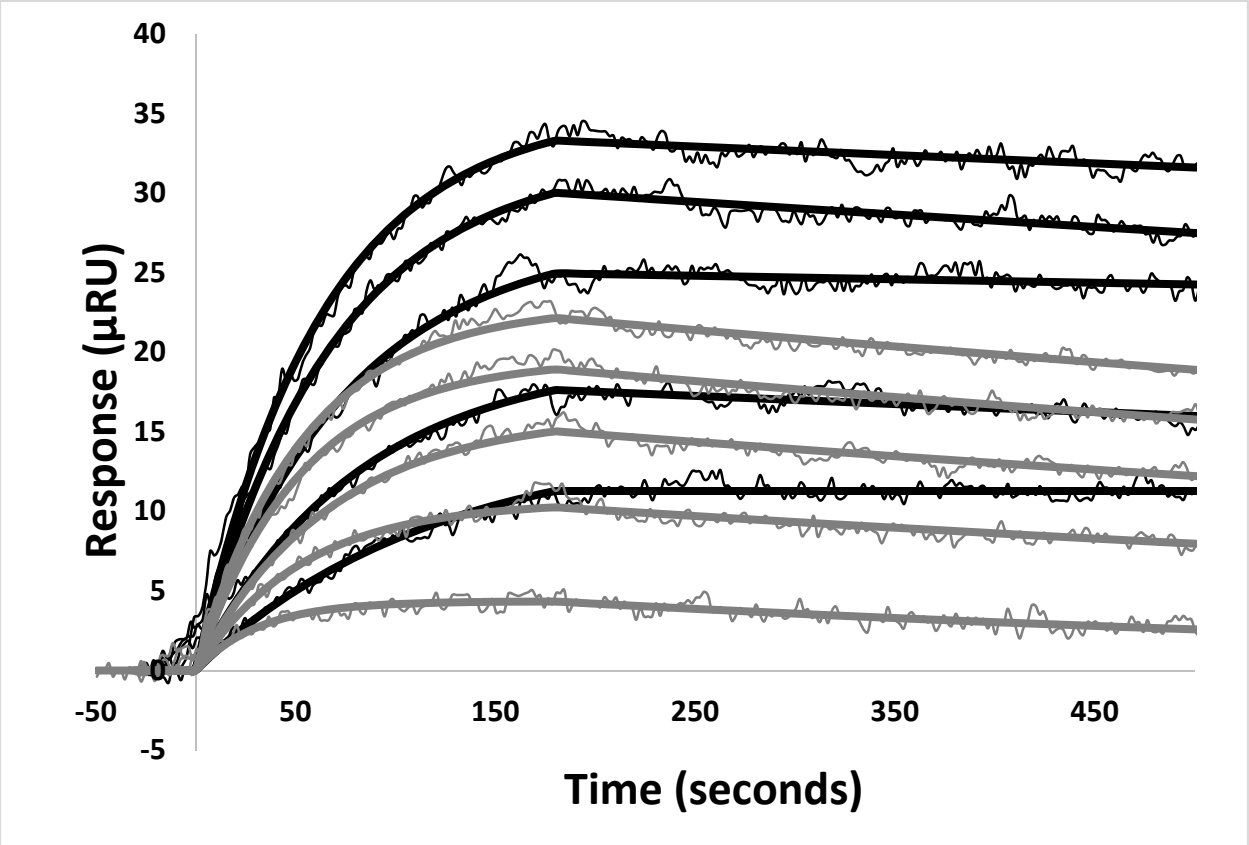
40
35
30
25
20
15
10
5
0
-5
Response (µRU)
-50
50
150
250
350
450
Time (seconds)

Figure 44

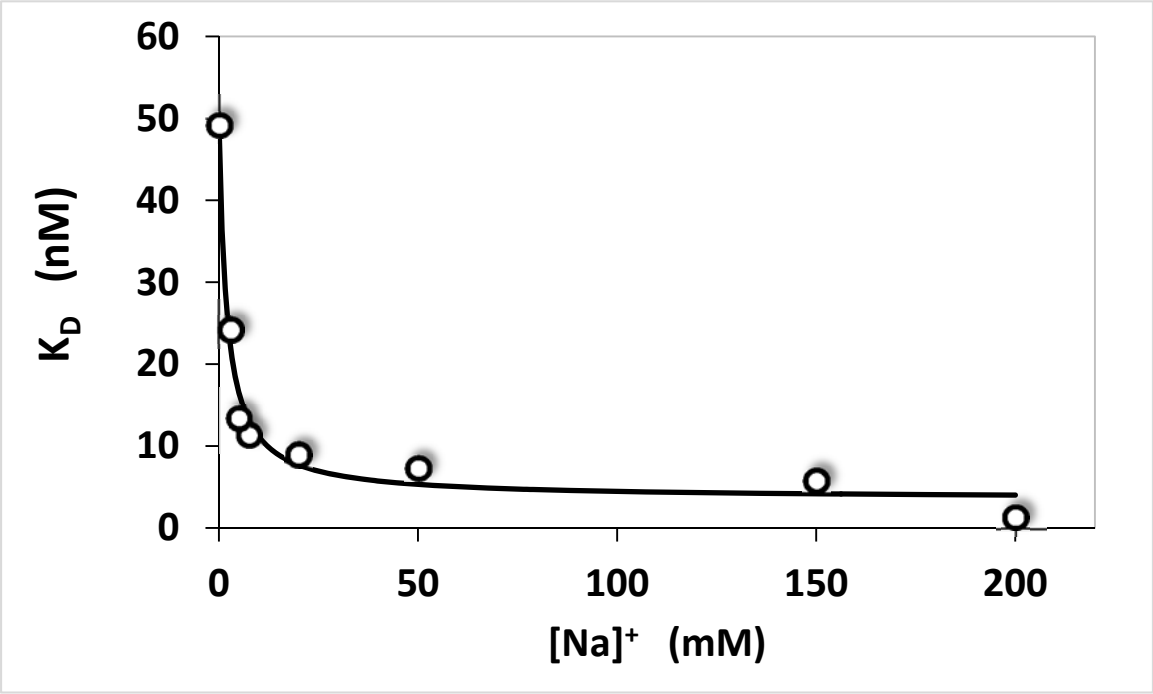

Figure 45

5.5. CONCLUSION

Dissecting the detailed interactions of polyelectrolytes with proteins has been established in literature as a substitute for structural data to obtain an insight about these complex structures. The study of the binding salt-dependency is an information rich method that indicates the number of ion-pairs formed between $CDSO_3$ or $FDSO_3$ and thrombin. The results corroborated the site-directed mutagenesis data obtained for both molecules and indicated more ionic interactions formed between $FDSO_3$ than $CDSO_3$ and thrombin. The thermodynamic signature indicated that the two inhibitors had positive ΔCp similar to heparin. This highlights the fact that burial of the polar surface of exosite 2 during complex formation, combined with the electrostatic interactions involved are shared features between LMWLs and heparin despite their structural difference.

The linkage between exosite 2 and thrombin was studied using $FDSO_3$ binding to surface immobilized thrombin. This allows direct, label-free measuring of the effect that sodium binding has on the binding at exosite 2, without interference from active site involvement. The increased sodium concentration led to a conformational change in exosite 2 that directly affected the K_D of $FDSO_3$. This data shows for the first time a positive correlation between sodium binding and the affinity of an exosite 2 ligand and refutes the idea that the origin of inhibition is due to sodium displacement leading to formation of "slow" thrombin.

Understanding how these complex polymers interact and inhibit thrombin on the molecular level is vital to the design of small molecule inhibitors bearing the same scaffold and recognition elements. This sheds new light on the control of allosteric signals in enzymes by adding another layer to the already complicated thrombin allostery.

Chapter 6: General Conclusion

Sulfated low molecular weight lignins (LMWLs), $CDSO_3$ and $FDSO_3$, designed recently as macromolecular mimetics of heparin, were found to exhibit potent anticoagulant activity. Small molecules based on the same scaffold, SBD and SBT, showed promising thrombin inhibition. We were able to address the mechanism of the inhibition using Michaelis-Menten kinetics. All the molecules were found to be allosterically impairing thrombin activity using either noncompetitive or uncompetitive mechanism.

Absence of competition with hirugen, an exosite 1 ligand, and competition with polymeric heparin points to exosite 2 as the site of interaction for these inhibitors. Yet mixed competition results with other exosite 2 ligands indicated that the molecules utilize different sub-sites within exosite 2 for interaction. Site-directed mutagenesis was used to pin point the key residues important for inhibition. All of all positively charged exosite 2 residues were mutated one at a time to alanine to abolish its charge. The data showed that Arg93 and Arg175 are the major residues involved in $CDSO_3$ binding. $FDSO_3$ showed a progressively greater defect in inhibition with double point mutations, the triple mutant Arg93,97,101Ala displayed a 50 fold drop in inhibition. A single mutant, Arg173Ala, displayed 22-fold reduction in IC_{50} of SBD, while Arg233Ala was the only mutation that impaired SBT inhibition. This proves the fact that in spite of the structural similarity between the two polymers and the two small molecules, the inhibitors do not share the same binding space in exosite 2.

To understand the types of interactions involved in thrombin interaction with the polymers, we resorted to salt-dependence studies. This showed that $CDSO_3$ had fewer ionic contacts with thrombin, with most of its binding energy derived from non-ionic interactions. $FDSO_3$ on the other

hand had a balanced contribution of ionic and non-ionic forces. Thermodynamic studies showed that both polymers have a positive ΔCp of binding, which proves the involvement of electrostatic forces and signals the burial of the polar residues on thrombin exosite 2.

These molecules offer a rare chance to study thrombin allostery. Little is known about the interplay between exosite 2, active site and sodium binding site. The allosteric nature of inhibition indicated that, for the first time, a link is proven to exist between exosite 2 and the active site that could be used to inhibit the enzyme. The presence of sodium was found to enhance the binding of $FDSO_3$ at exosite 2, which establish the energetic coupling between exosite 2 and sodium binding site. The results identify novel binding sub-sites within exosite 2 that are energetically coupled to thrombin's catalytic function and linked to the sodium binding site. The design of high affinity small molecules based on LMWLs scaffold presents major opportunities for developing clinically relevant, allosteric modulators of thrombin.

Literature Cited

Literature Cited

1. Henry, B. L. and Desai, U. R. Anticoagulants. In *Burger's Medicinal Chemistry, Drug Discovery and Development*; John Wiley & Sons, Inc.: **2010**; 365–408.
2. Girard, T. J., MacPhail, L. A., Likert, K. M., Novotny, W. F., Miletich, J. P., Broze Jr, G. J. Inhibition of factor VIIa-tissue factor coagulation activity by a hybrid protein. *Science* **1990***, 248*, 1421-1424.
3. Gailani, D., Broze Jr., G. J. Factor XI activation in a revised model of blood coagulation. *Science* **1991***, 253*, 909-912.
4. Coughlin, S. R. Thrombin signaling and protease-activated receptors. *Nature* **2000**, *407*, 258-264.
5. Mann, K. G. Thrombin formation. *Chest* **2003**, *124*, 4S-10S.
6. Esmon, C. T. The protein C pathway. *Chest* **2003**, *124*, 26S-32S.
7. Esmon, C. T., Xu, J., Gu, J. M., Qu, D., Laszik, Z., Ferrell, G., Stearns-Kurosawa, D. J., Kurosawa, S., Taylor Jr., F. B., Esmon, N.L. *Thromb. Haemost.* **1999**, *82*, 251-258.
8. Taylor Jr., F. B., Peer, G. T., Lockhart, M. S., Ferrell, G., Esmon, C. T. Endothelial cell protein C receptor plays an important role in protein C activation in vivo. *Blood* **2001**, *97*, 1685-1688.
9. Bjork, I.; Olson, S. T. Antithrombin. A bloody important serpin. *Adv. Exp. Med. Biol.* **1997**, *425,* 17-33.
10. Olson, S. T.; Swanson, R.; Raub-Segall, E.; Bedsted, T.; Sadri, M.; Petitou, M.; Herault, J. P.; Herbert, J. M.; Bjork, I. Accelerating ability of synthetic oligosaccharides on antithrombin inhibition of proteinases of the clotting and fibrinolytic systems. Comparison with heparin and low-molecular-weight heparin. *Thromb. Haemost.* **2004**, *92,* 929-939.

11. Larsen, K. S.; Ostergaard, H.; Bjelke, J. R.; Olsen, O. H.; Rasmussen, H. B.; Christensen, L.; Kragelund, B. B.; Stennicke, H. R. Engineering the substrate and inhibitor specificities of human coagulation Factor VIIa. *Biochem. J.* **2007**, *405,* 429-438.
12. Zhao, M.; Abdel-Razek, T.; Sun, M. F.; Gailani, D. Characterization of a heparin binding site on the heavy chain of factor XI. *J. Biol. Chem.* **1998**, *273,* 31153-31159.
13. Gettins, P. G. Serpin structure, mechanism, and function. *Chem. Rev.* **2002**, *102*, 4751-4804.
14. Meddahi, S.; Bara, L.; Fessi, H.; Samama, M. M. Pharmacologic modulation of thrombin generation associated with human clots by human purified antithrombin alone or in the presence of low molecular weight heparin or unfractionated heparin. *Blood Coagul. Fibrinolysis* **2000**, *11,* 51-59.
15. Crawley, J. T.; Lane, D. A. The haemostatic role of tissue factor pathway inhibitor. *Arterioscler. Thromb. Vasc. Biol.* **2008**, *28,* 233-242.
16. Weitz, J. I.; Hudoba, M.; Massel, D.; Maraganore, J.; Hirsh, J. Clot-bound thrombin is protected from inhibition by heparin-antithrombin III but is susceptible to inactivation by antithrombin III-independent inhibitors. *J. Clin. Invest.* **1990**, *86,* 385-391.
17. Weitz, J. I.; Leslie, B.; Hudoba, M. Thrombin binds to soluble fibrin degradation products where it is protected from inhibition by heparin-antithrombin but susceptible to inactivation by antithrombin-independent inhibitors. *Circulation* **1998**, *97,* 544-552.
18. Berry, C. N.; Girardot, C.; Lecoffre, C.; Lunven, C. Effects of the synthetic thrombin inhibitor argatroban on fibrin- or clot-incorporated thrombin: comparison with heparin and recombinant Hirudin. *Thromb. Haemost.* **1994**, *72,* 381-386.

19. Izaguirre, G.; Olson, S. T. Residues Tyr253 and Glu255 in strand 3 of beta-sheet C of antithrombin are key determinants of an exosite made accessible by heparin activation to promote rapid inhibition of factors Xa and IXa. *J. Biol. Chem.* **2006**, *281,* 13424-13432.
20. Izaguirre, G.; Swanson, R.; Raja, S. M.; Rezaie, A. R.; Olson, S. T. Mechanism by which exosites promote the inhibition of blood coagulation proteases by heparin-activated antithrombin. *J. Biol. Chem.* **2007**, *282,* 33609-33622.
21. Bedsted, T.; Swanson, R.; Chuang, Y. J.; Bock, P. E.; Bjork, I.; Olson, S. T. Heparin and calcium ions dramatically enhance antithrombin reactivity with factor IXa by generating new interaction exosites. *Biochemistry* **2003**, *42,* 8143-8152.
22. Desai, U. R. New antithrombin-based anticoagulants. *Med. Res. Rev.* **2004**, *24,* 151-181.
23. Olson, S. T.; Bjork, I.; Sheffer, R.; Craig, P. A.; Shore, J. D.; Choay, J. Role of the antithrombin-binding pentasaccharide in heparin acceleration of antithrombin-proteinase reactions. Resolution of the antithrombin conformational change contribution to heparin rate enhancement. *J. Biol. Chem.* **1992**, *267,* 12528-12538.
24. Duchaussoy, P.; Jaurand, G.; Driguez, P. A.; Lederman, I.; Ceccato, M. L.; Gourvenec, F.; Strassel, J. M.; Sizun, P.; Petitou, M.; Herbert, J. M. Assessment through chemical synthesis of the size of the heparin sequence involved in thrombin inhibition. *Carbohydr. Res.* **1999**, *317,* 85-99.
25. Li, W.; Johnson, D. J.; Esmon, C. T.; Huntington, J. A. Structure of the antithrombin-thrombin-heparin ternary complex reveals the antithrombotic mechanism of heparin. *Nat. Struct. Mol. Biol.* **2004**, *11,* 857-862.

26. Dementiev, A.; Petitou, M.; Herbert, J. M.; Gettins, P. G. The ternary complex of antithrombin-anhydrothrombin-heparin reveals the basis of inhibitor specificity. *Nat. Struct. Mol. Biol.* **2004**, *11,* 863-867.
27. Olson, S. T.; Bjork, I. Predominant contribution of surface approximation to the mechanism of heparin acceleration of the antithrombin-thrombin reaction. Elucidation from salt concentration effects. *J. Biol. Chem.* **1991**, *266,* 6353-6364.
28. Olson, S. T.; Halvorson, H. R.; Bjork, I. Quantitative characterization of the thrombin-heparin interaction. Discrimination between specific and nonspecific binding models. *J. Biol. Chem.* **1991**, *266,* 6342-6352.
29. Warkentin, T. E.; Greinacher, A. Heparin-induced thrombocytopenia: recognition, treatment, and prevention: the Seventh ACCP Conference on Antithrombotic and Thrombolytic Therapy. *Chest* **2004**, *126,* 311S-337S.
30. Pospisil, C. H.; Stafford, A. R.; Fredenburgh, J. C.; Weitz, J. I. Evidence that both exosites on thrombin participate in its high affinity interaction with fibrin. *J. Biol. Chem.* **2003**, *278,* 21584-21591.
31. Lovely, R. S.; Moaddel, M.; Farrell, D. H. Fibrinogen gamma' chain binds thrombin exosite II. *J. Thromb. Haemost.* **2003**, *1,* 124-131.
32. Fredenburgh, J. C.; Stafford, A. R.; Leslie, B. A.; Weitz, J. I. Bivalent binding to gammaA/gamma'-fibrin engages both exosites of thrombin and protects it from inhibition by the antithrombin-heparin complex. *J. Biol. Chem.* **2008**, *283,* 2470-2477.
33. Blick, S. K.; Orman, J. S.; Wagstaff, A. J.; Scott, L. J. Spotlight on fondaparinux sodium in acute coronary syndromes. *BioDrugs* **2008**, *22,* 413-415.

34. Antman, E. M.; Morrow, D. A.; McCabe, C. H.; Murphy, S. A.; Ruda, M.; Sadowski, Z.; Budaj, A.; Lopez-Sendon, J. L.; Guneri, S.; Jiang, F.; White, H. D.; Fox, K. A.; Braunwald, E.; ExTRACT-TIMI 25 Investigators Enoxaparin versus unfractionated heparin with fibrinolysis for ST-elevation myocardial infarction. *N. Engl. J. Med.* **2006**, *354,* 1477-1488.

35. Greinacher, A.; Alban, S.; Omer-Adam, M. A.; Weitschies, W.; Warkentin, T. E. Heparin-induced thrombocytopenia: a stoichiometry-based model to explain the differing immunogenicities of unfractionated heparin, low-molecular-weight heparin, and fondaparinux in different clinical settings. *Thromb. Res.* **2008**, *122,* 211-220.

36. Yusuf, S.; Mehta, S. R.; Chrolavicius, S.; Afzal, R.; Pogue, J.; Granger, C. B.; Budaj, A.; Peters, R. J.; Bassand, J. P.; Wallentin, L.; Joyner, C.; Fox, K. A.; OASIS-6 Trial Group Effects of fondaparinux on mortality and reinfarction in patients with acute ST-segment elevation myocardial infarction: the OASIS-6 randomized trial. *JAMA* **2006**, *295,* 1519-1530.

37. de Kort, M.; Buijsman, R. C.; van Boeckel, C. A. Synthetic heparin derivatives as new anticoagulant drugs. *Drug Discov. Today* **2005**, *10,* 769-779.

38. Walenga, J. M.; Jeske, W. P.; Fareed, J. Short- and long-acting synthetic pentasaccharides as antithrombotic agents. *Expert Opin. Investig. Drugs* **2005**, *14,* 847-858.

39. Harenberg, J.; Vukojevic, Y.; Mikus, G.; Joerg, I.; Weiss, C. Long elimination half-life of idraparinux may explain major bleeding and recurrent events of patients from the van Gogh trials. *J. Thromb. Haemost.* **2008**, *6,* 890-892.

40. Savi, P.; Herault, J. P.; Duchaussoy, P.; Millet, L.; Schaeffer, P.; Petitou, M.; Bono, F.; Herbert, J. M. Reversible biotinylated oligosaccharides: a new approach for a better management of anticoagulant therapy. *J. Thromb. Haemost.* **2008**, *6,* 1697-1706.

41. Lubenow, N.; Greinacher, A. Hirudin in heparin-induced thrombocytopenia. *Semin. Thromb. Hemost.* **2002**, *28,* 431-438.

42. Fischer, K. G.; Liebe, V.; Hudek, R.; Piazolo, L.; Haase, K. K.; Borggrefe, M.; Huhle, G. Anti-hirudin antibodies alter pharmacokinetics and pharmacodynamics of recombinant hirudin. *Thromb. Haemost.* **2003**, *89,* 973-982.

43. Mohapatra, R.; Tran, M.; Gore, J. M.; Spencer, F. A. A review of the oral direct thrombin inhibitor ximelagatran: not yet the end of the warfarin era.. *Am. Heart J.* **2005**, *150,* 19-26.

44. Testa, L.; Bhindi, R.; Agostoni, P.; Abbate, A.; Zoccai, G. G.; van Gaal, W. J. The direct thrombin inhibitor ximelagatran/melagatran: a systematic review on clinical applications and an evidence based assessment of risk benefit profile. *Expert Opin. Drug Saf.* **2007**, *6,* 397-406.

45. Eriksson, B. I.; Dahl, O. E.; Rosencher, N.; Kurth, A. A.; van Dijk, C. N.; Frostick, S. P.; Kalebo, P.; Christiansen, A. V.; Hantel, S.; Hettiarachchi, R.; Schnee, J.; Buller, H. R.; RE-MODEL Study Group. Oral dabigatran etexilate vs. subcutaneous enoxaparin for the prevention of venous thromboembolism after total knee replacement: the RE-MODEL randomized trial. *J. Thromb. Haemost.* **2007**, *5,* 2178-2185.

46. Hogg, P. J.; Jackson, C. M. Fibrin monomer protects thrombin from inactivation by heparin-antithrombin III: implications for heparin efficacy. *Proc. Natl. Acad. Sci. USA* **1989**, *86,* 3619-3623.

47. Hogg, P. J.; Jackson, C. M.; Labanowski, J. K.; Bock, P. E. Binding of fibrin monomer and heparin to thrombin in a ternary complex alters the environment of the thrombin catalytic site, reduces affinity for hirudin, and inhibits cleavage of fibrinogen. *J. Biol. Chem.* **1996**, *271,* 26088-26095.

48. Henry, B. L.; Monien, B. H.; Bock, P. E.; Desai, U. R. A novel allosteric pathway of thrombin inhibition: Exosite II mediated potent inhibition of thrombin by chemo-enzymatic, sulfated dehydropolymers of 4-hydroxycinnamic acids. *J. Biol. Chem.* **2007**, *282,* 31891-31899.

49. Monien, B. H.; Henry, B. L.; Raghuraman, A.; Hindle, M.; Desai, U. R. Novel chemo-enzymatic oligomers of cinnamic acids as direct and indirect inhibitors of coagulation proteinases. *Bioorg. Med. Chem.* **2006**, *14,* 7988-7998.

50. Sidhu, P. S.; Liang, A.; Mehta, A. Y.; Abdel Aziz, M. H.; Zhou, Q.; Desai, U. R. Rational design of potent, small, synthetic allosteric inhibitors of thrombin. *J. Med. Chem.* **2011**, *54,* 5522-5531.

51. Di Cera, E. A structural perspective on enzymes activated by monovalent cations. *J. Biol. Chem.* **2006**, *281*, 1305-1308.

52. Page, M. J., Di Cera, E. Role of Na^+ and K^+ in enzyme function. *Physiol. Rev.* **2006**, *86*, 1049-1092.

53. Di Cera, E. Thrombin. *Mol. Aspects Med.* **2008**, *29*, 203-254.

54. Dang, Q. D., Vindigni, A., Di Cera, E. An allosteric switch controls the procoagulant and anticoagulant activity activities of thrombin. *Proc. Natl. Acad. Sci. USA* **1995**, *92*, 5977-5981.

55. Dang, Q. D., Guinto, E. R., Di Cera, E. Rational engineering of activity and specificity in a serine protease. *Nat. Biotechnol.* **1997**, *15*, 146-149.

56. Di Cera, E. Thrombin as procoagulant and anticoagulant. *J. Thromb. Haemost.* **2007**, *5*, 196-202.

57. Bode, W., Turk, D., Karshikov, A. The refined 1.9-A X-ray crystal structure of D-Phe-Pro-Arg chloromethylketone-inhibited human alpha-thrombin: structure analysis, overall structure, electrostatic properties, detailed active-site geometry, and structure-function relationships. *Protein Sci.* **1992**, *1*, 426-471.

58. http://www.rcsb.org/pdb/home/home.do accessed on 12/18/12.

59. Page, M. J., Di Cera, E. Serine peptidases: classification, structure and function. *Cell Mol. Life Sci.* **2008**, *65*, 1220-1236.

60. Bode, W. Structure and interaction modes of thrombin. *Blood Cells Mol. Dis.* **2006**, *36,* 122-130.

61. Adams, T. E.; Huntington, J. A. Thrombin-cofactor interactions: structural insights into regulatory mechanisms. *Arterioscler. Thromb. Vasc. Biol.* **2006**, *26,* 1738-1745.

62. Huntington, J. A. Molecular recognition mechanisms of thrombin. *J. Thromb. Haemost.* **2005**, *3,* 1861-1872.

63. Fenton, J. W.,2nd; Villanueva, G. B.; Ofosu, F. A.; Maraganore, J. M. Thrombin inhibition by hirudin: how hirudin inhibits thrombin. *Haemostasis* **1991**, *21 Suppl 1,* 27-31.

64. Pospisil, C. H.; Stafford, A. R.; Fredenburgh, J. C.; Weitz, J. I. Evidence that both exosites on thrombin participate in its high affinity interaction with fibrin. *J. Biol. Chem.* **2003**, *278,* 21584-21591.

65. Ye, J.; Liu, L. W.; Esmon, C. T.; Johnson, A. E. The fifth and sixth growth factor-like domains of thrombomodulin bind to the anion-binding exosite of thrombin and alter its specificity. *J. Biol. Chem.* **1992**, *267,* 11023-11028.

66. Monteiro, R. Q. Targeting exosites on blood coagulation proteases. *An. Acad. Bras. Cienc.* **2005**, *77,* 275-280.

67. Zarpellon, A.; Celikel, R.; Roberts, J. R.; McClintock, R. A.; Mendolicchio, G. L.; Moore, K. L.; Jing, H.; Varughese, K. I.; Ruggeri, Z. M. Binding of alpha-thrombin to surface-anchored platelet glycoprotein Ib(alpha) sulfotyrosines through a two-site mechanism involving exosite I. *Proc. Natl. Acad. Sci. USA* **2011**, *108,* 8628-8633.

68. Prasad, S., Wright, K. J., Roy, D. B., Bush, L. A., Cantwell, A. M., Di Cera, E. Redesigning the monovalent cation specificity of an enzyme. *Proc. Natl. Acad. Sci. USA* **2003**, *100*, 13785-13790.

69. Fenton, J. W.,2nd; Olson, T. A.; Zabinski, M. P.; Wilner, G. D. Anion-binding exosite of human alpha-thrombin and fibrin(ogen) recognition. *Biochemistry* **1988**, *27,* 7106-7112.

70. Krishnaswamy, S. Exosite-driven substrate specificity and function in coagulation. *J. Thromb. Haemost.* **2005**, *3,* 54-67.

71. Di Cera, E.; Page, M. J.; Bah, A.; Bush-Pelc, L. A.; Garvey, L. C. Thrombin allostery. *Phys. Chem. Chem. Phys.* **2007**, *9,* 1291-1306.

72. Bah, A., Garvey, L. C., Ge, J., Di Cera, E. Rapid kinetics of Na+ binding to thrombin. *J. Biol. Chem.* **2006**, *281*, 40049-40056.

73. Pineda, A. O., Carrell, C. J., Bush, L. A., Prasad, S., Caccia, S., Chen, Z. W., Mathews, F. S., Di Cera, E. Molecular dissection of Na^+ binding to thrombin. *J. Biol. Chem.* **2004**, *279*, 31842-31853.

74. Bone, S. Dielectric studies of water clusters in cyclodextrins: relevance to the transition between slow and fast forms of thrombin. *J. Phys. Chem. B Condens. Matter Mater. Surf. Interfaces Biophys.* **2006**, *110*, 20609-20614.

75. Guinto, E. R., Di Cera, E. Large heat capacity change in a protein-monovalent cation interaction. *Biochemistry* **1996**, *35*, 8800-8804.

76. Griffon, N., Di Stasio, E. Thermodynamics of Na^+ binding to coagulation serine proteases. *Biophys. Chem.* **2001**, *90*, 89-96.

77. Kamath, P.; Huntington, J. A.; Krishnaswamy, S. Ligand binding shuttles thrombin along a continuum of zymogen- and proteinase-like states. *J. Biol. Chem.* **2010**, *285,* 28651-28658.

78. Liu, L. W.; Vu, T. K.; Esmon, C. T.; Coughlin, S. R. The region of the thrombin receptor resembling hirudin binds to thrombin and alters enzyme specificity. *J. Biol. Chem.* **1991**, *266,* 16977-16980.

79. Lai, M. T.; Di Cera, E.; Shafer, J. A. Kinetic pathway for the slow to fast transition of thrombin. Evidence of linked ligand binding at structurally distinct domains. *J. Biol. Chem.* **1997**, *272,* 30275-30282.

80. Gandhi, P. S.; Chen, Z.; Mathews, F. S.; Di Cera, E. Structural identification of the pathway of long-range communication in an allosteric enzyme. *Proc. Natl. Acad. Sci. USA* **2008**, *105,* 1832-1837.

81. Lechtenberg, B. C.; Johnson, D. J.; Freund, S. M.; Huntington, J. A. NMR resonance assignments of thrombin reveal the conformational and dynamic effects of ligation. *Proc. Natl. Acad. Sci. USA* **2010**, *107,* 14087-14092.

82. Ng, N. M.; Quinsey, N. S.; Matthews, A. Y.; Kaiserman, D.; Wijeyewickrema, L. C.; Bird, P. I.; Thompson, P. E.; Pike, R. N. The effects of exosite occupancy on the substrate specificity of thrombin. *Arch. Biochem. Biophys.* **2009**, *489,* 48-54.

83. Fredenburgh, J. C.; Stafford, A. R.; Weitz, J. I. Evidence for allosteric linkage between exosites 1 and 2 of thrombin. *J. Biol. Chem.* **1997**, *272,* 25493-25499.

84. Petrera, N. S.; Stafford, A. R.; Leslie, B. A.; Kretz, C. A.; Fredenburgh, J. C.; Weitz, J. I. Long range communication between exosites 1 and 2 modulates thrombin function. *J. Biol. Chem.* **2009**, *284,* 25620-25629.

85. Verhamme, I. M.; Olson, S. T.; Tollefsen, D. M.; Bock, P. E. Binding of exosite ligands to human thrombin. Re-evaluation of allosteric linkage between thrombin exosites I and II. *J. Biol. Chem.* **2002**, *277,* 6788-6798.

86. Carter, W. J.; Cama, E.; Huntington, J. A. Crystal structure of thrombin bound to heparin. *J. Biol. Chem.* **2005**, *280,* 2745-2749.

87. Oshima, G.; Uchiyama, H.; Nagasawa, K. Effect of NaCl on the association of thrombin with heparin. *Biopolymers* **1986**, *25,* 527-537.

88. Griffith, M. J.; Kingdon, H. S.; Lundblad, R. L. The interaction of heparin with human alpha-thrombin: effect on the hydrolysis of anilide tripeptide substrates. *Arch. Biochem. Biophys.* **1979**, *195,* 378-384.

89. Griffith, M. J. Kinetics of the heparin-enhanced antithrombin III/thrombin reaction. Evidence for a template model for the mechanism of action of heparin. *J. Biol. Chem.* **1982**, *257,* 7360-7365.

90. Liang, A.; Thakkar, J. N.; Desai, U. R. Study of physico-chemical properties of novel highly sulfated, aromatic, mimetics of heparin and heparan sulfate. *J. Pharm. Sci.* **2010**, *99,* 1207-1216.

91. Olson, S. T.; Chuang, Y. J. Heparin activates antithrombin anticoagulant function by generating new interaction sites (exosites) for blood clotting proteinases. *Trends Cardiovasc. Med.* **2002**, *12,* 331-338.

92. Hirsh, J.; Anand, S. S.; Halperin, J. L.; Fuster, V.; American Heart Association Guide to

anticoagulant therapy: Heparin : a statement for healthcare professionals from the American Heart Association. *Circulation* **2001**, *103,* 2994-3018.

93. Hirsh, J.; Fuster, V.; Ansell, J.; Halperin, J. L.; American Heart Association; American College of Cardiology Foundation American Heart Association/American College of Cardiology Foundation guide to warfarin therapy. *Circulation* **2003**, *107,* 1692-1711.
94. Henry, B. L.; Thakkar, J. N.; Martin, E. J.; Brophy, D. F.; Desai, U. R. Characterization of the plasma and blood anticoagulant potential of structurally and mechanistically novel oligomers of 4-hydroxycinnamic acids. *Blood Coagul. Fibrinolysis* **2009**, *20,* 27-34.
95. Henry, B. L.; Desai, U. R. Recent research developments in the direct inhibition of coagulation proteinases--inhibitors of the initiation phase. *Cardiovasc. Hematol. Agents Med. Chem.* **2008**, *6,* 323-336.
96. Henry, B. L.; Abdel Aziz, M.; Zhou, Q.; Desai, U. R. Sulfated, low-molecular-weight lignins are potent inhibitorsof plasmin, in addition to thrombin and factor Xa: Novel opportunity for controlling complex pathologies. *Thromb. Haemost.* **2010**, *103,* 507-515.
97. Bock, P. E.; Olson, S. T.; Bjork, I. Inactivation of thrombin by antithrombin is accompanied by inactivation of regulatory exosite I. *J. Biol. Chem.* **1997**, *272,* 19837-19845.
98. He, X.; Ye, J.; Esmon, C. T.; Rezaie, A. R. Influence of Arginines 93, 97, and 101 of thrombin to its functional specificity. *Biochemistry* **1997**, *36,* 8969-8976.
99. Yang, L.; Rezaie, A. R. Calcium-binding sites of the thrombin-thrombomodulin-protein C complex: possible implications for the effect of platelet factor 4 on the activation of vitamin K-dependent coagulation factors. *Thromb. Haemost.* **2007**, *97,* 899-906.
100. Russell, W. R.; Forrester, A. R.; Chesson, A.; Burkitt, M. J. Oxidative coupling during lignin polymerization is determined by unpaired electron delocalization within parent

phenylpropanoid radicals. *Arch. Biochem. Biophys.* **1996**, *332,* 357-366.

101. Neuenschwander, P. F.; Branam, D. E.; Morrissey, J. H. Importance of substrate composition, pH and other variables on tissue factor enhancement of factor VIIa activity. *Thromb. Haemost.* **1993**, *70,* 970-977.

102. Rezaie, A. R. Identification of basic residues in the heparin-binding exosite of factor Xa critical for heparin and factor Va binding. *J. Biol. Chem.* **2000**, *275,* 3320-3327.

103. Badellino, K. O.; Walsh, P. N. Localization of a heparin binding site in the catalytic domain of factor XIa. *Biochemistry* **2001**, *40,* 7569-7580.

104. Henry, B. L.; Thakkar, J. N.; Liang, A.; Desai, U. R. Sulfated, low molecular weight lignins inhibit a select group of heparin-binding serine proteases. *Biochem. Biophys. Res. Commun.* **2012**, *417,* 382-386.

105. Alexander, K. S.; Fried, M. G.; Farrell, D. H. Role of Electrostatic Interactions in Binding of Thrombin to the Fibrinogen gamma' Chain. *Biochemistry* **2012**, *51*, 3445-3450.

106. Bock, P. E.; Panizzi, P.; Verhamme, I. M. Exosites in the substrate specificity of blood coagulation reactions. *J. Thromb. Haemost.* **2007**, *5 Suppl 1,* 81-94.

107. Stone, S. R.; Dennis, S.; Hofsteenge, J. Quantitative evaluation of the contribution of ionic interactions to the formation of the thrombin-hirudin complex. *Biochemistry* **1989**, *28,* 6857-6863.

108. Betz, A.; Hofsteenge, J.; Stone, S. R. Ionic interactions in the formation of the thrombin-hirudin complex. *Biochem. J.* **1991**, *275 (Pt 3),* 801-803.

109. Yang, L.; Sun, M. F.; Gailani, D.; Rezaie, A. R. Characterization of a heparin-binding site on the catalytic domain of factor XIa: mechanism of heparin acceleration of factor XIa inhibition by the serpins antithrombin and C1-inhibitor. *Biochemistry* **2009**, *48,* 1517-1524.

110. Bode, W. The structure of thrombin: a janus-headed proteinase. *Semin. Thromb. Hemost.* **2006**, *32 Suppl 1,* 16-31.

111. Di Cera, E. Thrombin: a paradigm for enzymes allosterically activated by monovalent cations. *C. R. Biol.* **2004**, *327,* 1065-1076.

112. Evans, S. A.; Olson, S. T.; Shore, J. D. p-Aminobenzamidine as a fluorescent probe for the active site of serine proteases. *J. Biol. Chem.* **1982**, *257,* 3014-3017.

113. Desai, B. J.; Boothello, R. S.; Mehta, A. Y.; Scarsdale, J. N.; Wright, H. T.; Desai, U. R. Interaction of thrombin with sucrose octasulfate. *Biochemistry* **2011**, *50,* 6973-6982.

114. Liu, C. C.; Brustad, E.; Liu, W.; Schultz, P. G. Crystal structure of a biosynthetic sulfo-hirudin complexed to thrombin. *J. Am. Chem. Soc.* **2007**, *129,* 10648-10649.

115. Monteiro, R. Q.; Raposo, J. G.; Wisner, A.; Guimaraes, J. A.; Bon, C.; Zingali, R. B. Allosteric changes of thrombin catalytic site induced by interaction of bothrojaracin with anion-binding exosites I and II. *Biochem. Biophys. Res. Commun.* **1999**, *262,* 819-822.

116. Levi, M.; Schultz, M. Hematologic failure. *Semin. Respir. Crit. Care. Med.* **2011**, *32,* 651-659.

117. Linhardt, R. J. 2003 Claude S. Hudson Award address in carbohydrate chemistry. Heparin: structure and activity. *J. Med. Chem.* **2003**, *46,* 2551-2564.

118. Verghese, J.; Liang, A.; Sidhu, P. P.; Hindle, M.; Zhou, Q.; Desai, U. R. First steps in the direction of synthetic, allosteric, direct inhibitors of thrombin and factor Xa. *Bioorg. Med. Chem. Lett.* **2009**, *19,* 4126-4129.

119. Sabo, T. M.; Farrell, D. H.; Maurer, M. C. Conformational analysis of gamma' peptide (410-427) interactions with thrombin anion binding exosite II. *Biochemistry* **2006**, *45,* 7434-7445.

120. Saiah, E.; Soares, C. Small molecule coagulation cascade inhibitors in the clinic. *Curr. Top. Med. Chem.* **2005**, *5,* 1677-1695.

121. Smallheer, J. M.; Quan, M. L. Chapter 9 Recent Advances in Coagulation Serine Protease Inhibitors. In *Annual Reports in Medicinal Chemistry;* Academic Press: Vol. Volume 44, pp 189-208.

122. Straub, A.; Roehrig, S.; Hillisch, A. Oral, direct thrombin and factor Xa inhibitors: the replacement for warfarin, leeches, and pig intestines? *Angew. Chem. Int. Ed Engl.* **2011**, *50,* 4574-4590.

123. Lovely, R. S.; Rein, C. M.; White, T. C.; Jouihan, S. A.; Boshkov, L. K.; Bakke, A. C.; McCarty, O. J.; Farrell, D. H. gammaA/gamma' fibrinogen inhibits thrombin-induced platelet aggregation. *Thromb. Haemost.* **2008**, *100,* 837-846.

124. Adams, T. E.; Everse, S. J.; Mann, K. G. Predicting the pharmacology of thrombin inhibitors. *J. Thromb. Haemost.* **2003**, *1,* 1024-1027.

125. Ladbury, J. E.; Klebe, G.; Freire, E. Adding calorimetric data to decision making in lead discovery: a hot tip. *Nat. Rev. Drug Discov*. **2010**, 9, 23-27.

126. Manning, G. S. The molecular theory of polyelectrolyte solutions with applications to the electrostatic properties of polynucleotides. *Q. Rev. Biophys.* **1978**, *11,* 179-246.

127. Record, M. T.; Anderson, C. F.; Lohman, T. M. Thermodynamic analysis of ion effects on the binding and conformational equilibria of proteins and nucleic acids: the roles of ion association or release, screening, and ion effects on water activity. *Q. Rev. Biophys.* **1978**, *11,* 103.

128. Lohman, T. M.; deHaseth, P. L.; Record, M. T.,Jr Pentalysine-deoxyribonucleic acid interactions: a model for the general effects of ion concentrations on the interactions of proteins with nucleic acids. *Biochemistry* **1980**, *19,* 3522-3530.

129. Record, M. T.,Jr; Lohman, M. L.; De Haseth, P. Ion effects on ligand-nucleic acid interactions. *J. Mol. Biol.* **1976**, *107,* 145-158.

130. Record, M. T.,Jr; Woodbury, C. P.; Lohman, T. M. Na^+ effects on transition of DNA and polynucleotides of variable linear charge density. *Biopolymers* **1976**, *15,* 893-915.

131. Desai, U. R.; Petitou, M.; Bjork, I.; Olson, S. T. Mechanism of heparin activation of antithrombin: evidence for an induced-fit model of allosteric activation involving two interaction subsites. *Biochemistry* **1998**, *37,* 13033-13041.

132. Desai, U. R.; Petitou, M.; Bjork, I.; Olson, S. T. Mechanism of heparin activation of antithrombin. Role of individual residues of the pentasaccharide activating sequence in the recognition of native and activated states of antithrombin. *J. Biol. Chem.* **1998**, *273,* 7478-7487.

133. Baerga-Ortiz, A.; Rezaie, A. R.; Komives, E. A. Electrostatic dependence of the thrombin-thrombomodulin interaction. *J. Mol. Biol.* **2000**, *296,* 651-658.

134. Henry, B. L.; Connell, J.; Liang, A.; Krishnasamy, C.; Desai, U. R. Interaction of antithrombin with sulfated, low molecular weight lignins: opportunities for potent, selective modulation of antithrombin function. *J. Biol. Chem.* **2009**, *284,* 20897-20908.

135. Monien, B. H.; Cheang, K. I.; Desai, U. R. Mechanism of poly(acrylic acid) acceleration of antithrombin inhibition of thrombin: implications for the design of novel heparin mimics. *J. Med. Chem.* **2005**, *48,* 5360-5368.

136. Monien, B. H.; Desai, U. R. Antithrombin activation by nonsulfated, non-polysaccharide organic polymer. *J. Med. Chem.* **2005**, *48,* 1269-1273.

137. Prabhu, N. V.; Sharp, K. A. Heat capacity in proteins. *Annu. Rev. Phys. Chem.* **2005**, *56,* 521-548.

138. Vindigni, A.; White, C. E.; Komives, E. A.; Di Cera, E. Energetics of thrombin-thrombomodulin interaction. *Biochemistry* **1997**, *36,* 6674-6681.

139. Ayala, Y. M.; Vindigni, A.; Nayal, M.; Spolar, R. S.; Record, M. T.,Jr; Di Cera, E. Thermodynamic investigation of hirudin binding to the slow and fast forms of thrombin: evidence for folding transitions in the inhibitor and protease coupled to binding. *J. Mol. Biol.* **1995**, *253,* 787-798.

140. Niedzwiecka, A.; Stepinski, J.; Darzynkiewicz, E.; Sonenberg, N.; Stolarski, R. Positive heat capacity change upon specific binding of translation initiation factor eIF4E to mRNA 5' cap. *Biochemistry* **2002**, *41,* 12140-12148.

141. Kiraga-Motoszko, K.; Niedzwiecka, A.; Modrak-Wojcik, A.; Stepinski, J.; Darzynkiewicz, E.; Stolarski, R. Thermodynamics of molecular recognition of mRNA 5' cap by yeast eukaryotic initiation factor 4E. *J. Phys. Chem. B* **2011**, *115,* 8746-8754.

142. Homans, S. W. Water, water everywhere--except where it matters? *Drug Discov. Today* **2007**, *12,* 534-539.

143. Beeler, D.; Rosenberg, R.; Jordan, R. Fractionation of low molecular weight heparin species and their interaction with antithrombin. *J. Biol. Chem.* **1979**, *254,* 2902-2913.

144. Zhou, Y.; Liao, J.; Du, F.; Liang, Y. Thermodynamics of the interaction of xanthine oxidase with superoxide dismutase studied by isothermal titration calorimetry and fluorescence spectroscopy. *Thermochimica Acta* **2005**, 426, 173-178.

145. Luther, M. A.; Gilbert, H. F.; Lee, J. C. Self-association of rabbit muscle phosphofructokinase: role of subunit interaction in regulation of enzymatic activity. *Biochemistry* **1983**, *22,* 5494-5500.

146. Kiraga-Motoszko, K.; Niedzwiecka, A.; Modrak-Wojcik, A.; Stepinski, J.; Darzynkiewicz, E.; Stolarski, R. Thermodynamics of molecular recognition of mRNA 5' cap by yeast eukaryotic initiation factor 4E. *J. Phys. Chem. B* **2011**, *115,* 8746-8754.

147. Niedzwiecka, A.; Stepinski, J.; Darzynkiewicz, E.; Sonenberg, N.; Stolarski, R. Positive heat capacity change upon specific binding of translation initiation factor eIF4E to mRNA 5' cap. *Biochemistry* **2002**, *41,* 1214-12148.

148. Ziegler, A.; Seelig, J. Binding and clustering of glycosaminoglycans: a common property of mono- and multivalent cell-penetrating compounds. *Biophys. J.* **2008**, 94, 2142-2149.

149. Hileman, R. E.; Jennings, R. N.; Linhardt, R. J. Thermodynamic analysis of the heparin interaction with a basic cyclic peptide using isothermal titration calorimetry. *Biochemistry* **1998**, 37, 15231-15237.

150. Ziegler, A.; Seelig, J. Interaction of the protein transduction domain of HIV-1 TAT with heparan sulfate: binding mechanism and thermodynamic parameters. *Biophys. J.* **2004**, 86, 254-263.

151. Muzammil, S.; Ross, P.; Freire, E. A major role for a set of non-active site mutations in the development of HIV-1 protease drug resistance. *Biochemistry* **2003**, 42, 631-638.

152. Clarke, C.; Woods, R. J.; Gluska, J.; Cooper, A.; Nutley, M. A.; Boons, G. J. Involvement of water in carbohydrate-protein binding. *J. Am. Chem. Soc*. **2001**, 123, 12238-12247.

153. Lemieux, R. U. How Water Provides the Impetus for Molecular Recognition in Aqueous Solution. *Acc. Chem. Res.* **1996**, 29, 373-380.

154. Ladbury, J. E. Just add water! The effect of water on the specificity of protein-ligand binding sites and its potential application to drug design. *Chem. Biol.* **1996**, *3,* 973-980.

155. Bingham, R. J.; Findlay, J. B.; Hsieh, S. Y.; Kalverda, A. P.; Kjellberg, A.; Perazzolo, C.; Phillips, S. E.; Seshadri, K.; Trinh, C. H.; Turnbull, W. B.; Bodenhausen, G.; Homans, S. W. Thermodynamics of binding of 2-methoxy-3-isopropylpyrazine and 2-methoxy-3-isobutylpyrazine to the major urinary protein. *J. Am. Chem. Soc.* **2004**, *126,* 1675-1681.

156. Englert, L.; Biela, A.; Zayed, M.; Heine, A.; Hangauer, D.; Klebe, G. Displacement of disordered water molecules from hydrophobic pocket creates enthalpic signature: binding of phosphonamidate to the S(1)'-pocket of thermolysin. *Biochim. Biophys. Acta* **2010**, *1800,* 1192-1202.

157. Snyder, P. W.; Mecinovic, J.; Moustakas, D. T.; Thomas, S. W.,3rd; Harder, M.; Mack, E. T.; Lockett, M. R.; Heroux, A.; Sherman, W.; Whitesides, G. M. Mechanism of the hydrophobic effect in the biomolecular recognition of arylsulfonamides by carbonic anhydrase. *Proc. Natl. Acad. Sci. USA* **2011**, *108,* 17889-17894.

158. Barratt, E.; Bingham, R. J.; Warner, D. J.; Laughton, C. A.; Phillips, S. E.; Homans, S. W. Van der Waals interactions dominate ligand-protein association in a protein binding site occluded from solvent water. *J. Am. Chem. Soc.* **2005**, *127,* 11827-11834.

159. Dunitz, J. D. The entropic cost of bound water in crystals and biomolecules. *Science* **1994**, *264,* 670.

160. Biela, A.; Sielaff, F.; Terwesten, F.; Heine, A.; Steinmetzer, T.; Klebe, G. Ligand binding stepwise disrupts water network in thrombin: enthalpic and entropic changes reveal classical hydrophobic effect. *J. Med. Chem.* **2012**, *55,* 6094-6110.

161. Binder, F. P.; Lemme, K.; Preston, R. C.; Ernst, B. Sialyl Lewis(x): a "pre-organized water oligomer"? *Angew. Chem. Int. Ed Engl.* **2012**, *51,* 7327-7331.

APPENDIX A

Abbreviations Used

AT: antithrombin

DTIs: direct thrombin inhibitors

*f*FPR-Th: fluorescein labeled inhibited thrombin

FibP: γ' fibrinogen peptide

GAGs: glycosaminoglycans

H8: heparin-derived octasaccharide

HirP: hirugen peptide

LMWHs: low molecular weight heparins

LMWLs: low molecular weight lignins

PARs: protease-activated receptors

SBD: sulfated benzofuran dimer

SBT: sulfated benzofuran trimer

Serpin: serine protease inhibitor

SPR: surface plasmon resonance

UFH: unfractionated heparin

VKAs: vitamin K antagonists

VITA

May Hamdy Abdel Aziz was born on July 6, 1980 in Cairo, Egypt, and is an Egyptian citizen. She earned her Bachelor in Pharmaceutical Sciences degree in 2002 followed by Masters in Pharmaceutical Chemistry in 2008 from Cairo University. She worked as a teaching assistant in Misr International University in Egypt between 2002 and 2008 where she earned the university's Certificate of Excellence. She started her doctorate degree in the Department of Medicinal Chemistry at Virginia Commonwealth University in 2008. She coauthored a book chapter, Cardiovascular Agents. In The Chemistry of Drugs for Nurse Anesthetists (2nd Edition) and four research articles, Designing allosteric regulators of thrombin: Monosulfated benzofuran dimers selectively interact with Arg173 of exosite 2 to induce inhibition; Identification of the site of binding of sulfated low molecular weight lignins on thrombin; Rational design of potent, small, synthetic allosteric inhibitors of thrombin; Sulfated, low-molecular-weight lignins are potent inhibitors of plasmin, in addition to thrombin and factor Xa: Novel opportunity for controlling complex pathologies.